Targeting underlying mechanisms of uveal melanoma metastasis through anti-cancer drug mifepristone and proteomic characterization of extracellular vesicles

Alexander Laskaris B.Sc.

Dr. Julia V. Burnier's Laboratory

Department of Pathology

McGill University, Montreal

A thesis submitted to McGill University in partial fulfillment of the

requirements of the degree of Master of Science

Table of Contents

Acknowledgements

I would like to extend a heartfelt thank you to my supervisor, Dr. Julia Burnier, who has been my guiding light throughout. She is an inspiring force as someone with great professionalism and expertise in the field of research. Her open-hearted approach to our laboratory environment has created an unparalleled unit of like-minded individuals who are learning to adopt her nurturing yet instructive approach. I greatly appreciate the support Dr. Julia Burnier has given me during these few years with her. She has propelled my research career and scientific writing to new heights through shear encouragement, invaluable feedback and advocacy.

I would also like to thank the department of pathology for allowing me to begin this journey and gain the necessary skills I will need in my future career. Dr. Edith Zorychta, Dr. Hua Ling and the entire department of pathology at McGill University have been a wonderful support to me and other students. Dr. Edith Zorychta and Dr. Hua Ling run the program with focus on the students, improving our learning experience and providing the necessary foundations for us to succeed in academia. Especially during these difficult times, they have extended additional support to us and adapted the program to help provide a more tailored experience for our needs. Another thank you is extended to my committee advisors : Dr. Carlos Telleria and Dr. Carolyn Baglole, for their continued support and insightful suggestions on research directions and methodologies.

A special acknowledgement goes to Dr. Peter Metrakos and Dr. Miguel Burnier whose kindness, advice, and insight opened a window of opportunities in my research career. From them I gained an essential clinical perspective, learning research is only as important as the patients we fight for.

In addition, I would like to thank my lab family for fostering a wonderful learning environment. I will always remember all the laughs, encouragements, and importantly the invaluable research experience they have passed down to me. To be specific, our research assistant Thupten Tsering was as much a colleague as a friend, I admire his dedication to the academic community and his drive to share his knowledge with everyone around him. Our PhD candidate Prisca Bustamante who helped me grow, taught me everything she knew about experimental procedures and was always there for advice whenever I needed a little encouragement. Of course I will never forget my cheerleader and friend, Tadhg Ferrier, who has always been by my side for the up and downs of these past two years. Another thank you goes to Dr. Cristina Fonseca for being a great friend and supportive older sister. I would also like to thank Dr. Alicia Goyeneche

who has been there to help with every experimental technique and extended her motherly advice whenever we spoke.

This project was made possible by funding from Fonds de recherche du Québec – Santé (FRQS). Integral to all my projects was the help from everyone at the proteomic platform at the RI-MUHC.

Finally, to my family and friends who have stood by me with their constant love and support. I cannot thank you all enough and am truly grateful to everyone who has been there for me unconditionally.

Author Contributions

This is to confirm that I have conducted the experiments described in this thesis under the supervision of Dr Julia V. Burnier and in collaboration with our laboratory to produce two manuscripts for publication.

Chapter 2 (Manuscript 1)

Contributions of Alexander Laskaris to this manuscript included optimizing drug treatment of UM and NCM cell cultures, live IncuCyte tracking of dose dependent response, cellular cck8 and trypan blue viability assays, recovery assay, flow cytometry, statistical analysis and graphing results. Alexander Laskaris had an equal part in writing the original draft and producing the figures, preparing the manuscript for initial submission, reviewing and editing for final submission.

Contributions of Prisca Bustamante included cck8 and trypan blue viability assays, flow cytometry, caspase 3/7 activity, genomic DNA fragmentation, quantification of cfDNA release, and investigation of PR and GR receptor expression. Prisca Bustamante had an equal part in writing the original draft and producing the figures, preparing the manuscript for initial submission, reviewing and editing for final submission.

Contributions of Alicia A. Goyeneche included flow cytometry analysis, collectively aided in analysis of caspase 3/7 data, cck8 and trypan blue viability assays, and flow cytometry. Alicia A. Goyeneche oversaw and supported the study design.

Chapter 3 (Manuscript 2)

Contributions of Alexander Laskaris to this manuscript included optimization of an EV isolation protocol, collection and isolation of EVs from cell culture supernatant, validation of EV yield with NTA and TEM, extraction of EV proteins, and proteomic data analysis. Alexander Laskaris had an equal part in writing the original draft and producing the figures, preparing the manuscript for initial submission, reviewing and editing for final submission.

Contributions of Thupten Tsering included optimization of an EV isolation protocol, culturing and isolating EVs from NCMs, validation of EV yield with NTA and TEM, *in vitro* assays with recipient cells. Thupten Tsering had equal part in writing the original draft and producing the figures, preparing the manuscript for initial submission, reviewing and editing for final submission.

Contributions of Mohamed Abdouh included an *in vivo* model of UM-EV oncogenic potential. Mohamed Abdouh had equal part in writing the original draft and producing the figures, preparing the manuscript for initial submission, reviewing and editing for final submission.

English Abstract

Uveal melanoma (UM) is a malignant neoplasm of melanocytic origin residing in the vascular layer of the eye. Despite ocular melanomas occurring at a relatively low frequency, UM is recognized as the dominant intraocular malignancy in adults. UM is highly metastatic; independent of primary treatment, an alarming 50% of patients present with metastasis plummeting survival to 15%. Given the limited and ineffective treatment options for metastatic disease, our aims were to investigate the effects of a repurposed drug on metastatic phenotypes and elucidate underlying mechanisms of UM metastasis.

Following a traditional theory of metastasis, genetic reprogramming of primary tumor cells culminates in partial epithelial to mesenchymal transition (EMT). Acquisition of a mesenchymal phenotype enhances the migratory and invasive capacity of cells, facilitating dissemination to distance tissue microenvironments. Mifepristone (MF) is an antiprogestin abortifacient that has anti-cancer potential through selective inhibition of EMT and cancer associated hallmarks. Repurposing of MF in oncology is cost effective and provides a means for this preapproved drug with a good safety profile to become implemented into clinic. Our primary aim focused on the anti-cancer effects of MF in the context of UM. The study confirmed MF's ability to significantly impede the natural proliferative curves of UM cells in a dose dependent fashion. Higher doses of MF demonstrated a cytotoxic effect associated with late apoptotic phenotypes.

In parallel to the malignant transformation of individual cells, the tumor secretome has an essential supportive role in cancer metastasis. Extracellular vesicles (EVs) are nanoparticles ubiquitously secreted by tumors with functionally active biomolecules that can be isolated non-invasively from blood. We shifted focused onto EVs as studies have confirmed their propensity to mediate metastasis through oncogenic reprogramming of target cells creating a pre-metastatic niche. Here, we extensively characterized UM cancer cell-derived EVs. Mass spectrometry analysis elucidated differential proteomic expression patterns in UM-EVs as compared to EVs derived from normal choroidal melanocytes (NCMs). Moreover, investigating the tumorigenic potential of UM-derived EVs, treatment of BRCA1-deficient fibroblasts with UM-EVs significantly enhanced metastatic properties and resulted in tumor formation *in vivo*. In short the above results expand the scope of our knowledge on UM metastasis; investigating potential treatment avenues and providing insight into the functional significance of UM derived EVs in relation to tumor growth and dissemination.

French Abstract

Le mélanome de l'uvée (MU) est une tumeur maligne d'origine mélanocytaire résidant dans la couche vasculaire de l'œil. Même si les mélanomes oculaires surviennent à une fréquence relativement faible, le MU est reconnu comme la tumeur maligne intraoculaire la plus fréquente chez l'adulte. Le MU est hautement métastatique; indépendamment du traitement différentiel, 50% des cas présentent des métastases, faisant chuter la survie des patients à 15%. Compte tenu des taux de métastases accrus et des options de traitement inefficaces limitées, nos objectifs étaient d'étudier les effets d'un médicament réutilisé sur les phénotypes métastatiques et d'élucider les mécanismes sous-jacents de la métastase du MU.

Suivant une théorie traditionnelle des métastases; la reprogrammation génétique des cellules tumorales primaires aboutit à une transition épithéliale-mésenchymateuse partielle (TEM). L'acquisition d'un phénotype mésenchymateux améliore la capacité migratoire et invasive des cellules, facilitant la diffusion à distance des microenvironnements tissulaires. La mifépristone (MF) est un abortif antiprogestatif qui semble fournir une solution prometteuse grâce à l'inhibition sélective de l'TEM et des caractéristiques associées au cancer. La réutilisation de la MF en oncologie est rentable et permet à ce médicament préapprouvé ayant un bon profil d'innocuité d'être mis en œuvre plus rapidement en clinique. Notre objectif principal s'est concentré sur les effets anticancéreux de la MF dans le contexte du MU. L'étude a confirmé la capacité de la MF à entraver de manière significative les courbes de prolifération naturelles des cellules mélanocytaires de manière dose-dépendante. Des concentrations plus élevées de MF ont démontré un effet cytotoxique associé à des phénotypes apoptotiques tardifs.

Parallèlement à la transformation maligne de cellules individuelles, le sécrétome tumoral joue un rôle de soutien essentiel dans les métastases cancéreuses. Les vésicules extracellulaires (VE) sont des nanoparticules sécrétées de manière ubiquitaire par les tumeurs avec des biomolécules fonctionnellement actives qui peuvent être isolées du sang de manière non invasive. Nous avons porté notre attention sur les vésicules extracellulaires, car des études ont confirmé leur propension à médier les métastases par le biais d'une reprogrammation oncogène des cellules cibles créant une niche pré-métastatique. En étudiant le potentiel tumorigène des VE dérivés du mélanome de l'uvée, le traitement des fibroblastes déficients en BRCA1 avec des VE-MU a considérablement amélioré les propriétés métastatiques et entraîné la formation de tumeurs *in vivo*. L'analyse par spectrométrie de masse a élucidé les schémas d'expression protéomiques

différentiels entre les MU et les NCM-VE. En bref, les résultats ci-dessus élargissent la portée de nos connaissances sur les métastases du MU; étudier les voies de traitement potentielles et fournir un aperçu de l'importance fonctionnelle des vésicules extracellulaires dérivées du MU en relation avec la croissance et la dissémination des tumeurs.

List of Abbreviations

UM	Uveal melanoma
CM	Cutaneous melanoma
NCM	Human normal choroidal melanocytes
GNAQ	Guanine nucleotide-binding protein alpha Q
GNA11	Guanine nucleotide-binding protein alpha 11
NTA	Nanoparticle tracking analysis
TEM	Transmission electron microscopy
MAPK	Mitogen-activated protein kinase
EV	Extracellular vesicle
BRCA1	Breast cancer type 1 susceptibility protein
BRAF	V-RAF murine sarcoma viral oncogene homolog B
NRAS	Neuroblastoma RAS viral oncogene homolog
PLCB	Phospholipase C β4
CYSTLR2	Cysteinyl leukotriene receptor 2
TERT	Human Telomerase Reverse Transcriptase
CTLA-4	Cytotoxic T-lymphocyte-associated protein 4
DNA	Deoxyribonucleic acid
MIF	Migration inhibitory factor
NF- kB	Nuclear factor kappa-light-chain-enhancer of activated B-cells
mTOR	Mechanistic target of rapamycin kinase
ECM	Extracellular matrix
MVB	Multivesicular body
ILVs	Intraluminal vesicles
ISEV	International Society for Extracellular Vesicles
PIBF	Progesterone induced blocking factor
EGFR	Epidermal growth factor receptor
PCR	Polymerase chain reaction

List of Figures

Chapter 1 (Introduction)

1.Uveal Melanoma

Melanoma arises from the malignant transformation of melanocytes: neural crest derived cells located in various tissues, functioning in the production and regulation of cellular pigment melanin. A photoprotective agent, melanin shields cells from ultraviolet (UV) radiation and minimizes accumulated DNA damage within exposed cells. Melanocytes predominate in the basal layer of the epidermis where a proper protective barrier from the sun and external world is vital [1]. In perspective, melanocytic lesions are primarily of cutaneous or ocular origin [2-5].

Ocular melanomas comprise 5% of total melanoma cases [4, 6-8], with a distinction for uveal melanoma (UM) as the predominant intraocular malignancy in adults [9, 10]. UM occurs in the vascular portion of the inner eye or uveal tract [2, 10], and the median age of diagnosis hovers around 62 years [9, 11, 12]. Over a 41-year period, the age-adjusted incidence of primary UM in the United States was 5.2 per million [9]. While in Canada from 1992-2010, the annual incidence of UM was 3.75 per million, varying heavily by province with British Columbia at 6.38 per million annually [13].

Treatment options for primary UM are very effective to control local (ocular) disease, and have shifted from complete enucleation to eye-saving local irradiation [9, 10, 14]. Regardless, 5-year survival has remained relatively stagnant since 1973 [7, 9, 14], suggesting local treatments have little influence on survival and metastatic progression. Further, 25% of patients present with metastases within 5-years post initial diagnosis, spiking to an alarming 50% overall [2, 15, 16]. UM metastases primarily develop in the liver (60.5-89%), lungs (24.4-29%), bone (8.4-17%), skin and subcutaneous tissue (10.9-12%), and lastly the lymph nodes (11%) [6, 17-20]. Following diagnosis of metastasis, median survival is 13.4 months as a mere 8% of metastatic UM patients survive past 2 years, regardless of treatment [6, 19, 21].

1.1 Ocular Anatomy

The introduction of certain anatomical terms is integral for understanding ocular melanomas and their divergent developmental schemes. Ocular globes are composed of three consecutive layers: an outer protective sclera, the underlying uvea (choroid, ciliary body, and iris) and finally a photosensitive retina (Fig. 1) [22]. The conjunctiva is a mucous membrane covering the inner eyelids, continuing over the sclera, and ending at the beginning of the cornea [23]. Ocular

melanomas find origin either in the uvea (83%), the conjunctiva (5%) or other variable ocular locations (10%) [3, 4, 10].

Conjunctival and uveal melanomas have different tumor biology, genetics, and clinical presentations [2, 22-24]. Uveal melanomas are mutationally similar to melanomas of the central nervous system, both harbouring activating mutations in guanine nucleotide-binding proteins alpha Q (GNAQ) and alpha 11 (GNA11) [25]. In contrast, conjunctival melanomas parallel cutaneous melanoma (CM), with activating mutations in BRAF and NRAS [24].

In conjunctival melanoma developing lesions are immediately visible to the patient as a suspicious mass on the eyelid, while UM progression can be inconspicuous. A study of 8033 UM patients by Shields C.L. *et al.* reported 4% of cases were clearly visible in the iris, 6% resided in the ciliary body, and an estimated 90% were hidden in the choroid [10, 26].

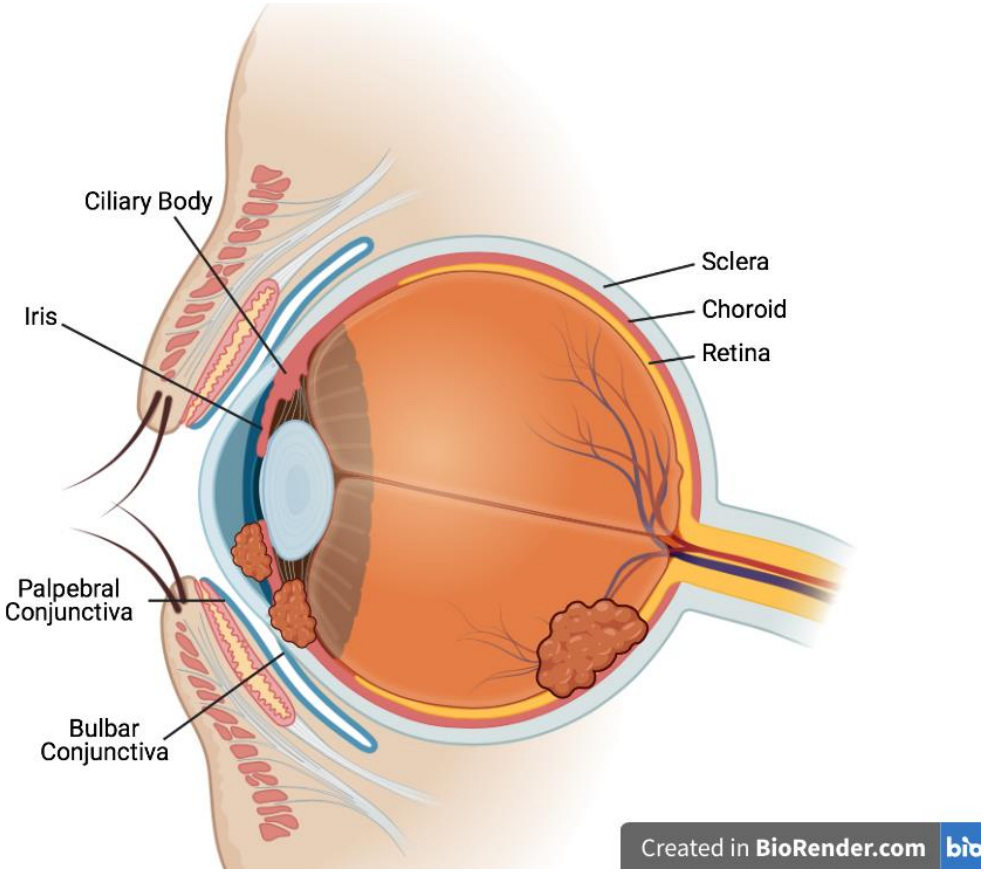

Figure 1: Ocular Anatomy and localization of UM (adapted from Ansari, M.W., & Nadeem, A., Atlas of Ocular Anatomy. Springer International Publishing, 2016 and Jager, M.J., Shields, C.L., Cebulla, C.M. *et al.*, Uveal melanoma. Nat Rev Dis Primers, 2020. 6: 24).

1.2 Predisposing factors

A meta-analysis of 10 studies and up to 1732 UM cases deemed light iris color (blue, green or grey), fair skin, and an inability to tan, as factors that significantly increased the risk of developing UM [27, 28]. A suggested explanation is routed in the photoprotective role of melanin in melanocytes. Lighter irises have an inherent vulnerability to UV radiation; a reduction in melanin permits increased penetration of rays onto the retina and choroid encouraging malignant transformations [27]. However, the foundations of this theory are unstable as researchers are struggling to find concrete links between UV exposure and UM development.

A meta-analysis of 12 studies was unable to correlate chronic UV light exposure (occupational sunlight, birthplace, lifetime exposure) with risk of UM [29]. The cornea and lens filter a large proportion of UV light and this is reflected in the lack of UV related genetic aberrations in UM. C >T transitions at dipyrimidine sites would be expected in a lesion dependent on UV-induced mutations, as found in cutaneous melanoma, yet are absent in UM [2]. However, blue light does penetrate through to the retina and choroid, and occupational welding has been correlated with a significant risk of UM [29].

A clear discrepancy persists: the genetic landscape of UM diverges from that of CM and other UV sensitive lesions. Exemplifying these claims, the promoter of human Telomerase Reverse Transcriptase (TERT) gene harbors UV-induced mutations in 70-80% of CM cases [2, 30-32], while in UM the mutational frequency drops to 1% [33, 34]. Therefore, UV-induced transformations may surface in a novel way or there may be unknown mechanisms independent of UV radiation involved in the development of UM.

Despite a lack of insight surrounding the causation of malignant transformations leading to UM, a generalized scheme provides the bare framework of UM development. A melanoma arises with direct genomic alterations of melanocytes, notably through activating mutations in oncogenes [35]. UM lesions can present through an intermediate stage or benign choroidal nevi; which are commonly pigmented (77%), have a mean diameter of 1.25-5 mm and thickness of 1.5mm [36, 37]. An estimated 6.2% of the US population have choroidal nevi, with 1 in 3664 individuals over age 80 developing UM [38, 39]. This transformation from begin to malignant is relatively low, with less than 1% of total choroidal nevi reported to develop into melanoma [36]. It remains unclear whether nevi are precursors to melanoma or whether they occur in a subset of cases [35, 38].

The subset of nevi which circumvent tumor suppressor mechanisms transform into aggressively malignant UM. The mutational accumulations required for such transformation are currently unknown, however important clinical features of nevi correlate with disease progression [35, 38]. These include, thickness (>2mm), subretinal fluid, visual acuity loss symptoms, orange lipofuscin pigment, melanoma acoustic hollowness and diameter (>5mm) [38, 40]. Other clinical presentations to consider are margin from optic disc (<3mm), absence of drusen (yellow fatty protein deposits), and absence of yellow halo around nevus [36]. Choroidal nevi between 2.1-3mm thickness have a 35.7 times greater risk of developing into melanoma compared to flat nevi [38]. Although rare, presenting with three or more of the aforementioned nevi factors can increase the risk of UM to over 50% [36].

Subsequent to full UM development, lesions can be subdivided into high, intermediate and low metastatic risk categories through clinical, histological and mutational features [41]. These features include size of initial tumor, mitotic activity of cells, cell type (epithelioid posing higher risk) and extraocular extensions [26, 41, 42]. Shields *et al.* conducted a study on 8,033 UM cases and found incremental 1 mm increase in thickness to correlate with a 5% increased risk of developing metastasis within ten years. Tumors over 8 mm had a 67% risk of metastasizing over 20 years [26].

1.3 Genetic Signatures

UM is defined by initiating mutations in one of four genes (*GNAQ, GNA11, PLCB4, CYSTLR2*) which constitutively activate the CYSLTR2-$G\alpha_{11/q}$-PLCβ pathway [41]. Compiling literature, mutually exclusive alterations in *GNAQ* or *GNA11* are found associated with anywhere from 80%-96% of UM cases [32, 33, 41, 43, 44]. These mutations are thought to be present in choroidal nevi suggesting they are initiating hits in UM [45]. While the remaining UM cohort harbors a mutation in phospholipase C β4 (*PLCB4*) or Cysteinyl Leukotriene Receptor 2 (*CYSTLR2*) [41, 46].

The signaling pathway commences as leukotrienes interact and activate transmembrane receptor CYSTLR2, triggering detachment and activation of the alpha G protein subunit [41, 46, 47]. From there, effectors PLCB4 or ADP-ribosylation factor 6 (ARF6) activate their respective downstream pathways [41, 48, 49]. The dominant scheme involves PLCB4 dependent activation of MAPK and AKT/mTOR pathways associated with cancer growth and development. In parallel, CM lesions with *BRAF* and *NRAS* mutations similarly thrive through activation of the MAPK pathway [50].

Independent from PLCB4, ARF6 can activate Yes-associated protein 1 (YAP1) a component of the Hippo signaling pathway involved in cellular growth, organ size and cancer development [41, 51, 52]. In a homeostatic state YAP activity occurs during proliferation and is regulated by tumor suppressor homologs 1 and 2 (LATS1 and LATS2), which phosphorylate YAP and impede uncontrolled growth [51, 53, 54]. However, in a pathological state these systems become dysregulated permitting unrestrained growth.

Though the CYSLTR2-$G\alpha_{11/q}$-PLCβ pathway contributes to the development of UM, subsequent hits required for full progression of UM to a malignant state remain unknown. The presence of three secondary oncogenic mutations in breast cancer associated protein 1 (BAP1), splicing factor 3b subunit 1 (SF3B1), or eukaryotic translation initiation factor 1A X-linked (EIF1AX), are known to correlate with long term disease progression and overall risk of metastasis. These mutations are mainly mutually exclusive although a small number of cases do present with mutations in both EIF1AX and SF3B1 (~3%) [44].

Loss or aberrant tumor suppressor gene BAP1 occurs in up to half of all primary UM and metastasizes in the majority of cases within the first five years [41, 55, 56]. BAP1 is a deubiquitinating enzyme that associates with breast cancer 1 (BRCA1) and functions in DNA double stranded break repair [41, 55, 57]. In absence of BAP1, frequency of non-homologous end joining increases the accumulation of mutations [41, 58]. However, UM lesions have significantly lower total mutational loads; in UM a single nucleotide variation per million pales relative to 100 mutations per million nucleotides in CM [41, 59]. Therefore, dysregulation of DNA repair does not seem to be the mechanism by which BAP1 negative tumors are developing, and instead researchers speculate the large array of BAP1 interactors may be responsible [60, 61]. Regardless, loss of BAP1 seems integral for acquisition of metastatic properties and therefore determining downstream mechanisms are vital to understanding metastatic UM.

Mutations in SF3B1 characterize the intermediate risk cohort which have relatively high metastasis rates over an extended dormancy phase of up to 15 years [44]. SF3B1 is integral to mRNA processing as it functions in recognition of branchpoints during pre-mRNA splicing. Similar spliceosome related mutations are observed in breast and pancreatic cancers [62, 63]. Finally, mutations in EIF1AX pose the lowest risk of metastasis and usually associate with disomy 3 status [33, 41, 44, 64]. 16-21% of UM cases are shown to harbor EIF1AX mutations, encoding

a protein known to stabilize the ribosome during binding to the 5' end of mRNA and aid in locating the start codon [41].

In addition, stratification of UM into low (Class 1) and high (Class 2) metastatic risk groups can be done with a gene expression profile test (GEP). The test includes 12 genes with differential expression between Class 1 and 2 groups providing accurate prognostication with a technical success of 97% [65]. Extraction of RNA from a fine needle biopsy of a Class 2 tumor will demonstrate an upregulation in E-cadherin, extracellular matrix protein 1, RAB31, member RAS oncogene family and 5-hydroxytryptamine (serotonin) receptor 2B [65]. The upregulated cluster of genes is linked to chromosome 8q, while downregulated genes are associated with chromosome 3 [65, 66]. This allows for clinicians to flag patients with heighten risk, alter adjuvant treatment plans and monitor for disease progression.

1.4 Diagnosis and Treatment

The ambiguity of UM symptoms remains an obstacle in early detection, contributing to heightened rates of tumor progression and metastasis. In a cohort of 2384 UM patients, 30.2% were asymptomatic and 23.1% reported their tumors had been initially missed when first consulted by a physician [67]. In absence of a visually apparent tumor, symptomatic presentations in UM can be attributed to other pathological conditions, extending the period between initial awareness and proper clinical diagnosis. 37.8% of UM patients experience blurred vision which can be overlooked and stem from a number of different ocular pathologies especially in an elderly patient cohort. While 8.6% of patients perceive flashing lights in absence of visual stimuli or photopsia [67]. Photopsia can result from a multitude of ocular and neurological pathologies including posterior vitreous detachment following trauma [68]. Additional UM symptoms include a general decrease in vision, perception of floating shadows, and ocular pain [67]. Due to difficulties in diagnosis of tumors, UM lesions often progress to substantial sizes uninterrupted for a time before appropriate diagnosis and treatment begin.

Histological examination of tissue biopsies used in the diagnosis of many tumors are not relevant in UM. In place less invasive imaging techniques in conjunction with clinical presentation suffice in obtaining a proper diagnosis [2, 69, 70]. Ocular tissue biopsies are initially avoided as sampling may not be reflective of the entire lesion and risk of complications are heightened due to the limited surface area with a high density of sensitive structures [70]. Imaging techniques,

including ultrasonography, allow a clear account of the size and location of the tumor while being least disruptive to the patient [71].

Though, tissue biopsies in UM have gained importance in prognostication as cytogenetic testing of tissue samples can assess risk of metastasis with great accuracy [72-74]. However, liquid biopsy techniques in UM are emerging as important workarounds to current challenges with invasive tissue biopsies. Identification of UM driving mutations in circulating tumor DNA can bypass the need for tissue, provide a faster more accurate diagnosis and has been shown to correlate with UM malignancy in patients [69].

Upon detection, globe-preserving and non-preserving treatment modalities are proposed to mitigate primary UM. Therapies are weighted based on tumor size, location, extraocular extension and extent to which functionality can be preserved [75]. Enucleation is performed under circumstances where tumors are relatively large, painful, have extensive extraocular growth and/or visual perception is already impaired [61]. In contrast, local resections (exoresection or endoresection), radiotherapy (brachytherapy), and laser therapy, are methods employed to preserve functionality while eradicating the melanoma [76, 77]. A recent report of 4999 UM cases in the US, demonstrated preferred treatment modalities have shifted focus drastically from 1973-2013. Surgical resections went from 94.2% to 24.7%, while globe preserving radiotherapy now predominates with 68.3% of patients receiving this treatment between 2012-2013 [9].

Regardless of initial local treatment, overall metastasis and as consequence mortality rates have remained constant. In a 12-year follow up study of 1317 patients by the COMS group, mortality after brachytherapy or enucleation was 43% and 41%, respectively [78]. While metastasis rates for either treatment were relatively high and comparable, concluding primary treatment regimens did not impact overall mortality or metastatic risk. In place, metastatic risk and death correlate with age of diagnosis (over 60 years) and tumor dimensions (over 11 mm diameter) [78].

Despite heightened metastatic risk, upon diagnosis a mere 4% of patients present with detectable metastases. To explain this disparity, estimation of tumor doubling suggests undetectable micro-metastases present upwards of 5 years prior to treatment of UM [79]. Further, these seeds may enter a dormant or quiescent state, providing an explanation for longitudinal reports of UM patients acquiring detectable metastases 15-20 years following initial treatment [9, 19, 41, 79]. These statistics stress the need for liquid biopsy based techniques to monitor disease

progression, provide real-time feedback on treatment response and metastatic development. Although preliminary, our group has shown mutant ctDNA in a rabbit model of UM is detectable before observable lesions can be discerned [69]. These findings further support the eventual use of liquid biopsies techniques in clinic to improve current detection and treatment of UM.

The reservoir of treatment options for metastatic UM is shallow, with a lack of effective adjuvant therapy to mitigate metastatic spread and improve overall survival [61]. Successful trials in metastatic CM, including immune checkpoint inhibitors (such as antibodies against CTLA-4 and PD-1), prove inadequate in the context of UM [59]. There are various clinical trials underway including chemotherapy, targeted therapy (ex. tyrosine kinase inhibitor crizotinib), and immunotherapy [61]. In a cohort of 661 metastatic UM patients, despite chemotherapy being the predominant treatment in 50% of cases, all treatment options improved median survival by 6.3 months [80]. Compiling data from 29 clinical trials, survival remains relatively consistent regardless of treatment with an estimated 3.3 month progression free survival and overall 1-year survival of 43% [81]. As consequence of these findings, a food and drug administration (FDA) approved treatment for metastatic UM is lacking.

Metastasis to the liver alone or in conjunction with disperse secondary metastases has been shown to represent an estimated 85-90% of cases [18, 80]. The burden of hepatic metastases plummets 1-year survival from 52.8% with strictly extrahepatic lesions to 18.4% [80]. Therefore, it lends to reason that hepatic-directed therapies may provide improved overall survival. In comparison to systemic treatment regimens (chemotherapy, immunotherapy and anti-angiogenic therapy) with an overall survival below 11 months, liver-directed therapy increased survival to 14.6 months [81]. Liver therapies include resection, radiofrequency ablation, and liver localized chemotherapy [61]. Though successful resection can in theory eradicate metastasis, the eligible patient cohort is extremely limited [82]. Further, resection is often not an endpoint, even in conjunction with radiofrequency ablation overall survival is 35% [17, 83].

2. Metastasis

While a primary lesion endangers the host by reducing the functionality of the organ of origin; secondary sites destroy additional organs in an already compromised host, are located in challenging visceral locations, become resistant to treatment, and contribute to a large proportion

of cancer related deaths. Two dominant sequences of events are thought to occur in parallel leading to the development and dissemination of cancer (Fig. 2).

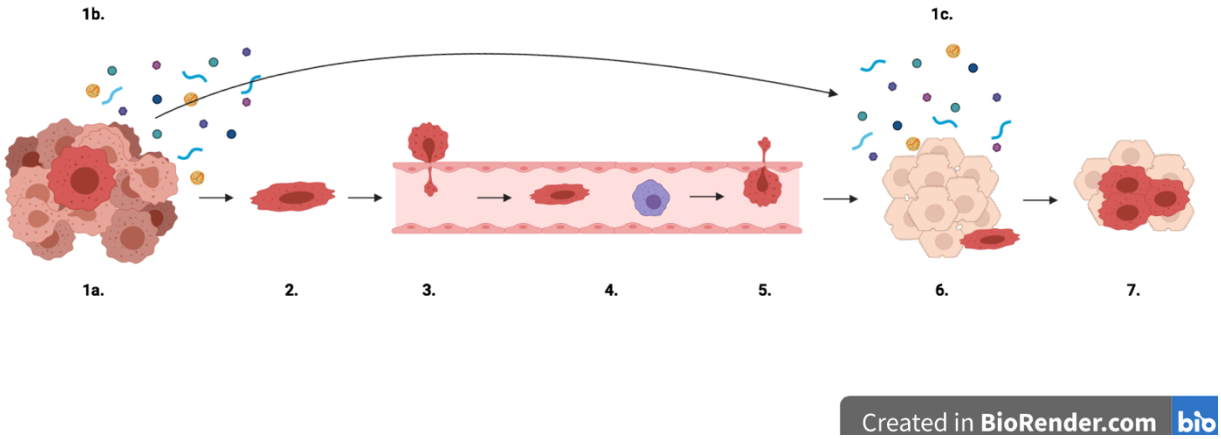

Figure 2: The two schemes of metastatic progression. Dominant pathway : (1A) primary tumor cells undergo genetic transformations, (2) partial EMT enhances migration and invasion, (3) intravasation, (4) dissemination through circulation, (5) extravasation, (6) colonization in distant tissue, and (7) formation of a metastatic seed. Parallel pathway : (1B) tumor cells secrete factors into circulation, (1C) cancer secretome primes distant tissue for future colonization.

Metastatic lesions come to fruition as individual cells evolve to evade characteristic cellular restraints and gain stem-like properties. This process occurs through a gradient as cells acquire capabilities slowly with the majority succumbing to tumor suppressor mechanisms and host defenses. As cells begin to surpass thresholds of malignancy through a series of genetic and epigenetic events, they invade and intravasate into the circulation or lymph, survive in harsh conditions, extravasate into a distant tissue, and colonize a novel organ. This scheme is a baseline for metastatic spread, however acquiring these capabilities takes place through variable means, is dependent on host treatment, location and mutational burden of the primary lesion [84-86].

Epithelial to mesenchymal transition (EMT) is a suggested route in which primary tumor cells phenotypically and transcriptionally alter themselves to gain metastatic traits [87, 88]. An integral indicator of EMT is loss of cell-cell adhesive junctions associated with absence or transcriptional repression of E-cadherin. This is a defining event that characterizes conversion from an epithelial phenotype and triggers a cascade in which epithelial markers of homeostasis become dysregulated [87, 89, 90]. Loss of apical-basal cell polarity and reorganization of the

cytoskeleton accompanies these adaptations and ultimately promotes cellular motility [87]. An invasive phenotype is gained in parallel, with increased expression of mesenchymal associated proteins vimentin and fibronectin, and expression of matrix metalloproteinases to allow for ECM remodeling during invasion [87, 89, 91, 92].

With differential acquisition of mesenchymal-like phenotypes, cellular migration, invasion into surrounding tissues and intravasation is achieved with varying success. Subsequently, if and only if malignant cells have undergone adequate evolution to evade and survive circulation, they will eventually extravasate into a distant tissue in an attempt to form the metastatic 'seed' [93, 94].

Though individual cells are thought to commence the process of colonization solely through shear malignancy and resistance to tumor suppressor defenses; research suggests in anticipation of metastatic spread a pre-metastatic niche is formed initially devoid of cancerous cells. As a lesion becomes aggressively malignant, pro-metastatic secretions can begin to modify a secondary environment, co-opt host mechanisms, and accommodate subsequent cellular colonization [95]. Tumors secrete a host of components, a pro-metastatic secretome, consisting of pro-angiogenic factors, growth factors, immune modulators [96, 97] and tumor derived extracellular vesicles (EVs, specifically delivering proteins, DNA and RNA) [95, 98, 99]. The end result is to transform the original properties of a future metastatic site. This occurs through immunomodulation, vascular remodelling, cellular transformations and selective recruitment of non-resident cells [93]. Niches encourage organotrophic colonization by becoming a malignantly inclined environment, improving the odds of single cancer cells to survive in distant tissues.

3. Mifepristone

The synthetic steroid mifepristone (MF), a potent anti-progesterone compound, originally found optimal use as an abortifacient [100, 101]. Branded with a reasonable safety profile (while rare minor and/or severe adverse effects have been reported), MF has been approved for use in various countries [102, 103]. As a progesterone regulator, other uses include emergency contraception, menstrual regulation, management of miscarriages, and facilitation of surgical abortion [103, 104]. Unrelated to reproductive medicine, MF has shown effectiveness in various other domains including treatment of Cushing's syndrome [105], in depression and mood disorders [106], and oncology [107].

Forming parallels between fetal and malignant growth, researchers have found a potential use for MF as an anti-cancer drug [101, 108-110]. MF is suggested to have dual effectiveness, inhibiting growth of primary lesions whilst simultaneously influencing mesenchymal phenotypes. *In vitro* assays confirm a potent effect on primary tumor cells in various cancers (glioma, ovarian, prostate, breast, gastric adenocarcinoma and osteosarcoma) regardless of progesterone receptor expression [110]. Further investigations have demonstrated an inhibitory effect on the migratory and invasive capacity of malignant cells suggesting a reasonable ability to influence metastatic phenotypes *in vitro* [109]. *In vivo* reports have shown MF to increase lifespan of mice with lung cancer [111], and in humans improved patient quality of life by reducing pain and possibly halting metastatic growth in advanced stage cancer [112].

3.1 Origin, Safety Profile, and Mechanism of Action

MF or RU 486 was synthesized for intended use as a pure anti-glucocorticoid, yet demonstrated higher affinities for the progesterone receptor (PR) [103, 113, 114]. Early recorded data on MF emerged in Paris around 1980 for menstrual regulation and termination of pregnancy [115-117]. Affinity testing confirmed the propensity of MF to interact with the progesterone receptor with five times greater affinity than progesterone itself, hence its subsequent use as an abortifacient [113, 118]. Initially sparking controversial beginnings, while approved for use as early as 1988 in France, the Vatican and lobbyists in the US deemed MF a dangerous treatment due to the religious implications of terminating a fetus [103].

In 2000, the FDA approved MF for use in the US, although countless other abortifacients were in use at the time. Under this directive a single dose of 600 mg of MF was administered for pregnancies of less than 49 days. Misoprostol, a prostaglandin, was taken in combination 48-hours following MF and a mandatory 2-week follow up was required to monitor for complications [103].

To date the World Health Organization's Clinical practice handbook for safe abortion care deems combination mifepristone/misoprostol as the standard for medically assisted abortion [119]. A woman with gestation time of up to 9 weeks (63 days) is administered 200 mg MF orally followed by 800 ug misoprostol (vaginally, buccally or sublingually) 24-48 hours after the initial MF dose. Depending on time of gestation, earlier than 7 or between 9-14 weeks, MF doses remain constant while misoprostol doses and route of administration vary [119]. This regimen effectively terminates over 90% of pregnancies with minimal adverse consequences for the patient [102, 103,

120-122]. With extensive use in gynecology, longitudinal and retrospective studies on MF have demonstrated an excellent efficacy and safety profile [102, 120, 123]. Common side effects of MF include cramping, vaginal bleeding, nausea, fever, weakness, vomiting, headache, and dizziness [123].

MF has modulatory effects on the progesterone receptor which are dependent on isoform dimerization, presence of excess cAMP, differential co-factors, and mutational aberrations in PR. Mirroring progesterone, MF interacts with PR triggering isoform dimerization (A:A, A:B, or B:B). At baseline, dimerization and activation of PR permits interaction with the DNA response element and commences transcription of progesterone related genes. The modulatory effects of MF on the progesterone pathway are dependent on PR conformation; A:A dimers silence transcription, A:B dimers are inhibitory and B:B dimers are active [124, 125].

3.2 Mifepristone and Cancer

Fetal and tumor development similarly involve extensive proliferation, migration, invasion, angiogenesis and tissue remodeling [126-128]. In 1985 translating theory into action, the potent effects of MF were investigated in breast cancer cell lines MCF7 and T47D, reporting a significant reduction in proliferation [129]. These conclusions brought a novel direction for the use of MF in cancer. Henceforth the application of MF as a potential adjuvant therapy has continued to be under investigation. Researchers are focusing on the extent to which MF can negatively influence cancer associated phenotypes and the possible mechanisms of action involved.

In hormone responsive tumors, *in vitro* MF treatment produces a cytostatic effect accompanied by cytotoxicity through a suggested apoptotic mechanism of cell death. In ovarian cancer, our collaborators Goyeneche *et al.* demonstrated a dose-dependent inhibition of proliferation associated with cellular arrest in G1. Further in response to MF, cyclin-dependent kinase inhibitors p21 and p27 were upregulated and localized to the nucleus, in conjunction with a decrease in cdk2 activity and localization. Authors proceeded with an *in vivo* mouse model of ovarian cancer, demonstrating 1mg of MF daily over 40 days was sufficient to reduce tumor growth [108]. Similar studies in breast cancer concluded MF induced G1 arrest, caspase associated apoptosis, and induction of p21 [130-132]. Finally in endometrial cancer, *in vitro* assays have found potent cell cycle arrest in S phase, apoptosis, and induction of p53 [133, 134].

While the majority of early accounts detailing MF's potency were in context of progesterone responsive tumors, Tieszen *et al.* challenged this theory by assessing the efficacy of MF in cancer of non-reproductive origin. A catalogue of 7 cancer types were investigated *in vitro* and included malignant glioma, human osteosarcoma, estrogen-unresponsive breast carcinoma, androgen-responsive and un-responsive prostate carcinoma and malignant meningioma. Independent of PR expression, all cell lines treated with MF demonstrated a significant cytostatic state transforming to cytotoxicity at heightened doses [110]. This group produced a follow up study detailing the inhibitory effects of MF on ovarian, breast, glioblastoma, and prostate cancer cell migratory and invasive capabilities [109]. Comparable findings are found in gastric cancer cell lines, in which MF impeded the invasive capacity of cells and down-regulated integrin β3 expression [126]. Though *in vitro* MF research had supported a suggested mechanism of action through hormone receptors [125, 135], the above accounts suggests varied mechanisms exist independent of hormone responsiveness [108, 109, 120].

In vivo animal models were conducted in BRCA1/p53-deficient mice, finding MF treatment to prevent breast cancer development [136]. While, in rats with mammary tumors, MF is shown to impede tumor growth by 75-90% in comparison to a 75% reduction with tamoxifen [137]. Various other *in vivo* models including lung, testicular and prostate cancer have concluded promising anti-tumor effects associated with MF treatment [111, 112].

In humans, clinical trials were undertaken for treatment of primary and metastatic breast cancer, endometrial cancer and meningioma. The three clinical trials in breast cancer provide positive results, but were dated prior to 2000 and are of limited cohort size [138-141]. In endometrial cancer, MF was found to stabilize disease progression in 25% of patients, but failed to improve overall quality of life [125, 142]. In meningiomas, a systemic literature review including 6 clinical trials found no significant results in terms of tumor regression or symptom improvement. In one report of 14 patients, tumor regression was observed in 36% of patients, symptom improvement in 21%, and progression of disease state in another 21% [143]. Extrapolating these findings, in 2001 researchers conducted a phase III trial enrolling 160 patients with meningioma demonstrating inconclusive results on the efficacy of MF [144]. Various other clinical trials involving MF follow similar paths. In advanced stage cancer patients with non-small cell lung cancer, thymic epithelial cell carcinoma, transitional cell carcinoma of the renal pelvis, leiomyosarcoma, colon adenocarcinoma, pancreatic adenocarcinoma, and malignant fibrous

histiocytoma; administration of 200-300mg of MF daily was shown to reduce or halt disease progression and improve overall symptoms [112, 145]. The reoccurring truths with every MF clinical trial are the limited cohort sizes, inconclusive findings regarding efficacy, and lack of mechanistic insights on how MF may be impacting tumor development.

4. Extracellular Vesicles

Extracellular vesicles (EV) are lipid bilayer nano-particles selectively loaded, secreted and targeted to recipient cells through different biogenesis pathways [146]. They are constitutively involved in homeostatic processes and recently have come under critical observation for their functionally significant influence on the growth and dissemination of cancer [147-152]. Release of EVs can be the result of a number of factors including host conditions, cellular communication and adaptation to environmental changes [153]. For example, T cells release exosomes (a subtype of EVs, see section 4.1) in response to T cell receptor activation [154]. In contrast, B cells or cancer cells can secrete exosomes in absence of receptor stimulation [153].

EV functions diverge greatly by biogenesis pathway, size, content, cell of origin and an entire host of factors still elusive to researchers [155, 156]. In face of a recipient cell they can initiate signaling through cell surface interactions, in which EV membrane lipids or surface proteins interact with cellular receptors directly. For example, dendritic cell secreted EVs have been shown to express MHC class I and II molecules on their surface in order to present antigens and activate T lymphocytes [157-159]. Direct interactions between EVs and cells are not a necessity to initiate signalling cascades. EVs can break down in the extracellular space and release their contents which in turn bind independently and activate receptors on recipient cells [147, 149, 155, 160-162]. Alternatively, EVs can become internalized through endocytosis or fuse with the plasma membrane ultimately releasing their contents intracellularly. In this manner EVs have been known, especially in cancer, to exchange proteins [163, 164], microRNA [165], double-stranded genomic DNA [166, 167], and even retrotransposon elements [168].

EVs are emerging as potential biomarkers in many malignancies due to their significant influence on the tumor microenvironment and immune system [148, 154, 166, 169, 170]. Importantly, EVs can be harnessed in liquid biopsies and isolated non-invasively from various bodily fluids [150, 171].

4.1 Extracellular Vesicle Emergence and Nomenclature

EVs were discovered as nanoparticles transporting cellular waste products from reticulocytes during the maturation process and misclassified as garbage collectors [172-174]. With technological advancements and nanoparticle tracking, it became apparent that EVs are essential for an entire host of homeostatic functions. Intercellular communication through EVs is implicated in the regulation of angiogenesis [175], immune signaling and responses [153, 176], crosstalk with the blood brain barrier [177], and regulation of skin homeostasis [178]. EVs are ubiquitous; the aforementioned functional responsibilities are far from exhaustive considering EVs are secreted by the majority of cells and involved in a multitude of signaling pathways.

The term extracellular vesicle encompasses a variety of nanoparticles diverging in biogenesis pathway, selective cargo, and functional intentions [146, 179, 180]. Two commonly utilized terms, microvesicle and exosome, classify EVs into subcategories based on differential surface marker expression and EV diameter [146, 155]. Exosomes range in size from 50-100nm in diameter and emerge from multivesicular bodies (MVB)[155]. MVBs are late endosomes which mature through the invagination of an endosomal limiting membrane creating intraluminal vesicles (ILVs). Subsequent to maturation, MVBs either fuse with the plasma membrane releasing ILVs as exosomes or fuse with lysosomes for degradation [181]. In contrast, microvesicles or ectosomes are loaded and released directly from the plasma membrane [155, 181, 182]. They were first reported in 1991 in neutrophils which were shedding vesicles by exocytosis [182]. Researchers have since defined microvesicles as 100-1000nm particles released by nearly any cell at significantly different secretion rates [155, 156, 181].

The EV community at times continues to follow older methods of classifying exosomes and microvesicles by surface markers, sedimentation rates, and size. Separating subclasses by any of the above means has proven to yield heterogeneous mixtures of exosomes and microvesicles [146, 147]. Contributing to this lack of purity: (1) reported subclass markers are rarely exclusive to exosomes or microvesicles, (2) subcategories overlap in size and sedimentation rates, (3) the cell of origin and extracellular conditions greatly influence EV subclass size and surface markers regardless of biogenesis pathway, and (4) isolation methods have considerable impact on EV yield and introduce biases for certain subclasses. With these inconsistencies it remains near impossible to ensure homogenous yields. In place, to classify a certain subtype one must confirm the biogenesis pathway of the EVs in question through live analysis [146, 147].

Before the International Society for Extracellular Vesicles (ISEV) set in place recommendations for proper EV standardization and reporting, EV subtypes were thought to be sufficiently purified by ultracentrifugation, with exosomes being preferentially pelleted at over 100,000*g* speeds and microvesicles at 10,000*g* [146, 153, 180]. There were flaws in this logic as researchers have found miniature microvesicles (40-100nm), confirmed through their direct budding from the membrane, to remain in the 100,000*g* pellet [183]. Further, heterogenous mixtures of non-EV particles (ex: low-density lipoproteins) can be pelleted with exosomes at 100,000*g*. When investigated, these lipoproteins were found to mimic plasma derived exosomes, skewing overall nanoparticle concentrations and downstream analyses [184]. Taken together, sedimentation speed and nanoparticle size alone cannot separate exosomes from microvesicles and poses a challenge of contamination from various extracellular factors [146, 150, 183, 184]. Therefore, according to the Minimal Information for Studies of Extracellular Vesicles (MISEV) 2018 guidelines, unless one can confirm a particular yield is solely of endosomal or plasma membrane origin authors should use the broader term of EV to classify their yield [146]. To reiterate, classification parameters are rarely mutually exclusive to an EV subtype and characteristic EV properties should be considered on an individualized basis by EV population obtained. However, the EV field continues to lack consensus on EV terms and traditional classification methods are still in wide use [146, 155].

4.2 Composition and Content

Through the biogenesis process, EVs adopt a lipid bilayer reflective of their cell of origin, comprising characteristic lipid patterns and harbouring distinctive surface proteins [151, 153]. The composition of an EV is a determinant of functional intentions, EV interactors and the mechanisms of communication with recipient cells [181, 185]. The lipidome of pure exosomal yields is enriched for cholesterol, sphingomyelin (SM), ceramide, and exposed phosphatidylserine (PS) [151, 153]. Phosphatidylserines on outer leaflets of EVs have demonstrated importance in vesicle docking, associated with recruitment of galectin 5 or annexin 5 [186-188]. Further, exposure of PS on the outer leaflet of oligodendrocyte EVs facilitates internalization by microglia cells [153, 189]. On an aside, lipid populations in an EV yield can hint at contamination; heightened levels of cardiolipin (CL) in EV yields suggests contamination with mitochondria as the inner mitochondrial membrane is enriched for CL [181].

It should be noted that lipid compositions can change drastically based on cellular origin, extracellular conditions and purification methods [146, 151, 153, 155]. Taken as example, adipocyte EVs have differential proportions of SM and PS in comparison to EVs derived from other cellular origins. Further depending on functional intention or extracellular stimuli, cells can secrete heterogenous populations of EVs. Small adipocyte derived EVs were found enriched for cholesterol while larger populations had abundant PS [190]. Skotland *et. al.* released two literature reviews on EV lipidomics incorporating an array of cell types and demonstrating an estimated 42.5% of the EV lipid membrane is cholesterol, 12.5% SM, 10.5% PS and 5.2% phosphatidylinositol (PI) [181].

The proteomic content of EVs are as heterogenous as the exterior lipidome, however there remains a relatively conserved set of EV specific markers associated with and integral to EV biogenesis pathways [149]. Included are surface tetraspanins (CD63, CD81, CD82), tumor susceptibility gene 101 (TSG 101), caveolins, and heat shock proteins. An exhaustive list of EV associated markers was compiled by ISEV and reviewed in Thery C. *et al.* [146]. The remaining proteomic composition of an EV is contingent on physiological conditions, cellular origin, intentions, extra- and intra-cellular stimuli, and diseased states [149, 191].

To initiate the process of EV-dependent intercellular communication, an EV must identify cellular targets, dock, activate host surface receptors, become internalized or fuse with the plasma membrane directly [149]. The process is multifactorial and requires a selective composition. Presence of integrins is an integral component on the surface of certain EVs to interact with intercellular adhesion molecules (ICAMs) of recipient dendritic cells [186]. EV integrins have further been reported to interact with extracellular matrix proteins such as fibronectin and laminin which further aid in the targeting and docking to recipient cells [149, 192]. Other important players for EV interactions include heparan sulfate proteoglycans such as Glypican 1, associated with pancreatic cancer EVs [193].

Identification of selective compositional patterns can predict specific targeting of an EV to a recipient cell. Exosomes enriched with CD63 indiscriminately interact with multiple brain cell subtypes, while in absence of CD63 and presence of amyloid precursor protein cargo they demonstrate a tendency to be selectively internalized by neurons [194]. Expression of CD47 by EVs seems to confer a protection and resist monocyte internalization [160]. To conclude the current thought, EVs are highly heterogeneous entities with a multitude of surface expression

markers that either facilitate their internalization or impede it and help target them to specific cells of interest [149, 160, 193-196].

4.3 Considerations for EV Isolation

Though the EV research scene is thriving, little consensus exists surrounding optimal isolation techniques. Current procedures rely on differential particle size, surface markers, density, and distinct morphological features. Techniques include differential ultracentrifugation, ultrafiltration, density gradient centrifugation, precipitation, size exclusion chromatography (SEC) and immunoaffinity-based capture [197, 198].

Over the past decade comprehensive isolation methods which produce relatively pure and reproducible EV yields have remained elusive [179, 180]. Complications arise in the accuracy and purity of EV yields as isolation methods are dependent on variables which overlap between EV subclasses (size, density, morphology and molecular markers) [146, 179]. Slight variations in method or within a protocol leads to enrichment of certain EV subtypes and cargo, hindering reproducibility and large meta-analyses [146, 179, 180]. Contaminants can further complicate the issue, as blood microparticles and protein aggregates co-isolate with EVs under specific experimental conditions especially when handling patient biofluids [199].

A crowdsourcing database of EV methodologies, EV-TRACK, revealed widespread heterogenicity in isolation procedures amongst EV publications. Differential ultracentrifugation which relies on sedimentation coefficients of particles was the conventional method employed in 45% of reports [179]. The generalized framework includes a series of centrifugation steps with centrifugal speeds in range of 500*g* for removal of larger particulate matter to final spins at 100,000*g* to pellet EVs [197]. A large proportion of these publications reported variations in *g*-forces, rotors and duration of ultracentrifugation [179].

The selection of a rotor during ultracentrifugation has a significant influence on EV cargo yield. Rotors have dissimilar sedimentation path lengthens which when interchanged create discrepancies in pelleting efficiency. Taking into consideration the rotor type is imperative when pelleting subclasses of EVs and standardizing a protocol. For instance, swinging bucket rotors are ideal for particles of similar densities while fixed angle rotors are ideal for particles with larger disparity in size and shortened protocols. However, 72% of EV publications fail to report the type of rotor which impedes standardization of acquired data as rotor type has been demonstrated to

significantly impact protein and RNA yield [179, 180]. Further, the *g*-force of a given protocol can skew data analysis as higher *g*-forces compact EVs into aggregates of heterogenous morphologies and phenotypes [200].

Standardized isolation techniques are critical for comparison and assay reproducibility. Regardless of cell type or medium in which EVs are contained, it is imperative to have consistency in isolation protocols when pelleting EVs. These inconsistencies in the quantity and purity of isolated materials makes it difficult to make comparisons between proteomic or nucleic acid compositions of EVs from different cancer types, mediums and even within the same conditions [146, 179, 180].

When attempting to isolate EVs, considerations must include a desired experimental endpoint, with tailored consistency in sample collection and method processing. Each EV isolation technique presents benefits and pitfalls which depend on the EV subclass of interest and downstream analyses. Briefly, immunoaffinity capture methods are excellent to acquire pure EVs with specific markers of interest; however, in this process the heterogenicity of an EV population is erased. While purification of a marker specific subclass of EVs could prove beneficial, this could likewise hinder discovery of EVs essential to a system of interest [201, 202]. Similarly, SEC and precipitation both reduce contamination in comparison to ultracentrifugation; however, they introduce other limitations. The precipitants are at times toxic to the EV yield disrupting their subsequent biological functionality [201], and the method in itself can result in structural and compositional alterations [203]. SEC techniques have their merits, namely in the removal of plasma contaminates [203] and in conjunction with ultrafiltration can result in a 58-fold increase in EV recovery compared with ultracentrifugation [204].

4.4 Extracellular Vesicles in Cancer

Subsequent to selective cellular targeting, EVs deliver their respective cargo or stimuli to recipient cells with diverse functional implications. In cancer, malignant cells are thought to adapt the biogenesis pathway to exploit EVs and transfer oncogenic messages systemically. Initially, Abdouh *et al.* demonstrated the ability of metastatic cancer patient sera to contain factors which provoked the malignant transformation of BRCA1-knockout fibroblasts *in vitro* [205]. Beginning to elucidate the culprits present in patient sera, the group discovered that treatment of fibroblasts with pure cancer patient derived EVs was sufficient to form carcinomas in a mouse model.

Intriguingly, histological analysis determined the developing lesions differentiated into carcinomas which mirrored that of the donor patient [169]. Evidence confirming the malignant potential of EVs is abundant. In colorectal cancer, EVs have been implicated in oncogenesis, immune evasion, metastasis and angiogenesis through their specific loaded cargo [162, 206]. Cancer-derived EVs from breast, pancreatic, glioblastoma, melanoma and numerous additional tumors have been implicated in metastasis and preparation of a pre-metastatic niche [162, 169, 207-209].

Shifting focus from the tumorigenic functions of EVs, researchers are investigating the biomarker potential of EV cargo. In contrast to vulnerable circulating tumor DNA, EV bilayers serve as a protective barrier impeding degradation by circulating DNases. As consequence large double-stranded DNA fragments (>10kb) have been detected in EVs and remain relatively stable over extended periods [167, 210]. A direct instance is the presence of mutated KRAS and p53 DNA in pancreatic cancer serum derived EVs [167]. In lung adenocarcinoma, EVs in patient pleural effusions contained characteristic mutated epidermal growth factor receptor (EGFR) DNA which was detectable with 100% sensitivity when compared to corresponding patient tissue [211].

This lends to promising potential for EVs as biomarkers in the detection and monitoring of UM. Under the scope of ctDNA, our group has validated a method of detection for driver mutations (*GNAQ, GNA11, PLCβ4* and *CYSTLR2*) in UM patient blood samples (liquid biopsy). Further, the presence and levels of ctDNA were found to correlate with UM malignancy and in a rabbit model predicted tumor growth before discernible lesions presented [69]. However, whether characteristic oncogenic DNA is present in UM-EVs has not been proven and is under investigation in our laboratory.

In UM, few studies have investigated the role of EVs as biomarkers and mediators of disease. Eldh *et al.* isolated EVs from liver perfusates of metastatic UM patients and demonstrated an elevation in total EVs present in peripheral blood compared to controls. Characterization of patient EV miRNA profiles found substantial overlap across the patient cohort suggesting UM specific miRNA patterns may be present in EVs [212]. Another UM study with focus on EV miRNA profiles provided a comparison of vitreal humor and patient serum with vitreal and serum derived EVs. The vitreal humor miRNA profile demonstrated a 90% overlap with that of vitreal EVs, indicating the majority of miRNAs detected in vitreous humor are encapsulated in EVs. Specific miRNAs such as miR-146a were identified as enriched across all UM samples, while

other miRNAs were specific to vitreous humor and vitreal EVs. Formalin-fixed, paraffin-embedded UM samples validated the upregulation of certain EV miRNAs suggesting EV miRNA profiles mirror that of the original tumor [213].

Of perhaps equal importance, the EV proteome has demonstrated biomarker potential and functional relevance in metastatic progression [98, 99, 152, 207]. In colon cancer cell line derived EVs, researchers comment tetraspanin 1 (TSPAN1) may be a future protein biomarker [163]. While in breast cancer, differential EV proteomes seem to correspond with specific molecular subtypes, hinting at the potential for non-invasive EV-based molecular subtyping [164].

In UM, a single paper investigated the glycosylation patterns and protein cargo in ectosomes released from a human UM cell line (Mel 202). Proteomic content was associated with cancer and metastasis related pathways: including proliferation, metabolism, invasion, and drug resistance. Differential glycosylation patterns were observed when comparing ectosomes to cellular membranes, supporting the theory that ectosomes are selectively formed, loaded and secreted [214]. Aside from this study, there continues to lack a comprehensive investigation into the proteomic content of EVs in UM.

Short of summarizing the immense log of tumorigenic cargo found associated with cancer derived EVs, it would suffice to conclude these cargo hold promising diagnostic and therapeutic applications [163, 167, 169, 170, 207, 209, 215]. With each characterization of EV cargo, researchers further elucidate tumor biology and the functional significance of EVs in metastasis [165, 166, 169, 189, 207]. While extrapolations using data on other cancer types can be made, EVs in UM have not been extensively characterized. Therefore, further investigating UM-EVs would provide insight into how UM may be communicating systemically and metastasizing.

Research Aims and Relevance

While rare, UM displays an alarming ability to spread throughout the body in almost half of all patients. Consequences of our current gaps in knowledge surrounding UM progression becomes a burden to individual patients. Upon detection, UM metastases are often too far progressed and systemic treatments fail to adequately control the disease. Extrapolating targeted therapies in CM to UM has not proven sufficient, as they often target genetic and molecular burdens not seen in UM.

Part 1.

To contribute to current data on potential adjuvant treatment options in UM, our group investigated the efficacy of the potent anti-cancer growth inhibitor MF. Cancer hallmarks and metastatic progression flow through the theory of tumor cell detachment, dissemination and seeding. MF has proven its effectiveness to alter known metastatic phenotypes and inhibit tumor growth. As UM is often not included in studies testing new drugs, we aimed to add UM to the cohort of cancers already tested with MF. In the manuscript presented in Chapter 2 we investigate the effects of MF on a panel of human UM cell lines and demonstrate its potential against this disease. Further we determine the feasibility of liquid biopsy based techniques to monitor response of UM cells to MF treatment as this may be the future in patient care.

Specific subaims included in the manuscript:

1. Dose-dependent effects of MF on cellular proliferation and viability in a panel of primary and metastatic human UM cells
2. Morphological alterations and recovery capability of UM cells under MF treatment
3. Mechanisms of cytotoxicity
4. Presence of classical and/or non-classical progesterone and glucocorticoid receptors in UM cells

Due to the aggressive nature of UM and the potency of MF on a range of aggressive cancer types regardless of hormone receptor expression, we hypothesize these *in vitro* assays will demonstrate the ability of MF to influence the growth and viability of UM. Parallel to various cancer types, we suspect MF may act through cell cycle arrest and result in cytotoxicity at higher

concentrations. The study design involved a varied panel of cell lines which represent UM disease in terms of behaviour, morphology and genetic characteristics (Table 1).

Table 1 : Mutational status of UM cell lines

Cell lines	Mutation status	Primary/Metastatic
MP41	GNA11 (Q209L) c.626 A>T	Primary
MP46	GNAQ (Q209L) c.626 A>T	Primary
92.1	GNAQ (Q209L) c.626 A>T	Primary
MEL270	GNAQ (Q209P) c.626 A>C	Primary
OMM2.5	GNAQ (Q209) c.626A>C	Liver metastasis

Part 2.

While targeting the primary and secondary lesions with MF can prove promising and may allow clinicians to focus in on impeding the hallmarks of cancer, other factors contribute to metastasis. These include the adjacent normal cells (lymphocytes, macrophages, cancer associated fibroblasts), the microenvironment, communication with distant tissues and systemic inflammation and signaling. EVs have long been established as potential mediators of tumor metastasis. Our group is attempting to link this alternative theory to UM metastasis in a hope to further understand disease progression. Chapter 3 focuses on elucidating the proteomic composition of EVs extracted from human UM cell lines to determine how EVs may influence metastasis in UM.

Specific subaims included in the manuscript are:

1. Determining the transforming potential of UM-derived EVs on recipient cells *in vitro* and *in vivo*
2. Characterizing the differential proteomic cargo of UM-derived EVs in comparison to normal choroidal melanocyte EVs isolated from patient donor eyes
3. Datamining to cluster proteomic profiles by gene ontology and pathway mapping to identify individual proteins and classes of putative biomarkers of UM progression and metastasis

Following previous research on the role of EVs in the process of metastasis, we speculate that UM cells secrete EVs capable of mediating tumor-microenvironment communication through

recipient cells. Investigating the oncogenic potential *in vitro* on recipient cells and *in vivo* will provide additional confirmation of UM-EVs as possible mediators of metastasis. This study adheres to the MISEV 2018 guidelines for EV characterization and seeks to begin a discussion on the proteomic profile of UM-derived EVs to address the lack of knowledge surrounding metastasis of this disease.

Both sets of data in Chapter 2 and 3 also demonstrate the role of liquid biopsies in monitoring treatment response and as a source of potential biomarkers. This is especially important in UM, where intraocular biopsies and resections are not commonly performed for diagnosis.

Chapter 2:

This chapter is based on a published manuscript in Cancer Cell International

Alvarez PB, Laskaris A, Goyeneche AA, Chen Y, Telleria CM, Burnier JV. Anticancer effects of mifepristone on human uveal melanoma cells. Cancer Cell Int. 2021 Nov 17;21(1):607. doi: 10.1186/s12935-021-02306-y. PMID: 34789240; PMCID: PMC8597220.

Introduction and Rationale:

The cytostatic and cytotoxic effects of MF influence metastatic phenotypes *in vitro* and *in vivo* in various cancer types in hormone responsive and non-responsive settings. Before now, no study had investigated the potency of MF in the context of UM. We sought to broaden the range of cancer types investigated for the application of MF as an anti-cancer drug. In this chapter we investigated whether MF had a dose-dependent influence on UM cell line growth, cell cycle, and viability with subsequent exploration of possible mechanisms of cell death. We wished to expand our current repertoire of possible therapies for treatment of UM. In future, MF, an already approved drug with a safe profile could become repurposed in cancer medicine as an adjuvant therapy.

Anticancer effects of mifepristone on human uveal melanoma cells

Alexander Laskaris[1,2]*, Prisca Bustamante Alvarez[1,2]*, Alicia A. Goyeneche[1,2], Yunxi Chen[1,2], Carlos M. Telleria[1,2]**† and Julia V. Burnier[1,2,3]**†

[1]Experimental Pathology Unit, Department of Pathology, McGill University, Montreal, QC, Canada

[2]Cancer Research Program, Research Institute of the McGill University Health Centre, Montreal, QC, Canada

[3]Gerald Bronfman Department of Oncology, McGill University, Montreal, QC, Canada

†Correspondence to:

Julia Burnier; Email: julia.burnier@mcgill.ca; or Carlos Telleria; Email carlos.telleria@mcgill.ca

*These authors equally contributed to this work.

**These authors share senior co-authorship.

Abstract

Background: Uveal melanoma (UM), the most prevalent intraocular tumor in adults, is a highly metastatic and drug resistant lesion. Recent studies have demonstrated cytotoxic and anti-metastatic effects of the antiprogestin and antiglucocorticoid mifepristone (MF) in vitro and in clinical trials involving meningioma, colon, breast, and ovarian cancers. Drug repurposing is a cost-effective approach to bring approved drugs with good safety profiles to the clinic. This current study assessed the cytotoxic effects of MF in human UM cell lines of different genetic backgrounds.

Methods: The effects of incremental concentrations of MF (0, 5, 10, 20, or 40 μM) on a panel of human UM primary (MEL270, 92.1, MP41, and MP46) and metastatic (OMM2.5) cells were evaluated. Cells were incubated with MF for up to 72 hours before subsequent assays were conducted. Cellular functionality and viability were assessed by Cell Counting Kit-8, trypan blue exclusion assay, and quantitative label-free IncuCyte live-cell analysis. Cell death was analyzed by binding of Annexin V-FITC and/or PI, caspase-3/7 activity, and DNA fragmentation. Additionally, the release of cell-free DNA was assessed by droplet digital PCR, while the expression of progesterone and glucocorticoid receptors was determined by quantitative real-time reverse transcriptase PCR.

Results: MF treatment reduced cellular proliferation and viability of all UM cell lines studied in a concentration-dependent manner. A reduction in cell growth was observed at lower concentrations of MF, with evidence of cell death at higher concentrations. A significant increase in Annexin V-FITC and PI double positive cells, caspase-3/7 activity, DNA fragmentation, and cell-free DNA release suggests potent cytotoxicity of MF. None of the tested human UM cells expressed the classical progesterone receptor in the absence or presence of MF treatment, suggesting a mechanism independent of the modulation of the cognate nuclear progesterone receptor. In turn, all cells expressed non-classical progesterone receptors and the glucocorticoid receptor.

Conclusion: This study demonstrates that MF impedes the proliferation of UM cells in a concentration-dependent manner. We report that MF treatment at lower concentrations results in cell growth arrest, while increasing the concentration leads to lethality. MF, which has a good safety profile, could be a reliable adjuvant of a repurposing therapy against UM.

Keywords: Uveal melanoma, mifepristone, drug repurposing, cancer therapy

Background

Melanomas are predominantly of cutaneous or ocular origin [1, 2] and present a host of distinct clinical challenges in relation to detection, treatment, and metastasis [3-5]. Ocular melanomas remain a diagnostic burden to oncologists as upwards of 83% arise in the vascular portion of the inner eye or uvea [1]. Uveal melanomas (UM) predominate in an inaccessible region, the choroid, growing undetected and often becoming highly metastatic [6, 7]. Despite effective local treatment, including plaque brachytherapy or enucleation [5, 8], up to 50% of patients develop metastases during the course of their lifetime [7, 9, 10]. Metastatic lesions emerge in the liver (89%), lung (29%), and bone (17%), and overall survival decreases below 20% within the first 2 years [9, 11-13].

To date, metastatic UM patients enter an abyss where a shallow understanding of their disease compounds the minimal efficacy of systemic treatment regimens. Clinically approved therapies in metastatic cutaneous melanoma, if applied to UM, have suboptimal or inconclusive results [3, 14]. For instance, checkpoint inhibitor (PD-1/ PD-L1 or CTLA-4) immunotherapies are emerging as a promising treatment in cutaneous melanoma; ipilimumab, an effective CTLA-4 inhibitor, has been FDA approved as treatment in metastatic cutaneous melanoma, yet it has dismal success rates of 0-5% in UM (reviewed in [14]). This can be attributed in part to the divergent biology, mutational profile and localization of cutaneous melanoma and UM metastases [11, 15, 16]. While metastatic disease in cutaneous melanoma follows through lymphatics, in UM disease, given the lack of lymphatics in the eye, metastasis occurs hematogenously, mainly in the liver (reviewed in [15]).

Unfortunately, liver metastases continue to be a challenge, resisting systemic therapies and reoccurring at unfavorable rates [11, 15]. Systemic combination chemotherapy regimens remain the gold standard for treatment of liver metastases; however, response rates are poor and dependent on individual patient variability [11, 15]. A 30-year study of 661 metastatic UM patients reported a 3-year survival rate of only 2.9% in patients with liver localized lesions compared to 19.8% in patients with extrahepatic metastasis. Dominant treatments were chemotherapy (50%), or combination of treatment modalities (34%), improving median survival from 1.7 months in absence of intervention to 6.3 months [11]. While preventative adjuvant therapies have shown little promise due to a combined lack of research, there is an unclear understanding of metastatic risk, and insufficient evidence that any one therapy can improve patient survival [15, 17, 18]. In

short, the UM community of clinicians and researchers lack effective methods to mitigate the propagation of metastatic UM.

Mifepristone (MF) has drawn attention as a potential cancer treatment as its potent cytotoxic effects have been demonstrated to disrupt the growth of several cancer cell types [19-21]. MF was originally synthesized in the 1980's as an antiglucocorticoid agent, yet due to its unexpected potent antiprogesterone activity, it was rapidly repurposed to the field of reproductive medicine for early termination of pregnancy, emergency contraception, and menstrual cycle regulation [22-25]. MF was further recognized for its ability to inhibit cell growth in endometriosis, uterine fibroids, and benign cases of meningioma; in cancer, MF demonstrated antiproliferative effects toward cells of cervical, breast, endometrial, ovarian, gastric, lung, brain, and prostate origin (reviewed in [26, 27]). These initial conclusions on MF's anti-cancer effects were in the context of hormone sensitive tumors, however our group has proven its effectiveness regardless of progesterone, androgen, and estrogen receptor expression [28]. Moreover, we have shown that MF-induced growth inhibition is associated with blockage of the cell cycle and inhibition of DNA synthesis [20, 21]. The influence on cell proliferation is independent of the level of chemosensitivity or genetic background of the cancer cells [29, 30]. As a growth inhibitor, we have also shown that MF prevents the repopulation of cells that escape the lethality of chemotherapeutic agents such as cisplatin or paclitaxel [30-32].

In the present work, we evaluated the effect of MF on UM cells to establish whether the repurposing of this safe drug can become an effective adjuvant therapy for the treatment of UM. The anti-growth effect of MF was evaluated against a panel of human UM cells of different phenotypic origins and genetic backgrounds. We demonstrate that MF impairs the functionality, growth capacity, and viability of UM cells in a concentration-related manner. Lethal concentrations were associated with induction of caspase-3/7-related apoptosis and release of cell-free DNA. Further, we prove that the potency of MF observed in UM is unrelated to the expression of cognate progesterone receptors.

Materials and methods

Cell lines, culture conditions, and treatments

Primary human uveal melanoma cell lines MP41 and MP46 were acquired from the American Type Culture Collection (ATCC, Manassas, VA, USA). Primary MEL270 and metastatic

OMM2.5 cell lines were kindly gifted by Dr. Vanessa Morales (University of Tennessee). Primary UM cells 92.1 were kindly gifted from Dr. Martine Jager [33]. MCF-7 breast cancer cells utilized as a positive control for classical progesterone receptor expression were obtained from ATCC. All previous cell lines were cultured in Roswell Park Memorial Institute media (RPMI 1640, Corning, Corning, NY, USA). Media was supplemented with 2 mM L-Alanyl-L-Glutamine (Glutagro, Corning), 100 U/ml penicillin and 100 µg/ml streptomycin (Corning), 10 mM HEPES (Corning), 10 µg/ml insulin (Roche, Basel, Switzerland), 1 mM sodium pyruvate (Corning), and 10% fetal bovine serum (FBS, Corning). Cells were kept at 37ºC and 5% CO_2 in a humidified incubator. Cell lines were authenticated by Short Tandem Repeat (University of Arizona Genetic Core).

Wild type choroidal melanocytes (wtCM) were isolated from donor eyes following a previously established protocol [34]; mutant CM (mutCM) carrying a point mutation [GNAQ(Q209L)] were generated from wtCM by viral transduction using plasmids psd44-GqQL, pMD2.G, and psPAX2 (Addgene, Watertown, MA, USA); the mutation reduces GTPase activity resulting in a constitutively active phenotype. Both wtCM and mutCM were cultured in serum-free melanocyte growth medium M2 (PromoCell, Heidelberg, Germany). Human eyes were used in accordance with the McGill University Health Centre (MUHC) Research Ethics Board (2019-5314).

Mifepristone (MF; Corcept Therapeutics, Menlo Park, CA, USA) was dissolved in dimethyl sulfoxide (DMSO) to generate a 40 mM stock solution that was stored at -20 ºC. Prior to each experiment, the drug was thawed and freshly prepared in media to reach a final concentration of 5, 10, 20, or 40 µM. The final concentration of DMSO (Corning) in the media was 0.1% and served as vehicle control in the absence of MF.

Cellular confluence

Cellular morphology and magnitude of confluence were assessed in real time using the Incucyte® S3 Live-Cell Analysis System (Sartorius, Ann Arbor, MI, USA). Cells were seeded in 12-well plates (Corning) at 8 x 10^4 cells per well for 24 h. Thereafter, cells were treated with 5, 10, 20, or 40 µM MF and placed in the Incucyte® System. The software was adjusted to take 9 images per well every 6 h over the 72-h period of treatment. The Incucyte® System phase contrast software provided an average percent confluence for each well. Cell proliferation is quantified by counting

the number of phase objects overtime. Occupied area (% of confluence) represents cells imaged over time.

Cellular functionality

1.5 x 10^4 cells per well were seeded in a 96-well plate (Corning) 24 h prior to treatment. Cells were kept under 5, 10, 20, or 40 μM MF treatment for 72 h. 10 μl of cell counting kit 8 solution (CCK8, Dojindo Molecular Technologies, Kumamoto, Japan) was added. After 1 h of incubation at 37 ºC and 5% CO_2, absorbance was read at 450 nm using an Infinite M200 Pro plate reader (Tecan Trading AG, Männedorf, Switzerland). Cells with no treatment were used as a negative control. Media and CCK8 solution in the absence of cells were used as a blank control. Percentage of metabolic activity was calculated according to the following equation: sample - blank / negative control - blank x 100.

Trypan blue exclusion test

2 x 10^5 cells per well were seeded in a 6-well plate (Corning) 24 h prior to treatment. Cells were then exposed for 72 h to 5, 10, 20, or 40 μM MF. Thereafter, the cells were dissociated by enzymatic solution (0.05% trypsin, Corning), and 10 μl of cell suspension were mixed with 10 μl of 0.4 % trypan blue solution (Corning). The number of dead and live cells was measured using a TC20 automated cell counter (Bio-Rad Laboratories, Hercules, CA, USA).

Recovery assay

Cells were seeded at a density of 9 x 10^4 cells per well in a 12-well plate (Corning), and treated with varying concentrations of MF (0, 20, or 30 μM). Throughout the 72-h treatment period, cells were imaged every 6 h using the Incucyte® S3 Live-Cell Analysis System at 4x magnification. Following the initial 72 h of treatment, media was aspirated, and fresh media lacking MF was added to all wells. Cells were then imaged for a subsequent period of 72 h to assess their recovery capacity. Images obtained were then analyzed by the Incucyte® S3 Live-Cell Analysis software, and cellular confluence data was exported for further quantitative analysis.

Cell cycle analysis

After MF treatment, single cell suspensions were fixed with 4% paraformaldehyde (PFA) at room temperature for 1 h. Suspensions were centrifuged at 300 *g* for 5 min and pelleted cells were washed twice with phosphate-buffered saline (PBS). A suspension containing 2 x 10^5 cells were re-pelleted and resuspended in 0.2 ml of propidium iodide (PI) solution containing 7 U/ml RNase A, 0.05 mg/ml PI, 0.1 % v/v Triton X-100, and 3.8 mM sodium citrate (Sigma Chemical Co., St. Louis, MO, USA) for 20 min at room temperature or overnight at 4 °C protected from light. Cells were analyzed with the Guava Muse Cell Analyzer (Luminex Corporation, Austin, TX, USA), that takes advantage of the capacity of PI to stain DNA allowing detecting different DNA contents along the cell cycle. The cell cycle application of the Muse software was used to analyze the results and to determine relative stages of the cell cycle.

Flow cytometric assessment of cell death

Early apoptosis and late apoptosis as well as necrosis were evaluated using the Dead Cell Apoptosis Kit with Annexin V-Fluorescein isothiocyanate (FITC) and PI, for flow cytometry double labelling (Thermo Fisher Scientific, Waltham, MA, USA) following the manufacturer's instructions, and then analyzed in a BD FACSCanto II Cell Analyzer (BD, Evembodegem, Belgium). Cells staining with Annexin V-FITC without PI were considered early apoptotic, cells with double staining were considered late apoptotic, whereas cells that incorporated only PI were considered necrotic.

DNA fragmentation

In a 100-mm dish, 1 x 10^6 cells were seeded and cultured for 24 h, and then treated with MF for 72 h. Genomic DNA (gDNA) was isolated following a previous described protocol [35]. gDNA was separated in 2% agarose gels, stained with SYBR Gold nuclei acid stain (Thermo Fisher), and visualized in a ChemiDoc MP (Bio-Rad Laboratories).

Caspase-3/7 activity

Cells were plated in a 96-well plate at 2 x 10^3 cells per well and incubated for 24 h to allow attachment. MF treatment was added in a 1 X medium containing Essen Bioscience Incucyte® Caspase-3/7 activity reagent (Sartorius, Ann Arbor, MI, USA). The caspase-3/7 dye crosses the cell membrane and is specifically recognized and cleaved by activated caspase-3/7 resulting in the

release of a dye that binds to DNA and fluoresces green. The 96-well plate was placed in the Incucyte® Live-Cell analysis system for live cell imaging for 72 h. Images from the scan interval were analyzed in the IC Incucyte® software.

Cell free DNA detection

Cell-free DNA (cfDNA) was detected using a known mutation in the UM cell lines. First, 3 x 10^5 cells were seeded in a 6-well plate. Following 72 h of MF treatment at concentrations of 5, 10, 20, or 40 μM, 3 ml of culture supernatant was collected and spun at 300 *g* for 5 min. cfDNA was isolated using the QIAamp Circulating Nucleic Acid kit (QIAGEN, Hilden, Germany) following the urine protocol. cfDNA was kept in AVE buffer (RNase-free water with 0.04 % sodium azide; QIAGEN), and quantified by a fluorometric method using a Qubit 4 (Thermo Fisher). Droplet digital PCR (ddPCR) (Bio-Rad Laboratories) was performed to measure the number of copies of cfDNA using wild type sequences and hotspot mutations GNAQ (Q209L and Q209P) and GNA11 (Q209L) by following a previously reported protocol [36]. No template control was added in each assay. Individual runs were performed in triplicates.

Quantitative real-time reverse transcriptase (qPCR)

Gene expressions of progesterone receptor (PR), progestin and adipoQ receptor family member 8 (PAQR8), membrane-associated progesterone receptor component 1 (PGRMC1), and component 2 (PGRMC2), the glucocorticoid receptor: receptor subfamily 3 group C member 1 (NR3C1), and β-Actin (as a reference gene) were quantified using SybrGreen-based Real Time PCR in a CFX96 Touch Real Time PCR detection system (Bio-Rad Laboratories). qPCR reactions were conducted in 20 μl volume for 40 cycles at 61°C annealing temperature using SsoAdvanced Universal SYBR Green supermix (Bio-Rad Laboratories) and primers (ID Technologies, Coralville, IA, USA). RNA was extracted using the RNeasy Plus Micro kit (QIAGEN). Complementary DNA (cDNA) was synthetized using iScript (Bio-Rad Laboratories). The MCF-7 cell line was used as a positive control for the expression of classical progesterone receptor mRNA. No template control and no reverse transcriptase control were added in each assay. Individual runs were performed in triplicates. Data was analyzed using CFX Maestro Software (Bio-Rad Laboratories).

Statistical analysis

Experiments were conducted at least three times in biological and technical replicates for each cell line. Results are expressed as the mean ± SD. Graphpad Prism 9 (Graphpad Software, La Jolla, CA, USA) allowed for statistical analysis of data using repeated measures two-way ANOVA followed by Tuckey's multiple comparison test, two-way ANOVA followed by Dunnett's multiple comparison test, or Student's *t*-test depending on the experiment. Differences were significant if $p<0.05$.

Results

Mifepristone inhibits functionality, growth capacity, and viability of human primary and metastatic UM cell lines in a concentration-related manner

To determine whether MF treatment influences the functionality and viability of UM in vitro, a range of human primary UM cell lines (MP46, 92.1, MP41, MEL270) and a metastatic UM line (OMM2.5) were investigated. Cells were treated with increasing concentrations of MF (0, 5, 10, 20, or 40 μM), and incubated over a period of 72 h. A colorimetric assay, in which reduction of water-soluble tetrazolium salt (WST-8) produces orange formazan, was utilized as a means to determine metabolic activity of UM cells upon MF treatment. A concentration-dependent decrease in cellular dehydrogenase activity was observed for all UM cell lines (Fig.1A). For concentrations of 5 to 40 μM of MF, UM cell lines all demonstrated reduction in functionality and significant cytotoxicity at 40 μM. To quantify the live cells in each sample and investigate late-stage cell death through disturbances in membrane permeability, a trypan blue exclusion assay was conducted. Concentrations of 5, 10 or 20 μM of MF resulted in no decrease in cellular viability except in MP46 cells that showed statistical significant reduction in viability upon incubation with 20 μM MF; 40 μM concentrations of MF caused a significant reduction in live cell count in all UM lines tested (Fig.1B). To determine how MF affects population doubling of UM cell lines, cells were treated and imaged at 6-h intervals in the Incucyte live cell-imaging incubator over 72 h. We report a concentration-related reduction in cellular confluence across all UM cells (Fig.1C). A significant deviation in cellular confluence was noted at 10 μM MF for MP41 cells only; 20 μM and 40 μM MF reduced confluence in MP41 as well as MEL270, 92.1, OMM2.5 and MP46 cells. A concentration of 40 μM had the strongest effect showing plateauing of the growth curves. As a visual example of the effect of MF we present in Fig.S1 how increased concentrations of MF cause a decrease in the confluence of MP41 cells when using label free-phase masking quantification;

the toxicity of MF is also revealed in the rounding and detachment of cells with the highest concentration of the drug. Wild type primary choroidal melanocytes (wtCM) isolated from donor eyes were used as control cells to estimate effects of MF on potential adjacent normal tissue. These wtCM display a steady confluence over time, which was not affected by concentrations of MF up to 20 μM (Fig.S2A). When however the CM carry a point mutation [GNAQ(Q209L)] (mutCM), the cells acquired growth advantage reflected in their slight yet consistent increased confluence over time of incubation when compared to wtCM; in this case 20 μM MF did inhibit such sustained yet slow growth (Fig.S2B).

High concentrations of mifepristone cause permanent impairment in the proliferative abilities of UM cells

To assess whether MF treatment has a long-term impact on cellular proliferation, we performed a recovery assay. Following treatment with 20 or 30 μM MF for 72 h, drug-supplemented media was replaced with regular growth media and cells were left to grow for another 72 h. All UM-cell growth curves significantly deviated from control, plateaued, or declined at concentrations of 20 or 30 μM during the initial 72 h period of incubation. Once MF treatment was withdrawn at 72 h, cells either were able to partially, or totally repopulate the culture regaining confluence. In contrast, the confluence of cell populations treated with 30 μM MF did not recover regardless of the cell line studied (Fig.2).

Mifepristone at higher concentrations triggers accumulation of hypo-diploid DNA content, fragmented DNA, and of cells undergoing apoptosis

To determine the extent to which MF causes cytotoxicity, we quantified the particles with hypo-diploid DNA content, which coincides with DNA located in the Sub-G1 region of the cell cycle histograms. No rise in hypo-diploid DNA content was observed in cells treated with MF at concentrations ranging from 5 to 20 μM (data not shown). In contrast, a large increase in hypo-diploid DNA content was observed in all UM cell lines treated with 40 μM MF (Fig.3A). When gDNA isolated from 40 μM MF-treated cells were run in agarose gels, we observed that the DNA shows fractionation typical of cells that are undergoing apoptotic cell death (Fig.3B). In Fig.S3 we clearly observe how the Sub-G1 region of the cell cycle histogram increases with the concentration of 40 μM MF, in all UM cell lines, when compared to the histograms displayed by cells receiving

vehicle or 20 μM MF; of interest, the latter have a tendency of accumulating cells in the G1 phase of the cell cycle, yet without reaching statistical significance.

To further examine whether gDNA fragmentation and hypo-diploid DNA content accumulated in response to lethal concentrations of MF involves an apoptotic process, we incubated all UM cell lines with vehicle, 20 or 40 μM MF, and subjected them to double labeling with Annexin V-FITC conjugate and propidium iodide (PI). Fig.4A depicts the flow cytometric histograms of each one of the UM cell lines treated with vehicle or MF. Fig.4B shows the quantification of early apoptosis denoted by cells binding only Annexin V-FITC; Fig.4D shows that only two cell lines, 92.1 and MEL270, display some level of necrosis as denoted by the cells binding PI.

Lethal concentrations of mifepristone activate executer caspase-3/7

To assess whether apoptosis induced by lethal concentrations of MF in UM cells involves activation of executer caspases, we studied the activation of caspases 3 and 7 following 72 h of treatment with either vehicle or 40 μM MF by using the Essen Bioscience Incucyte® Caspase-3/7 activity reagent. Caspase-3/7 activities were found highly increased by the lethal concentrations of MF in all UM cell lines studied (Fig.5A, B), as well as in wtCM and mutCM (Fig.S4). The green fluorescence cellular content denoting caspase-3/7 activation in all cell lines shown in Fig.5 can also be observed overlaid with phase contrast imaging (Fig.S5).

Mifepristone treatment induces the release of cell-free DNA into the culture media

Various studies have shown cell-free DNA (cfDNA) to be released from cells undergoing cell death [37]. We have previously shown the ability to utilize driver mutations in UM (GNAQ and GNA11 c626A>T and A>C) to detect and monitor circulating tumor DNA (ctDNA) in UM cell lines following drug treatment [36]. Here, we evaluated the release of GNAQ mutant (MP46, 92.1, MEL270, OMM2.5) and GNA11 mutant (MP41), as well as GNAQ/11 wild type cfDNA in the absence or presence of increasing concentrations of MF using ddPCR. After 72 h of MF treatment, we detected a concentration-dependent increase in both wild type and mutant cfDNA (Fig.6A, B). The number of mutant and wild type copies detected upon treatment of each UM cell line with increasing concentrations of MF are depicted in Fig.6C; they clearly denote a highly significant increase in cfDNA at the lethal concentration of 40 μM MF. Of interest, release of cfDNA was

noted in MP46 and 92.1 cells in response not only to lethal concentrations of MF, but also to non-lethal ones.

Mifepristone does not require the presence of classical nuclear progesterone receptors to inhibit growth and kill UM cells of different genetic backgrounds

It has been previously demonstrated that the antiproliferative action of MF can be independent of the presence of nuclear progesterone receptor (PR), and instead be potentially mediated by membrane progesterone receptors or glucocorticoid receptors [28] (reviewed in [27]). To investigate whether UM cells express cognate progesterone receptors or the other alternative putative receptors, we analyzed their mRNA expression. This included the cognate progesterone receptor (PR), progestin and adipoQ receptor family member 8 (PAQR8), membrane-associated progesterone receptor component 1 (PGRMC1), and component 2 (PGRMC2), as well as the glucocorticoid receptor subfamily 3 group C member 1 (NR3C1). We used MCF-7 breast cancer cells as a positive control for the expression of the cognate PR [28]. qPCR results indicate that primary MP41, MP46, 92.1, and MEL270 cells, as well as metastatic OMM2.5 cells, all express the glucocorticoid receptor (NR3C1). Furthermore, all UM cells express non-classical progesterone receptors (PAQR8, PGRMC1, PGRMC2); however, the cognate nuclear PR is absent in all UM cells. Of interest, of the detected receptor's mRNAs, all are downregulated in the presence of MF (Fig.7).

Discussion

There is a clear gap in treatment options that succeed in mitigating the progression of metastatic UM and ameliorate the survival of patients. Our group elected to improve this current situation by determining whether the promising literature on MF as an anti-cancer agent held in the context of UM. At concentrations of 10 μM and higher, MF significantly disturbed the natural proliferative curves of human UM cell lines. This potent inhibition in proliferation was accompanied by a significant reduction in cellular viability. We found the lower concentrations studied—5 μM—to affect the metabolic activity of the cells while higher concentrations resulted in disruption of membrane permeability, associated with later stage cell death. These results were consistent across all cell lines tested, including the highly metastatic line OMM2.5. The results found in UM cells

are in line with previous reports in ovarian, cutaneous melanoma, and various additional cancer types [20, 28, 38].

MF has potent actions independently from cell line donors, clinical history, or mutational signatures. From the five UM cell lines in our study, 92.1 and MEL270 were originally derived from primary UM patient tumors [39]. The donor for line 92.1 presented with a large primary mass which resulted in complete exenteration of the orbit due to extension into rectus muscles [33, 39]. In contrast, MEL270 cells were obtained following enucleation of a patient who had previously undergone plaque irradiation treatment for primary UM. The cell line OMM2.5 was cultured from liver metastases discovered in the same patient, making MEL270 and OMM2.5 a primary and metastatic donor matched pair [39, 40]. Finally, MP41 and MP46 were cultured from patient derived xenografts of primary UM [41]. All cell lines tested were susceptible to the toxicity of MF in a concentration-related manner.

UM is characterized by mutually exclusive early guanine nucleotide-binding protein alpha Q (*GNAQ*) or alpha 11 (*GNA11*) activating mutations present in each of the cell lines studied here [42, 43]. Moreover, our panel of UM cell lines covers a variety of additional and differential mutational statuses. For example, MP46 has loss of heterozygosity of chromosome 3 and no BRCA-1 associated protein 1 (BAP1) expression, both associated with increased metastatic risk and function as prognostic indicators of metastasis [5, 44-46]. In contrast, cell line 92.1 has disomy 3 and a eukaryotic translation initiator factor 1A X-linked (*EIF1AX*) mutation [39, 41], both correlated with a significantly lowered risk of metastasis [44, 47]. Regardless of genetic background and metastatic potential, MF influenced the growth and viability of all cell lines in a relatively similar manner.

The MF-induced growth inhibition observed in UM is consistent with that observed in other cancer types [21]. We demonstrated that at lower concentrations, MF induced a cytostatic effect in UM, while higher concentrations resulted in high cytotoxicity associated with reduction in cellular viability. A MF-dependent decrease in cyclin dependent kinase-2 (Cdk2) was suggested as the mechanism underlying growth arrest. We previously demonstrated an increase in the abundance of cell cycle inhibitors $p21^{cip1}$ and $p27^{kip1}$ with a simultaneous decrease in Cdk2 activity and cyclin E abundance, all supporting the notion that MF blocks cell cycle progression at the G1/S transition [20, 21, 28].

In terms of the lethality caused by MF at higher concentrations in UM cells, we found that the most prominent effect was the double labeling of the cells with Annexin V-FITC and PI indicating that the majority of the cells, upon 72-h incubation with MF, are in a stage of late apoptosis. Nevertheless, we found that the slowest proliferating cells, MP46 and OMM2.5, showed signs of early apoptosis as marked by Annexin V-FITC-only labeling at the 20 μM concentration of MF. In addition, we found two cell lines (92.1 and MEL270) with a very slight proportion of cells undergoing necrosis associated with apoptosis. The concomitant accumulation of hypodiploid-DNA content, DNA fragmentation, and double labelling Annexin V FITC-PI, denotes that UM cells treated with lethal concentrations of MF mostly die by a classical process of apoptosis. This apoptosis also is associated with the activation of executer caspase-3/7. We have shown that MF causes lethality of other cancer cell types associated with accumulation of cells with hypodiploid DNA content and DNA fragmentation [21, 31]. Given that UM usually presents with a phenotype not very prone to undergo apoptosis [48], manipulation of proapoptotic pathways using an external agent such as MF may represent a potent therapeutic approach for the management of this disease.

During cellular death or cancer progression, the release of highly fragmented cfDNA is amplified, and can be detected in bodily fluids. cfDNA is mainly released through processes of apoptosis, necrosis and cellular secretions, and can inform us of the current state of a tumor or cellular system [49, 50]. cfDNA derived from a tumor, also referred to as circulating tumor DNA (ctDNA), can be detected in a liquid biopsy such as blood, and allow for earlier detection, help classify a lesion, inform on mutational burden, and provide real-time disease monitoring in response to treatment [51-54]. We previously optimized a protocol to detect the dominant driver mutations in UM, especially wild type and mutant GNAQ and GNA11 (c626A>T and A>C) [55]. With this, our group had conducted in vivo studies of ctDNA in a rabbit model of UM and a clinical study in a UM patient cohort, finding ctDNA in blood and aqueous humor correlated with growth, malignancy, and enabled earlier detection of UM and premalignant nevus [55]. Here we applied these methods to detect GNAQ/11 cfDNA released by a panel of UM cells in the presence or absence of MF treatment. Consistent with the cytotoxicity of MF, the release of wild type and mutant cfDNA increased in a concentration-dependent manner. An increase in cancer cfDNA could signal widespread cytotoxicity and successful treatment or be indicative of adaptive mechanisms resulting in resistant populations [37]. Because UM cells were able to repopulate a

culture upon removal of a 20 μM concentration of MF, then the amplification of cfDNA observed in these cultures may be consequence of actively secreted DNA [56]. Conversely, the large increase in cfDNA observed upon 40 μM MF treatment is most likely consequence of widespread cell death only, as UM cells were no longer capable of repopulating a culture plate upon drug removal. Importantly, the dose-dependent increase in ctDNA detection following MF suggests that such an assay could be used through a liquid biopsy as a non-invasive monitoring tool of MF treatment response in patients.

MF acts through PR modulation having inhibitory effects on proliferation and cell cycle progression in hormone responsive tumors [20, 27, 57]. The current reservoir of knowledge on PR expression in UM is scarce, dated, and contradictory [58, 59]. Questioning the relevance of PR to drive the observed effects of MF in UM, we sought to update the field and found that the panel of UM cells here studied does not express classical nuclear PR. However, as progesterone has functional affinity also for non-classical receptors, it is likely that MF may similarly have widespread functionality via such receptors [60-62]. Expanding our search we found that all non-classical surface progesterone receptors PAQR8, PGRMC1, PGRMC2, as well as the other known receptor for MF, the glucocorticoid receptor NR3C1, were present in the UM cells. Interestingly, PAQR8 and PGRMC1 where found stimulated by progesterone and associated with anti-apoptotic signaling cascades [63, 64]. PGRMC1 has been involved in a multitude of other cancer associated signaling pathways [64]. In vitro studies of uterine sarcoma and cervical cancers have demonstrated PGRMC1 to enhance the epithelial mesenchymal transition phenotypes, promote chemoresistance, and have a possible role in progression of metastasis [65, 66]. PGRMC2, similar to PGRMC1, have been implicated in different cancer signaling cascades, yet with likely tumor suppressor properties [60, 67, 68]. Of interest, in the UM cells studied here, 20 μM MF treatment resulted in the downregulation of PAQR8, PGRMC1, PGRMC2, and NR3C1. The later gene, which encodes for the glucocorticoid receptor, is of interest; most effects of the glucocorticoids are mediated by the alpha isoform of the glucocorticoid receptor (reviewed in [69]); however, we have shown that cells devoid of mRNA for the alpha GR isoform but expressing the beta mRNA isoform still respond to MF with growth inhibition [28]. Therefore, we cannot exclude that MF may elicit its anticancer effect targeting the beta isoform of the glucocorticoid receptor, which however seems to operate as a dominant negative regulator of the traditional alpha isoform [70, 71]. Finally, another existing option behind the mechanism of action of MF to explore in UM is

its capacity to induce stress of the endoplasmic reticulum while blocking the growth of cancer cells as we have shown in ovarian cancer [72]. Further studies are therefore required to investigate whether MF is indeed functioning through non-classical means and the mechanisms by which selective receptor modulation is occurring.

The repurposing or repositioning of MF into the clinic for treatment of cancer, in this case UM, could be very rapid; this is due to the fact that the safety profile in humans has been already tested as the drug is currently approved for two clinical conditions: 1) to ameliorate the hyperglycemia associated with Cushing's syndrome; and 2) to terminate early pregnancies when accompanied with a prostaglandin analogue (reviewed in [27]). We anticipate that the concentrations of MF needed to be reached in vivo to inhibit functionality and growth of UM cells are achievable. According to pharmacological studies done in patients when MF was administered orally in doses up to 800 mg, the drug reached blood concentrations of up to 20 μM [73-76]. We provide evidence that concentrations higher than 20 μM not only impair functionally and arrest UM cells, but also kill them. However, in order to reach such concentrations in the circulatory system, either new derivatives of MF with higher potencies need to be synthesized, or new formulations of the drug, such as MF-carrying nanoparticles, should be developed in order to deliver higher amounts of MF into the microenvironment of the UM.

Conclusion

This report is the first to investigate the anti-cancer effects of MF in the context of UM. Our results demonstrate potent growth inhibitory and lethal effects of MF on primary and metastatic UM cell lines in a concentration-dependent manner. These effects seem to be independent of cognate PR as no mRNA expression was detected for this receptor in any of the UM cell lines studied. The lethal effect of MF occurred in association with increased Annexin V-FITC/ PI double-labelled cells, DNA fragmentation, and caspase-3/7 activation, all consistent with the induction of apoptotic cell death. Of novelty, cfDNA levels of wild type and mutant copies of critical UM genes were recorded under MF treatment proving that a significant increase in DNA release occurs when MF is used at lethal concentrations. MF is a safe FDA approved drug with promising potential as a potent anti-cancer treatment. Repurposing MF would be a cost-effective means of finding new treatment options for patients with UM.

Abbreviations

Analysis of variance (ANOVA); BRCA-1 associated protein 1 (BAP1); cell free DNA (cfDNA); circulating tumor DNA (ctDNA); Cyclin-dependent kinase (cdk); droplet digital Polymerase Chain Reaction (ddPCR); eukaryotic translation initiator factor 1A X-linked (EIF1AX); guanine nucleotide-binding protein G subunit alpha (GNAQ); guanine nucleotide-binding protein G subunit alpha 11 (GNA11); membrane-associated progesterone receptor component 1 (PGRMC1) and component 2 (PGRMC2); mifepristone (MF); Choroidal Melanocytes (CM); propidium iodide (PI); progesterone receptor (PR); progestin and adipoQ receptor family member 8 (PAQR8); Real time Polymerase Chain Reaction (qPCR); receptor subfamily 3 group C member 1 (NR3C1); uveal melanoma (UM).

Author's contributions

PB and AL carried out all experiments. AAG oversaw and supported the study design, and collection and analysis of data. YC generated the primary wild type and mutant choroidal melanocytes. CMT and JVB designed the study, provided the funding, and supervised the graduate students. All authors helped in drafting the manuscript.

Acknowledgements

We thank Drs. Robert Roe and Hazel Hunt (Corcept Therapeutics) for supplying pharmaceutical-grade mifepristone. The authors would also like to thank the Immunophenotyping Platform of the RI-MUHC.

Competing interests

The authors declare that they have no competing interests

Availability of data and materials

Not applicable

Consent for publication

Not applicable

Ethics approval and consent to participate

Human eyes were used in accordance with the McGill University Health Centre (MUHC) Research Ethics Board (2019-5314).

Funding

The work was supported in part by funds from the Rivkin Center (to CMT). AL was the recipient of a FRQS scholarship, PB was supported by fund# 739468 from CONACYT.

References

1. Chang AE KL, Menck HR.: **The National Cancer Data Base report on cutaneous and noncutaneous melanoma: a summary of 84,836 cases from the past decade. The American College of Surgeons Commission on Cancer and the American Cancer Society.** *Cancer* 1998, **83(8)**:1664-1678.
2. Ghazawi FM, Darwich R, Le M, Rahme E, Zubarev A, Moreau L, Burnier JV, Sasseville D, Burnier MN, Litvinov IV: **Uveal melanoma incidence trends in Canada: a national comprehensive population-based study**. *Br J Ophthalmol* 2019, **103**(12):1872-1876.
3. Rozeman EA, Dekker TJA, Haanen J, Blank CU: **Advanced Melanoma: Current Treatment Options, Biomarkers, and Future Perspectives**. *Am J Clin Dermatol* 2018, **19**(3):303-317.
4. van der Kooij MK, Speetjens FM, van der Burg SH, Kapiteijn E: **Uveal Versus Cutaneous Melanoma; Same Origin, Very Distinct Tumor Types**. *Cancers (Basel)* 2019, **11**(6).
5. Yang J, Manson DK, Marr BP, Carvajal RD: **Treatment of uveal melanoma: where are we now?** *Ther Adv Med Oncol* 2018, **10**:1758834018757175.
6. Damato EM, Damato BE: **Detection and time to treatment of uveal melanoma in the United Kingdom: an evaluation of 2,384 patients**. *Ophthalmology* 2012, **119**(8):1582-1589.
7. Shields CL FM, Thangappan A, Nagori S, Mashayekhi A, Lally DR et al.: **Metastasis of uveal melanoma millimeter-by-millimeter in 8033 consecutive eyes.** *Arch Ophthalmol* 2009, **127(8)**:989–998.
8. Amaro A, Gangemi R, Piaggio F, Angelini G, Barisione G, Ferrini S, Pfeffer U: **The biology of uveal melanoma**. *Cancer Metastasis Rev* 2017, **36**(1):109-140.

9. Diener-West M, Reynolds SM, Agugliaro DJ, Caldwell R, Cumming K, Earle JD, Hawkins BS, Hayman JA, Jaiyesimi I, Jampol LM *et al*: **Development of metastatic disease after enrollment in the COMS trials for treatment of choroidal melanoma: Collaborative Ocular Melanoma Study Group Report No. 26**. *Arch Ophthalmol* 2005, **123**(12):1639-1643.
10. Kujala E, Makitie T, Kivela T: **Very long-term prognosis of patients with malignant uveal melanoma**. *Invest Ophthalmol Vis Sci* 2003, **44**(11):4651-4659.
11. Lane AM, Kim IK, Gragoudas ES: **Survival Rates in Patients After Treatment for Metastasis From Uveal Melanoma**. *JAMA Ophthalmol* 2018, **136**(9):981-986.
12. CollaborativeOcularMelanomaStudyGroup: **Assessmentofmetastaticdisease status at death in 435 patients with large choroidal melanoma in the Collabora- tive Ocular Melanoma Study (COMS). COMS Report No. 15.** . *Arch Ophthalmol* 2001, **119**:670-676.
13. Kaliki S, Shields CL, Shields JA: **Uveal melanoma: estimating prognosis**. *Indian J Ophthalmol* 2015, **63**(2):93-102.
14. Wessely A, Steeb T, Erdmann M, Heinzerling L, Vera J, Schlaak M, Berking C, Heppt MV: **The Role of Immune Checkpoint Blockade in Uveal Melanoma**. *Int J Mol Sci* 2020, **21**(3).
15. Bustamante P, Piquet L, Landreville S, Burnier JV: **Uveal melanoma pathobiology: Metastasis to the liver**. *Semin Cancer Biol* 2020.
16. Milette S, Sicklick JK, Lowy AM, Brodt P: **Molecular Pathways: Targeting the Microenvironment of Liver Metastases**. *Clin Cancer Res* 2017, **23**(21):6390-6399.
17. Carvajal RD, Schwartz GK, Tezel T, Marr B, Francis JH, Nathan PD: **Metastatic disease from uveal melanoma: treatment options and future prospects**. *Br J Ophthalmol* 2017, **101**(1):38-44.
18. Triozzi PL, Singh AD: **Adjuvant Therapy of Uveal Melanoma: Current Status**. *Ocul Oncol Pathol* 2014, **1**(1):54-62.
19. Ritch SJ, Brandhagen BN, Goyeneche AA, Telleria CM: **Advanced assessment of migration and invasion of cancer cells in response to mifepristone therapy using double fluorescence cytochemical labeling**. *BMC Cancer* 2019, **19**(1):376.

20. Goyeneche AA, Caron RW, Telleria CM: **Mifepristone inhibits ovarian cancer cell growth in vitro and in vivo**. *Clin Cancer Res* 2007, **13**(11):3370-3379.
21. Goyeneche AA, Seidel EE, Telleria CM: **Growth inhibition induced by antiprogestins RU-38486, ORG-31710, and CDB-2914 in ovarian cancer cells involves inhibition of cyclin dependent kinase 2**. *Invest New Drugs* 2012, **30**(3):967-980.
22. Baulieu EE, Segal,S.J.: **The antiprogestin steroid RU 486 and human fertility control**. *New York: Plenum Press* 1985.
23. Goldstone P, Walker C, Hawtin K: **Efficacy and safety of mifepristone-buccal misoprostol for early medical abortion in an Australian clinical setting**. *Aust N Z J Obstet Gynaecol* 2017, **57**(3):366-371.
24. Schaff EA: **Mifepristone: ten years later**. *Contraception* 2010, **81**(1):1-7.
25. Spitz IM, Bardin CW: **Clinical pharmacology of RU 486--an antiprogestin and antiglucocorticoid**. *Contraception* 1993, **48**(5):403-444.
26. Telleria CM, Goyeneche AA: **Antiprogestins in Ovarian Cancer**. In: *Ovarian Cancer - Clinical and Therapeutic Perspectives.* Edited by Farghaly S, vol. 11: InTechopen; 2012: 207-230.
27. Goyeneche AA, Telleria CM: **Antiprogestins in gynecological diseases**. *Reproduction* 2015, **149**(1):R15-33.
28. Tieszen CR, Goyeneche AA, Brandhagen BN, Ortbahn CT, Telleria CM: **Antiprogestin mifepristone inhibits the growth of cancer cells of reproductive and non-reproductive origin regardless of progesterone receptor expression**. *BMC Cancer* 2011, **11**:207.
29. Freeburg EM, Goyeneche AA, Seidel EE, Telleria CM: **Resistance to cisplatin does not affect sensitivity of human ovarian cancer cell lines to mifepristone cytotoxicity**. *Cancer Cell Int* 2009, **9**:4.
30. Gamarra-Luques CD, Hapon MB, Goyeneche AA, Telleria CM: **Resistance to cisplatin and paclitaxel does not affect the sensitivity of human ovarian cancer cells to antiprogestin-induced cytotoxicity**. *J Ovarian Res* 2014, **7**:45.
31. Freeburg EM, Goyeneche AA, Telleria CM: **Mifepristone abrogates repopulation of ovarian cancer cells in between courses of cisplatin treatment**. *Int J Oncol* 2009, **34**(3):743-755.

32. Kapperman HE, Goyeneche AA, Telleria CM: **Mifepristone inhibits non-small cell lung carcinoma cellular escape from DNA damaging cisplatin**. *Cancer Cell Int* 2018, **18**:185.
33. De Waard-Siebinga I, Blom DJ, Griffioen M, Schrier PI, Hoogendoorn E, Beverstock G, Danen EH, Jager MJ: **Establishment and characterization of an uveal-melanoma cell line**. *Int J Cancer* 1995, **62**(2):155-161.
34. Tsering T, Laskaris A, Abdouh M, Bustamante P, Parent S, Jin E, Ferrier ST, Arena G, Burnier JV: **Uveal Melanoma-Derived Extracellular Vesicles Display Transforming Potential and Carry Protein Cargo Involved in Metastatic Niche Preparation**. *Cancers (Basel)* 2020, **12**(10).
35. Goyeneche AA, Harmon JM, Telleria CM: **Cell death induced by serum deprivation in luteal cells involves the intrinsic pathway of apoptosis**. *Reproduction* 2006, **131**(1):103-111.
36. Bustamante PM, D; Goyeneche, A; Garcia de Alba Graue, P; Jin, E; Tsering, T; Dias, AB; Burnier, M.N.; Burnier, J.V.: **Beta-blockers exert potent anti-tumor effects in cutaneous and uveal melanoma**. *Cancer Medicine* 2019, **00**:1-13.
37. Heitzer E, Auinger L, Speicher MR: **Cell-Free DNA and Apoptosis: How Dead Cells Inform About the Living**. *Trends in Molecular Medicine* 2020, **26**(5):519-528.
38. Zheng N, Chen J, Liu W, Wang J, Liu J, Jia L: **Metapristone (RU486 derivative) inhibits cell proliferation and migration as melanoma metastatic chemopreventive agent**. *Biomed Pharmacother* 2017, **90**:339-349.
39. Jager MJ, Magner, J.A.B, Ksander, B.R., Dubovy, S.R.: **Uveal Melanoma Cell Lines: Where do they come from? (An American Ophthalmological Society Thesis)**. *Trans Am Ophthalmol Soc* 2016, **114:T5**.
40. Griewank KG, Yu X, Khalili J, Sozen MM, Stempke-Hale K, Bernatchez C, Wardell S, Bastian BC, Woodman SE: **Genetic and molecular characterization of uveal melanoma cell lines**. *Pigment Cell Melanoma Res* 2012, **25**(2):182-187.
41. Amirouchene-Angelozzi N, Nemati F, Gentien D, Nicolas A, Dumont A, Carita G, Camonis J, Desjardins L, Cassoux N, Piperno-Neumann S *et al*: **Establishment of novel cell lines recapitulating the genetic landscape of uveal melanoma and preclinical validation of mTOR as a therapeutic target**. *Mol Oncol* 2014, **8**(8):1508-1520.

42. Dono M, Angelini G, Cecconi M, Amaro A, Esposito AI, Mirisola V, Maric I, Lanza F, Nasciuti F, Viaggi S *et al*: **Mutation frequencies of GNAQ, GNA11, BAP1, SF3B1, EIF1AX and TERT in uveal melanoma: detection of an activating mutation in the TERT gene promoter in a single case of uveal melanoma**. *Br J Cancer* 2014, **110**(4):1058-1065.

43. Vader MJC, Madigan, M.C., Versluis, M., Suleiman, H.M., Gezgin, G., Gruis, N.A., Out-Luiting, J.J., Bergman, W., Verdijk, R.M., Jager, M.J., van der Velden, P.A.: **GNAQ and GNA11 mutations and downstream YAP activation in choroidal nevi.** . *Br J Cancer* 2017, **117**:884–887.

44. Ewens KG, Kanetsky PA, Richards-Yutz J, Purrazzella J, Shields CL, Ganguly T, Ganguly A: **Chromosome 3 status combined with BAP1 and EIF1AX mutation profiles are associated with metastasis in uveal melanoma**. *Invest Ophthalmol Vis Sci* 2014, **55**(8):5160-5167.

45. Harbour JW, Onken MD, Roberson ED, Duan S, Cao L, Worley LA, Council ML, Matatall KA, Helms C, Bowcock AM: **Frequent mutation of BAP1 in metastasizing uveal melanomas**. *Science* 2010, **330**(6009):1410-1413.

46. Smit KN, Jager MJ, de Klein A, Kili E: **Uveal melanoma: Towards a molecular understanding**. *Prog Retin Eye Res* 2020, **75**:100800.

47. Violanti SS, Bononi I, Gallenga CE, Martini F, Tognon M, Perri P: **New Insights into Molecular Oncogenesis and Therapy of Uveal Melanoma**. *Cancers (Basel)* 2019, **11**(5).

48. Landreville S, Agapova OA, Harbour JW: **Emerging insights into the molecular pathogenesis of uveal melanoma**. *Future Oncol* 2008, **4**(5):629-636.

49. Heitzer E, Haque IS, Roberts CES, Speicher MR: **Current and future perspectives of liquid biopsies in genomics-driven oncology**. *Nat Rev Genet* 2019, **20**(2):71-88.

50. Jin E, Burnier JV: **Liquid Biopsy in Uveal Melanoma: Are We There Yet?** *Ocul Oncol Pathol* 2021, **7**(1):1-16.

51. Wan JCM, Massie C, Garcia-Corbacho J, Mouliere F, Brenton JD, Caldas C, Pacey S, Baird R, Rosenfeld N: **Liquid biopsies come of age: towards implementation of circulating tumour DNA**. *Nat Rev Cancer* 2017, **17**(4):223-238.

52. Mouliere F, El Messaoudi S, Gongora C, Guedj AS, Robert B, Del Rio M, Molina F, Lamy PJ, Lopez-Crapez E, Mathonnet M *et al*: **Circulating Cell-Free DNA from Colorectal**

Cancer Patients May Reveal High KRAS or BRAF Mutation Load. *Transl Oncol* 2013, **6**(3):319-328.

53. Jiang P, Chan CW, Chan KC, Cheng SH, Wong J, Wong VW, Wong GL, Chan SL, Mok TS, Chan HL *et al*: **Lengthening and shortening of plasma DNA in hepatocellular carcinoma patients**. *Proc Natl Acad Sci U S A* 2015, **112**(11):E1317-1325.
54. Diehl F, Schmidt K, Choti MA, Romans K, Goodman S, Li M, Thornton K, Agrawal N, Sokoll L, Szabo SA *et al*: **Circulating mutant DNA to assess tumor dynamics**. *Nat Med* 2008, **14**(9):985-990.
55. Bustamante P, Tsering T, Coblentz J, Mastromonaco C, Abdouh M, Fonseca C, Proenca RP, Blanchard N, Duge CL, Andujar RAS *et al*: **Circulating tumor DNA tracking through driver mutations as a liquid biopsy-based biomarker for uveal melanoma**. *J Exp Clin Cancer Res* 2021, **40**(1):196.
56. Bronkhorst AJ, Wentzel JF, Aucamp J, van Dyk E, du Plessis L, Pretorius PJ: **Characterization of the cell-free DNA released by cultured cancer cells**. *Biochim Biophys Acta* 2016, **1863**(1):157-165.
57. KB. H: **The antiprogestin RU38 486: receptor-mediated progestin versus antiprogestin actions screened in estrogen-insensitive T47Dco human breast cancer cells.** *Endocrinology* 1985, **116(6)**:2236-2245.
58. Foss AJE, Alexander RA, Phil M, Guille MJ, Hungerford JL, McCartney ACE, Lightman S: **Estrogen and Progesterone Receptor Analysis in Ocular Melanomas**. *Ophthalmology* 1995, **102**(3):431-435.
59. Pache M, Glatz-Krieger K, Sauter G, Meyer P: **Expression of sex hormone receptors and cell cycle proteins in melanocytic lesions of the ocular conjunctiva**. *Graefes Arch Clin Exp Ophthalmol* 2006, **244**(1):113-117.
60. Islam MS, Afrin S, Jones SI, Segars J: **Selective Progesterone Receptor Modulators-Mechanisms and Therapeutic Utility**. *Endocr Rev* 2020, **41**(5).
61. Lösel R WM: **Nongenomic actions of steroid hormones.** *Nat Rev Mol Cell Biol* 2003, **4(1)**:46–56.
62. Garg D NS, Baig KM, Driggers P, Segars J. : **Progesterone-mediated non-classical signaling.** *Trends Endocrinol Metab* 2017, **28(9)**:656–668.

63. Dressing GE AR, Pang Y, Thomas P. : **Membrane progesterone receptors (mPRs) mediate progestin induced antimorbidity in breast cancer cells and are expressed in human breast tumors.** . *Horm Cancer* 2012, **3(3)**:101-112.

64. Cahill MA, Jazayeri JA, Catalano SM, Toyokuni S, Kovacevic Z, Richardson DR: **The emerging role of progesterone receptor membrane component 1 (PGRMC1) in cancer biology**. *Biochim Biophys Acta* 2016, **1866**(2):339-349.

65. S.T. Lin EWM, J.F. Chang, R.Y. Hu, L.H. Wang, H.L. Chan: **PGRMC1 contributes to doxorubicin-induced chemoresistance in MES-SA uterine sarcoma**. *Cell Mol Life Sci* 2015, **72**:2395–2409.

66. Shih CC, Chou HC, Chen YJ, Kuo WH, Chan CH, Lin YC, Liao EC, Chang SJ, Chan HL: **Role of PGRMC1 in cell physiology of cervical cancer**. *Life Sci* 2019, **231**:116541.

67. Cahill MA, Neubauer H: **PGRMC Proteins Are Coming of Age: A Special Issue on the Role of PGRMC1 and PGRMC2 in Metabolism and Cancer Biology**. *Cancers (Basel)* 2021, **13**(3).

68. Wendler A, Wehling M: **PGRMC2, a yet uncharacterized protein with potential as tumor suppressor, migration inhibitor, and regulator of cytochrome P450 enzyme activity**. *Steroids* 2013, **78**(6):555-558.

69. Timmermans S, Souffriau J, Libert C: **A General Introduction to Glucocorticoid Biology**. *Front Immunol* 2019, **10**:1545.

70. Oakley RH, Jewell CM, Yudt MR, Bofetiado DM, Cidlowski JA: **The dominant negative activity of the human glucocorticoid receptor beta isoform. Specificity and mechanisms of action**. *J Biol Chem* 1999, **274**(39):27857-27866.

71. Yudt MR, Jewell CM, Bienstock RJ, Cidlowski JA: **Molecular origins for the dominant negative function of human glucocorticoid receptor beta**. *Mol Cell Biol* 2003, **23**(12):4319-4330.

72. Zhang L, Hapon MB, Goyeneche AA, Srinivasan R, Gamarra-Luques CD, Callegari EA, Drappeau DD, Terpstra EJ, Pan B, Knapp JR *et al*: **Mifepristone increases mRNA translation rate, triggers the unfolded protein response, increases autophagic flux, and kills ovarian cancer cells in combination with proteasome or lysosome inhibitors**. *Mol Oncol* 2016, **10**(7):1099-1117.

73. Heikinheimo O: **Pharmacokinetics of the antiprogesterone RU 486 in women during multiple dose administration**. *J Steroid Biochem* 1989, **32**(1A):21-25.

74. Heikinheimo O, Lahteenmaki PL, Koivunen E, Shoupe D, Croxatto H, Luukkainen T, Lahteenmaki P: **Metabolism and serum binding of RU 486 in women after various single doses**. *Hum Reprod* 1987, **2**(5):379-385.

75. Shoupe D, Mishell DR, Jr., Lahteenmaki P, Heikinheimo O, Birgerson L, Madkour H, Spitz IM: **Effects of the antiprogesterone RU 486 in normal women. I. Single-dose administration in the midluteal phase**. *Am J Obst Gynecol* 1987, **157**(6):1415-1420.

76. Kawai S, Nieman LK, Brandon DD, Udelsman R, Loriaux DL, Chrousos GP: **Pharmacokinetic properties of the antiglucocorticoid and antiprogesterone steroid RU 486 in man**. *J Pharmacol Exp Ther* 1987, **241**(2):401-406.

Figure legends

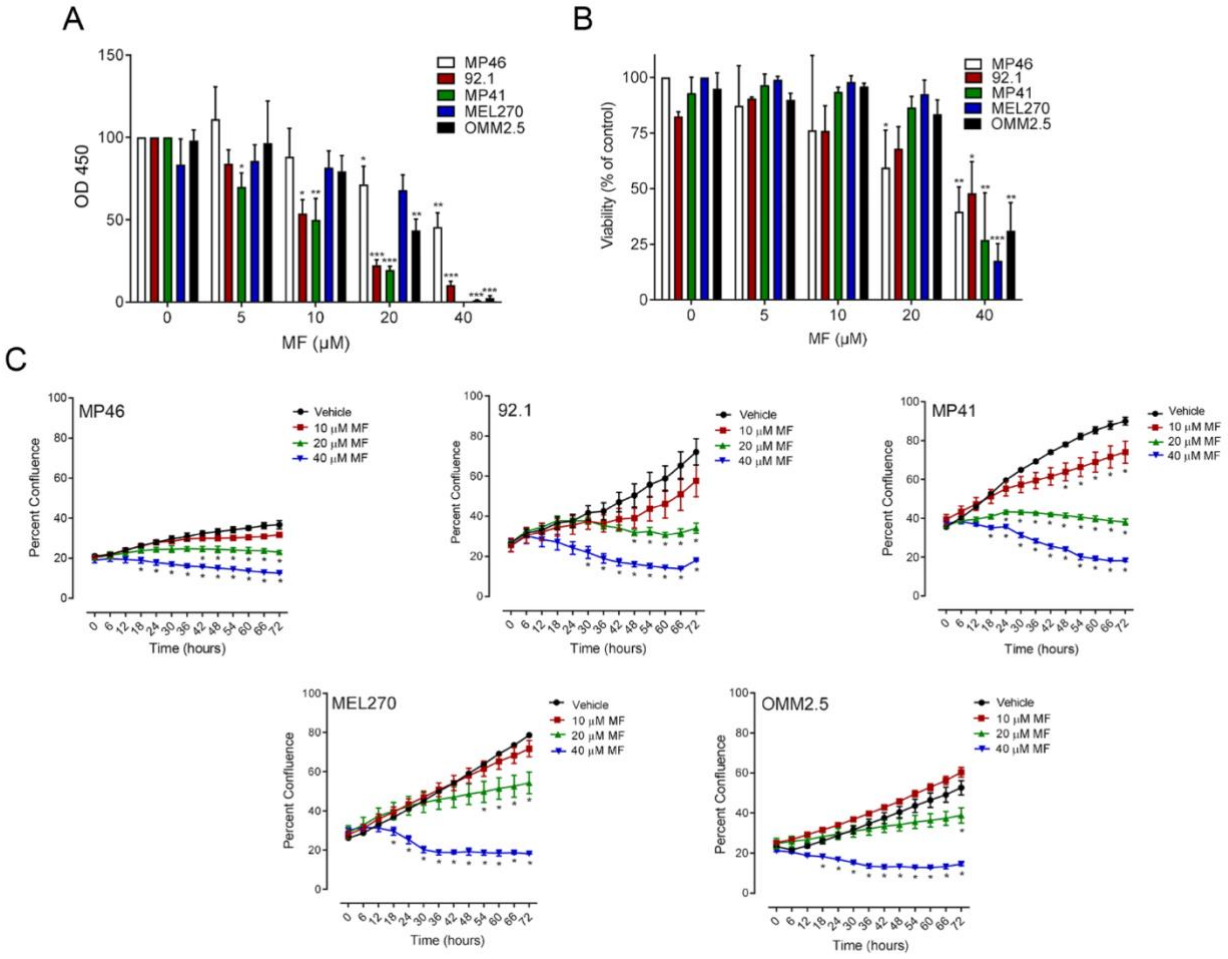

Fig. 1 MF inhibits functionality, growth capacity, and viability of UM cell lines in a concentration-related manner. Graphs represent the level of cellular functionality or viability respectively as detected via a CCK8 colorimetric assay (**A**) or Trypan Blue exclusion assay (**B**) after cells were treated with increasing concentrations of MF (0, 5, 10, 20, or 40 μM) for 72 h. (**C**) Growth curves obtained through Incucyte live cell imaging system, tracking cellular confluency. In **A** and **B**, data were analyzed using two-way ANOVA followed by Dunnett's multiple comparison test. In **C**, data were analyzed using repeated measures ANOVA followed by Tuckey's multiple comparison test.* Indicates $p<0.05$, ** indicates $p<0.01$, whereas *** indicates $p<0.001$ compared against vehicle-treated controls.

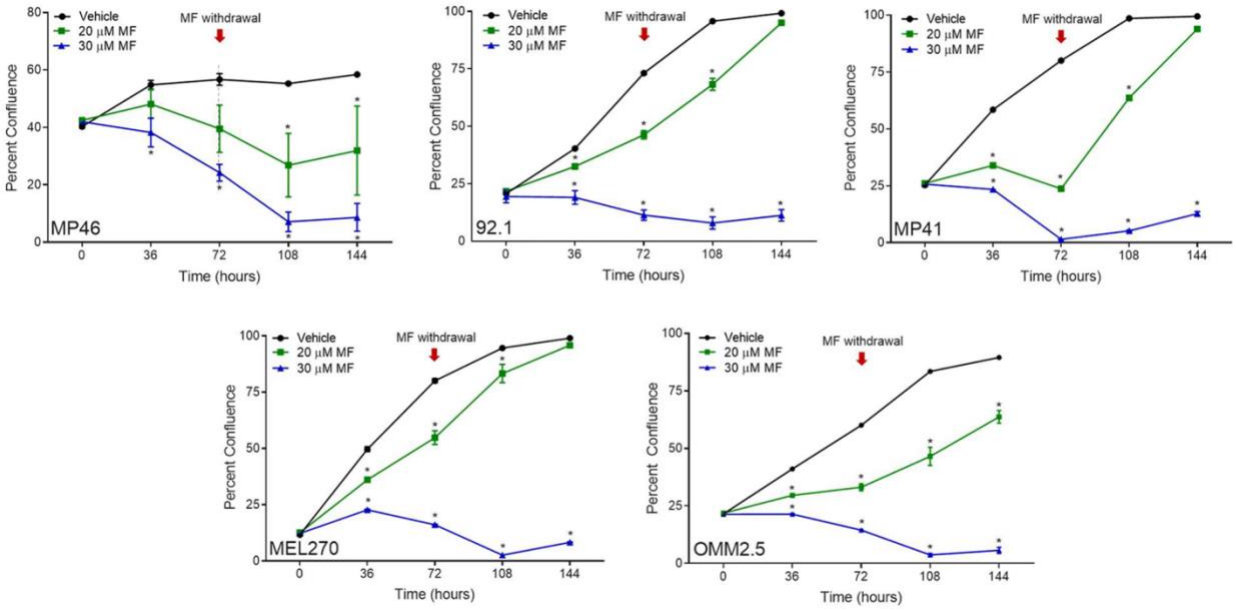

Fig. 2 Long-term toxicity of MF towards UM cell lines and the consequence of MF withdrawal. UM cells were treated with MF at concentrations of either 0, 20, or 30 μM for 72 h and imaged every 6 h in the Incucyte. Following the initial 72 h, media was aspirated, replaced with regular growth media, and placed back into the Incucyte to be imaged for another 72 h. The red arrows at 72 h indicate the moment in which MF was removed from the media. Data were analyzed using repeated measures ANOVA followed by Tuckey's multiple comparison test. * Indicates $p<0.05$, ** indicates $p<0.01$, whereas *** indicates $p<0.001$ compared against vehicle-treated controls.

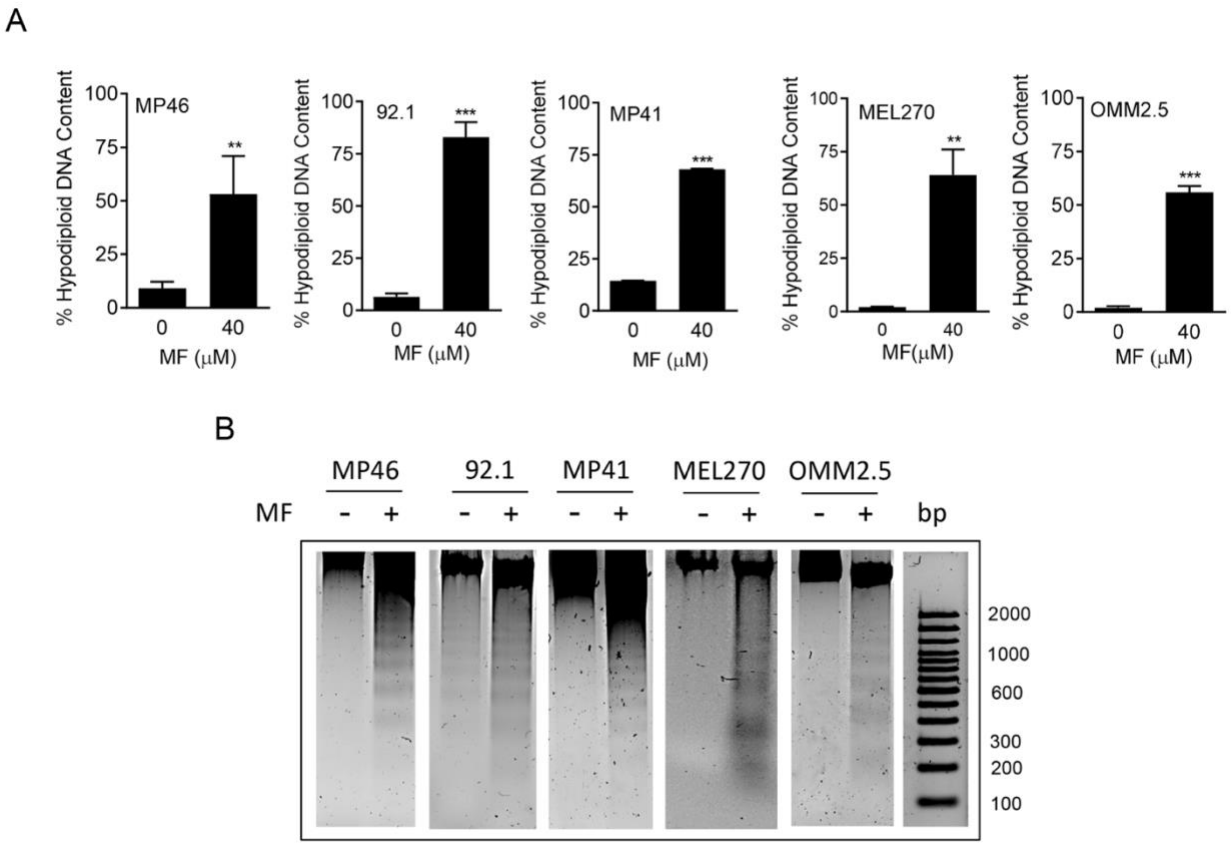

Fig. 3 MF induces accumulation of hypodiploid DNA content and DNA ladder. (**A**) Quantification of particles with hypodiploid DNA content upon 72 h of MF treatment in a panel of UM cell lines. The hypodiploid DNA content corresponds to the Sub-G1 DNA content extrapolated when performing the cell cycle analysis of the cells treated with MF (the quantitative details are shown in the green-stained sections of the histograms in Fig.S3). (**B**) A similar experiment was done in which all floating and adherent cells were pelleted, gDNA isolated, subjected to agarose electrophoresis, stained with SYBR Gold nuclei acid stain, and imaged. A 100 base pair (bp) maker was run in parallel. -: vehicle; +: 40 μM MF.

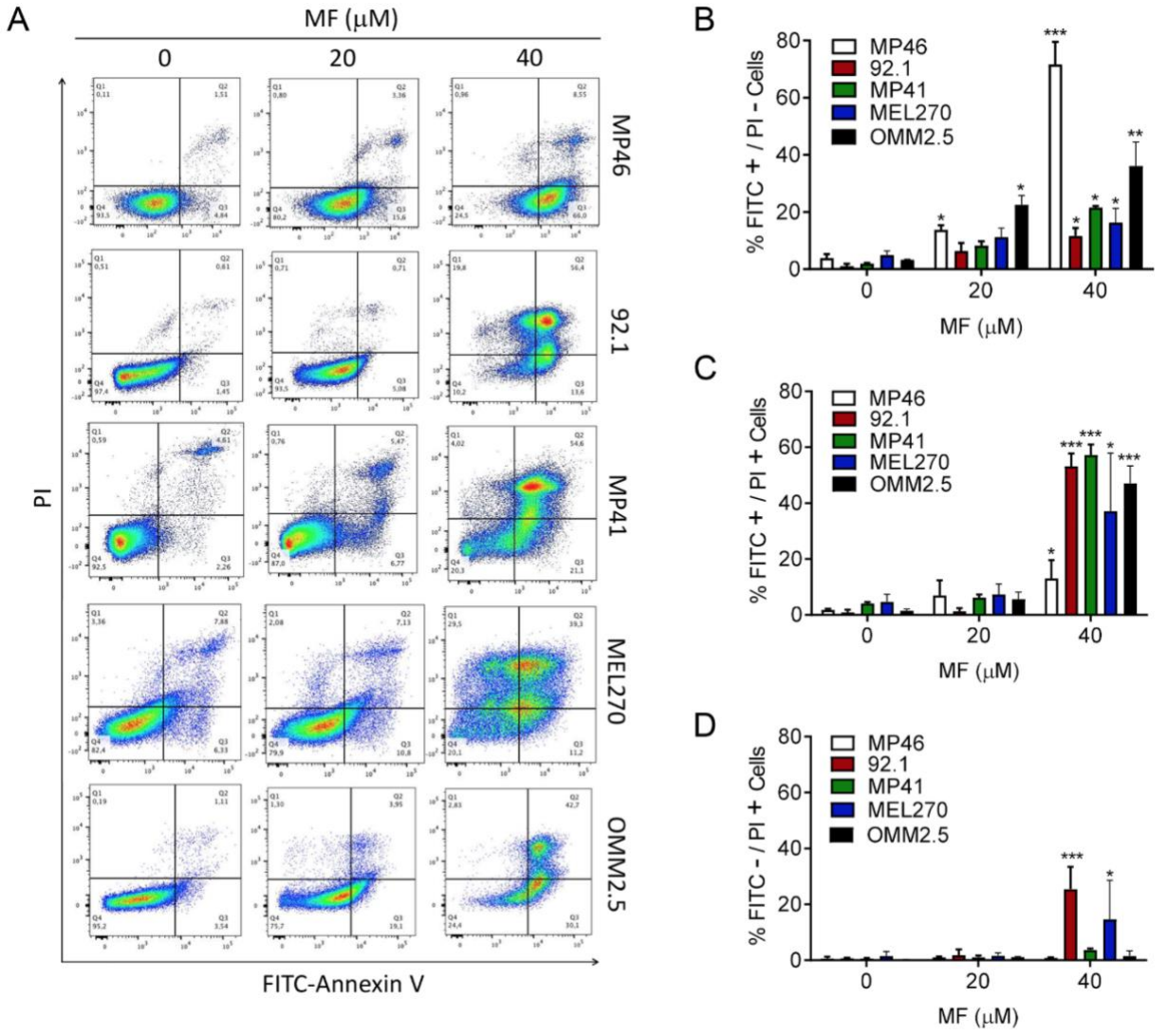

Fig.4 MF induces apoptosis in UM cells. (**A**) Representative histograms depicting the distribution of UM cells exposed to vehicle, 20, or 40 μM MF, and stained with Annexin V-FITC and/or PI after 72 h of incubation. The histograms represent flow cytometry data. (**B**) The bar graphs depict the percent of UM cells undergoing early apoptosis as marked by the labeling with only Annexin V-FITC. (**C**) Results show the percent of UM cells undergoing late apoptosis represented by cells double labeled with Annexin V-FITC and PI. (**D**) The percent of cells likely undergoing necrosis is shown as PI only stained cells. Data were analyzed using two-way ANOVA followed by Dunnett's multiple comparison test. * Indicates $p<0.05$, ** indicates $p<0.01$, whereas *** indicates $p<0.001$ compared against vehicle-treated controls.

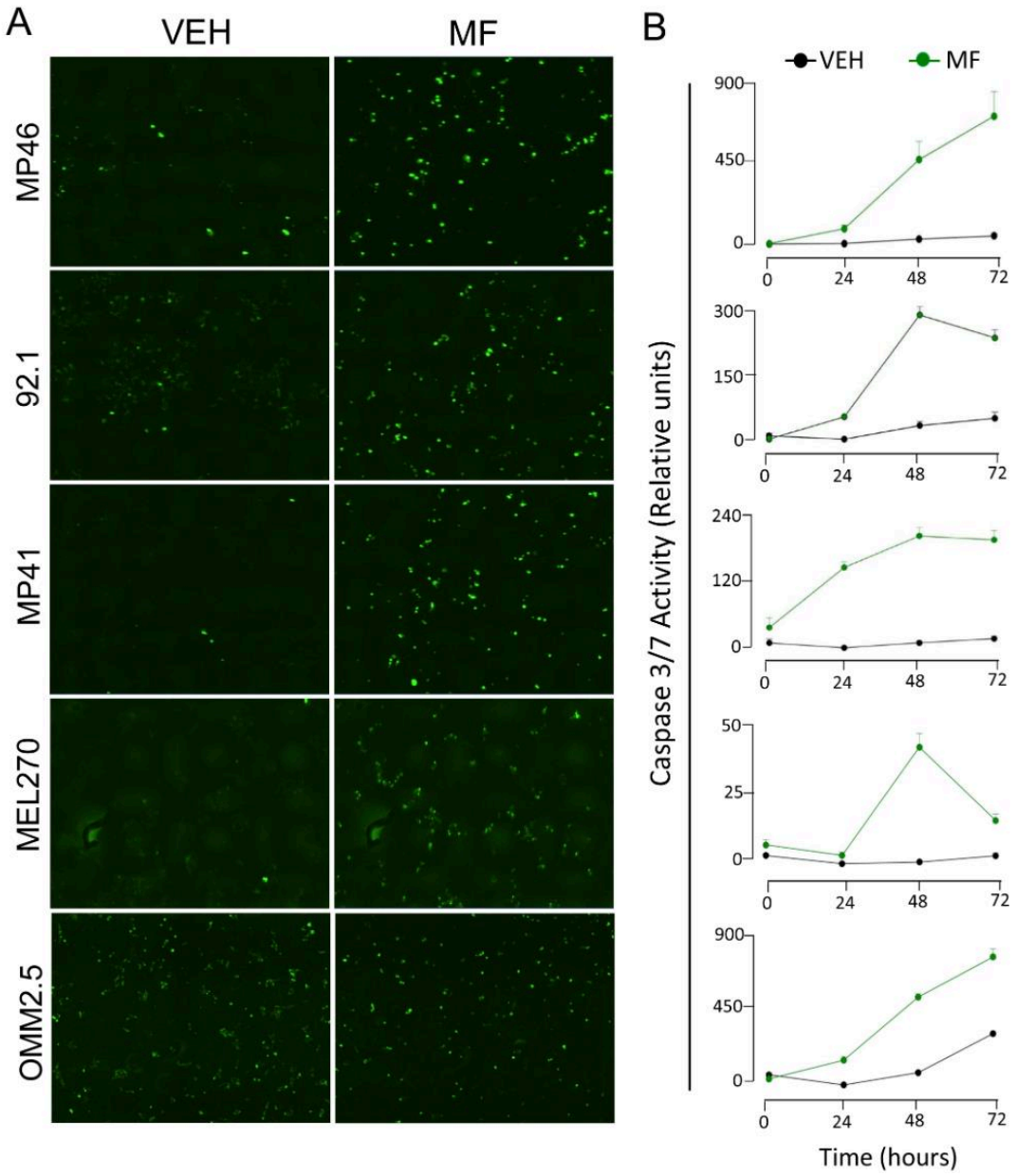

Fig.5 MF-associated UM cell death is related with the activation of executer caspase-3/7. **(A)** Green nuclear staining is generated upon a chemical reaction catalyzed by either active caspases 3 or 7. The images shown represent the endpoint of an experiment done for 72 h following MF treatment at a 40 μM concentration. These images can be observed over imposed with phase contrast in Fig.S5. (**B**) Depicted are the time-course quantifications of the green fluorescence expressed as relative activity with respect to the fluorescence generated by vehicle-treated cells.

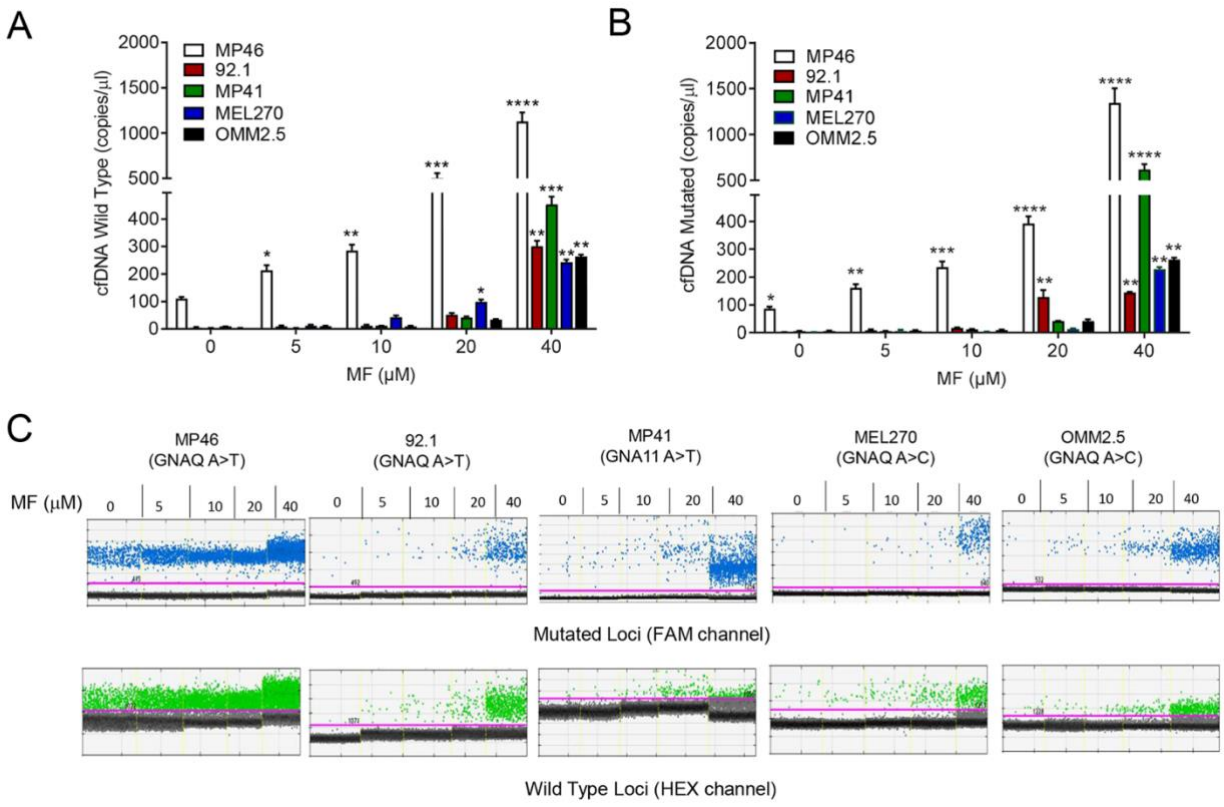

Fig. 6 MF treatment induces the release of cell-free DNA into the media supernatant. Graphs show number of wild type (**A**) and mutant (**B**) copies of cfDNA per µl of cell-free media obtained 72 h after incubation with vehicle, 5, 10, 20, or 40 µM MF. (**C**) Representative one-dimensional plot of mutant GNAQ/GNA11 or wild type cfDNA extracted from conditioned media after treatment for 72 h with the depicted concentrations of MF. Channel compatible with FAM dye shows droplets with mutant target in blue. Wild type target is shown in green using a HEX label. Threshold (pink line) set in between positive (mutant or wild type) and no DNA target (black) droplets.

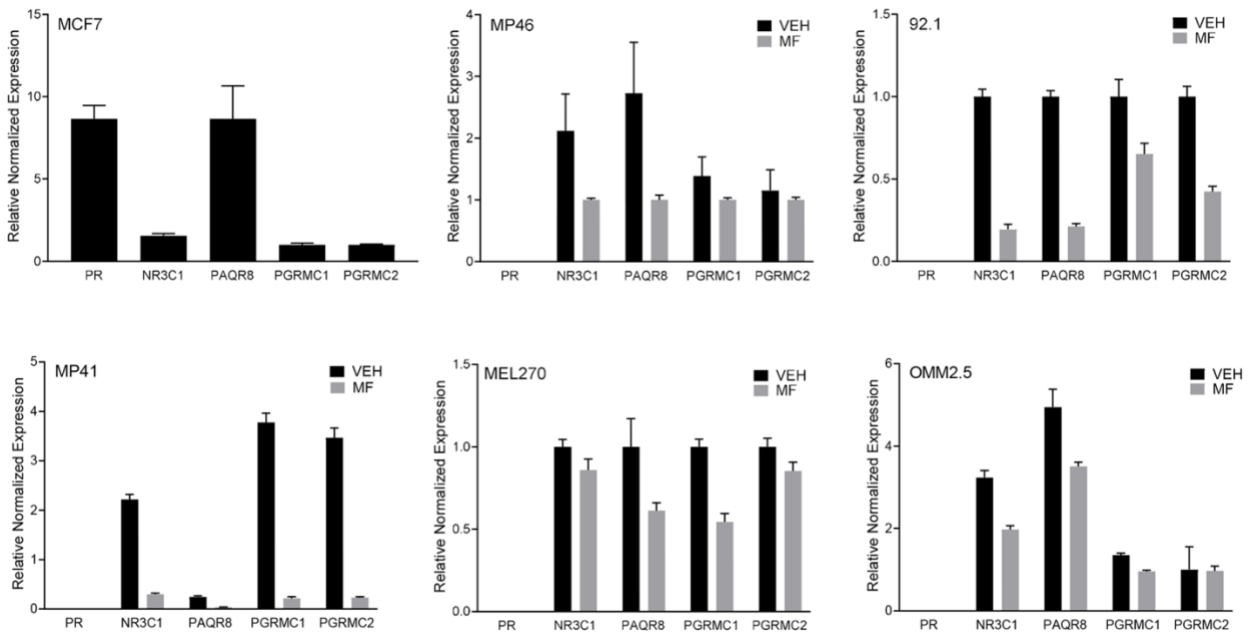

Fig. 7 The effect of MF in UM cells is independent from the classical nuclear progesterone receptor**.** SybrGreen-based Real Time PCR quantified the gene expression profiles of PR, PAQR8, PGRMC1, PGRMC2, and NR3C1. β-Actin was used as a reference gene. mRNAs were amplified from either untreated cells or cells treated with 20 μM MF. The mRNA from MCF-7 cells was used as a positive control for the expression of the classical PR. No template control and no reverse transcriptase control were added in each assay. Individual runs were performed in triplicates.

Supplementary Figures

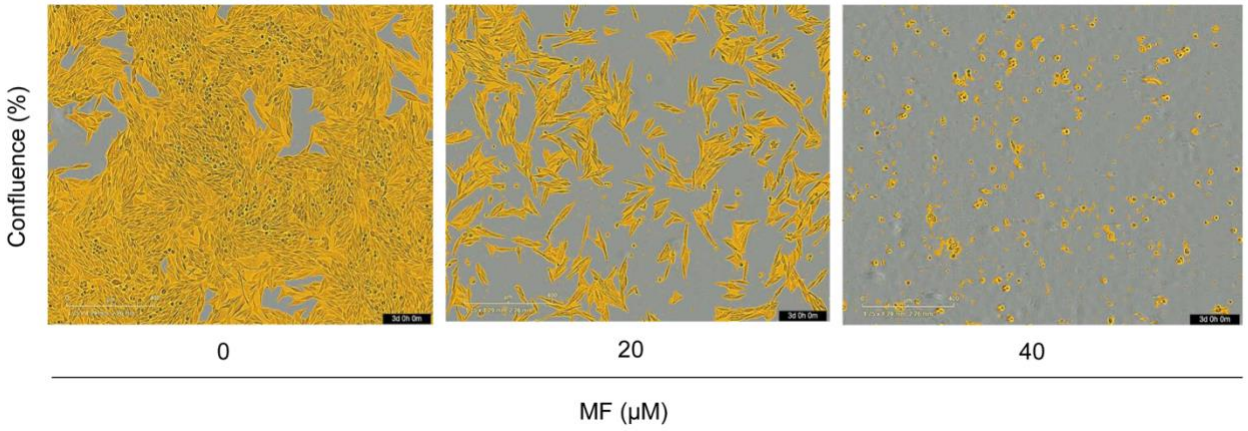

Fig. S1 Depiction of confluency as assessed using the Incucyte software. Representative are masked images of MF41 cells treated with the indicated concentrations of MF for 72 h.

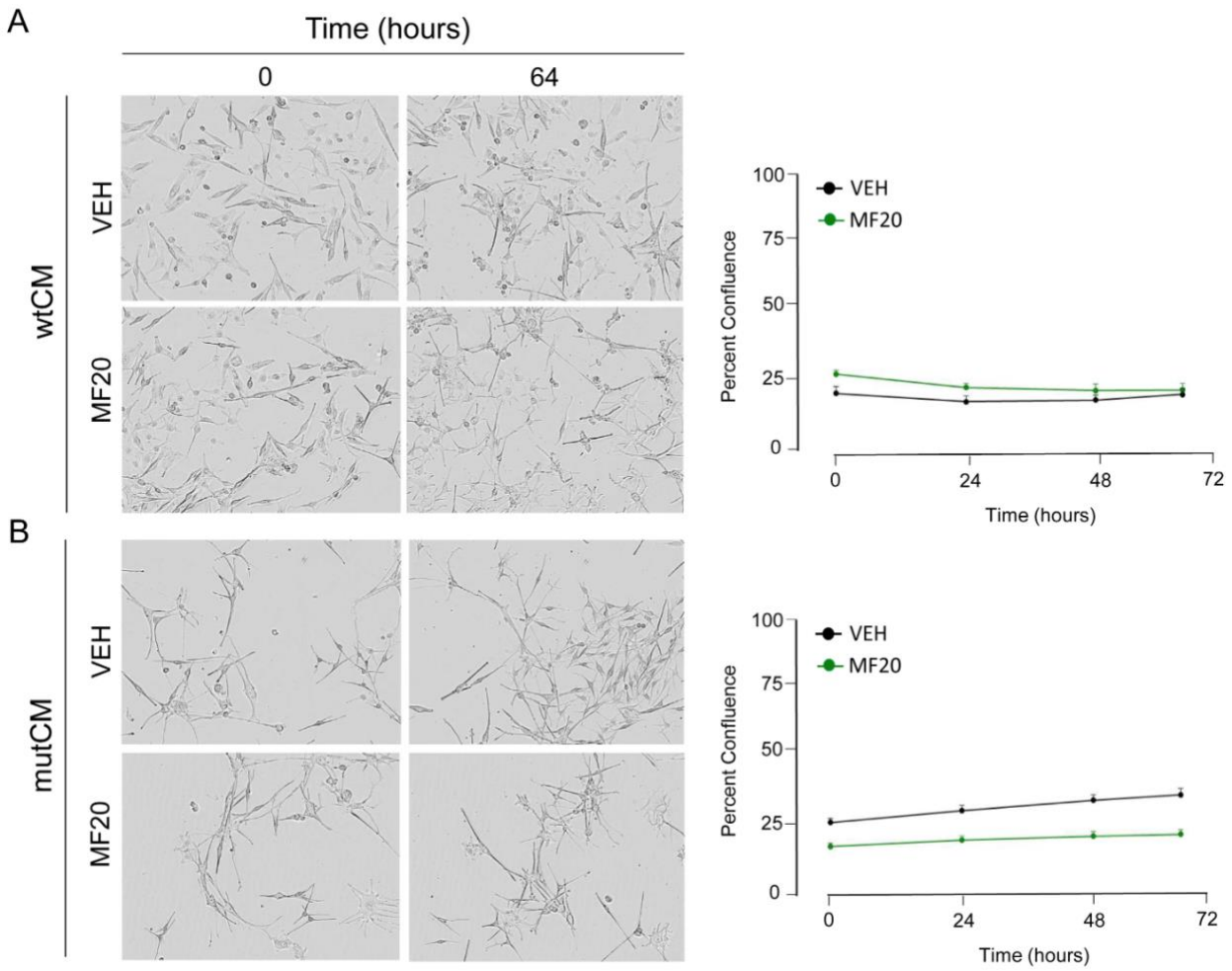

Fig. S2 Assessment of growth of wild type choroidal melanocytes (wtCM) (**A**) or mutant CM (mutCM) (**B**) in the presence or absence of 20 μM MF. Right panels in (**A**) and (**B**) represent the percent confluence of the cells in the absence or presence of MF. MF20: 20 μM MF; VEH: vehicle.

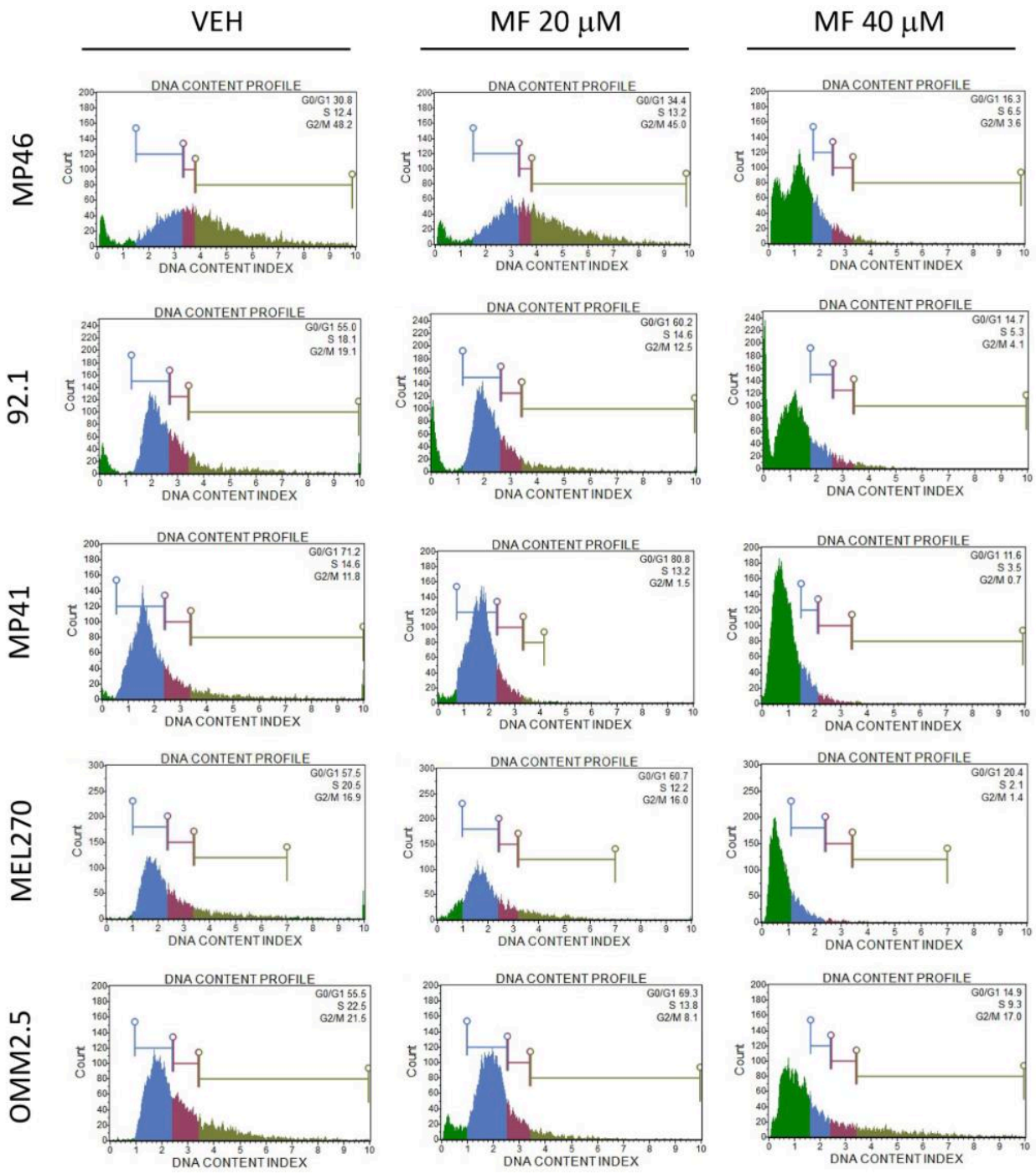

Fig. S3 Representative cell cycle histograms of UM cell lines exposed to vehicle or MF at 20 μM or 40 μM concentrations. Results were generated using the Guava Muse microcytometer. Colored in dark green are the hypodiploid DNA contents (a.k.a. Sub-G1 regions). Cells in G1 phase are colored in blue, those in S phase in red, whereas the light green represents the cells having G2/M content plus hyperploid DNA.

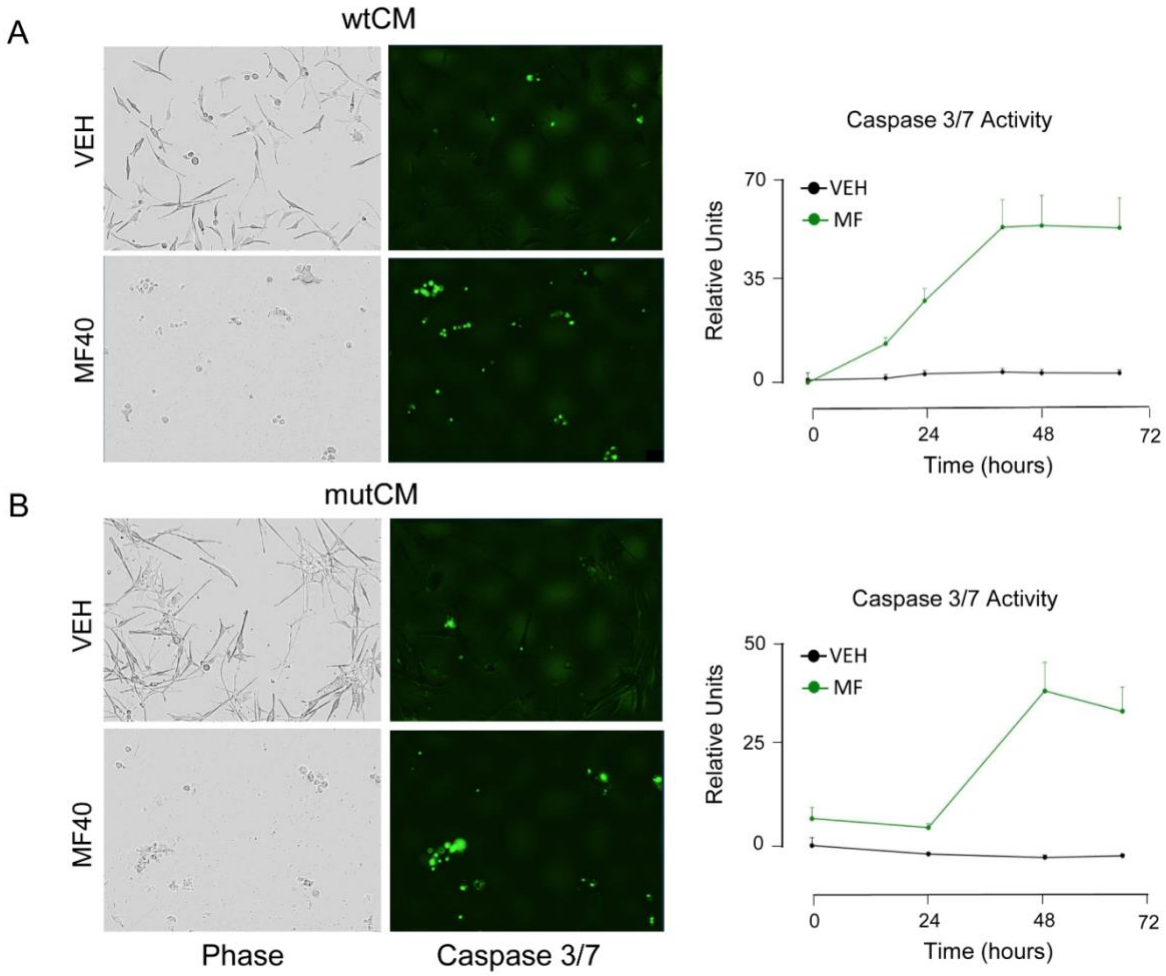

Fig.S4. Caspase-3/7 activity in wild type CM (wtCM) (**A**) or mutant CM (mutCM) (**B**) exposed for 60 h to vehicle (VEH) or 40 μM MF (MF40). Left panels in (**A**) and (**B**) show phase contrast images, whereas the middle panels represent the staining denoting caspase-3/7 activity; the quantitation of the activity of caspase-3/7 is depicted in the right panels.

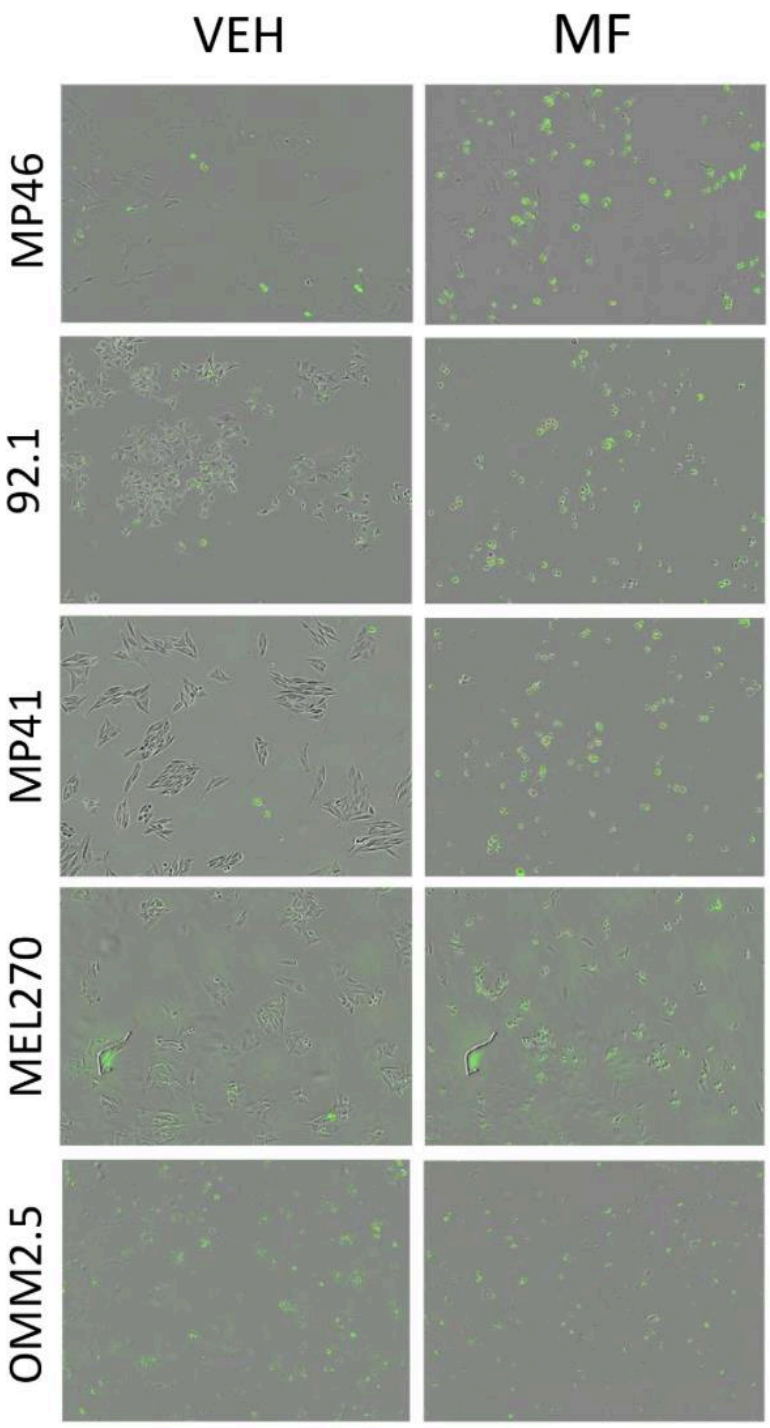

Fig. S5 Overlay images of phase contrast with green fluorescence representing nuclear regions within the cells that accumulate a product of the enzymatic activity of executer caspase-3 7. These images represent the same fields shown in Fig.5.

Chapter 3:

This chapter is based on a published manuscript in Cancers

Tsering T, Laskaris A, Abdouh M, Bustamante P, Parent S, Jin E, Ferrier ST, Arena G, Burnier JV. Uveal Melanoma-Derived Extracellular Vesicles Display Transforming Potential and Carry Protein Cargo Involved in Metastatic Niche Preparation. Cancers (Basel). 2020 Oct 11;12(10):2923. doi: 10.3390/cancers12102923. PMID: 33050649; PMCID: PMC7600758.

Introduction and Rationale:

The previous chapter focused on targeting the traditional model of cancer metastasis, initiated by cellular detachment, migration, invasion and finally colonization of distant tissues. However, there are theories which suggest tumors secrete factors such as EVs that may be aiding in formation of the pre-metastatic niche to accommodate disseminating cancer cells. Further, various papers have confirmed the ability of EV secretions from different primary cancers to carry oncogenic cargo which aids in pre-metastatic niche formation *in vivo* [98, 99, 169, 207].

Few papers to date have undertaken investigation into the oncogenic potential and proteomic profile of EVs in UM. The majority of current research in UM-EVs is either focused on miRNA profiles or provides proteomic patterns for a subset of EV classes [165, 213, 214]. In this chapter, we provide for the first time a comprehensive mass spectrometry analysis of the proteomic content of a panel of UM cell line derived EVs. With further functional assays investigating their inclination to transform recipient cells and promote metastasis in mice. This work lays the foundation for future studies attempting to elucidate the metastatic potential of UM-EV secretions.

Article :

Uveal Melanoma-Derived Extracellular Vesicles Display Transforming Potential and Carry Protein Cargo Involved in Metastatic Niche Preparation

Thupten Tsering [1], Alexander Laskaris [1], Mohamed Abdouh [1], Prisca Bustamante [1], Sabrina Parent [1], Eva Jin [1], Sarah Tadhg Ferrier [1], Goffredo Arena [1,2,3] and Julia V. Burnier [1,4,*]

[1] Cancer Research Program, Research Institute of the McGill University Health Centre, 1001 Decarie Blvd, Montreal, QC H4A 3J1, Canada; thupten.tsering@mail.mcgill.ca (T.T.); alexander.laskaris@mail.mcgill.ca (A.L.); mohamed.abdouh@muhc.mcgill.ca (M.A.); prisca.bustamantealvarez@mail.mcgill.ca (P.B.); sabparent@icloud.com (S.P.); eva.jin@mail.mcgill.ca (E.J.); sarah.ferrier@mail.mcgill.ca (S.T.F.); goffredo.arena@mcgill.ca (G.A.)

[2] Ospedale Giuseppe Giglio Fondazione San Raffaele Cefalu Sicily, 90015 Cefalu, Italy

[3] Mediterranean Institute of Oncology, 95029 Viagrande, Italy

[4] Experimental Pathology Unit, Department of Pathology, McGill University, QC H3A 2B4, Canada

* Correspondence: julia.burnier@mcgill.ca; Tel.: +1-514-934-1934 (ext. 76307)

Received: 13 September 2020; Accepted: 7 October 2020; Published: 11 October 2020

Simple summary: Uveal melanoma is a rare but deadly cancer that shows remarkable metastatic tropism to the liver. Extracellular vesicles (EVs) are nanometer-sized, lipid bilayer-membraned particles that are released from cells. In our study we used EVs derived from primary normal choroidal melanocytes and matched primary and metastatic uveal melanoma cell lines from a patient. Analysis of these EVs revealed important protein signatures that may be involved in tumorigenesis and metastatic dissemination. We have established a model to study EV functions and phenotypes which can be used in EV-based liquid biopsy.

Abstract: Extracellular vesicles (EVs) carry molecules derived from donor cells and are able to alter the properties of recipient cells. They are important players during the genesis and progression of tumors. Uveal melanoma (UM) is the most common primary intraocular tumor in adults and is associated with a high rate of metastasis, primarily to the liver. However, the mechanisms underlying this process are poorly understood. In the present study, we analyzed the

oncogenic potential of UM-derived EVs and their protein signature. We isolated and characterized EVs from five UM cell lines and from normal choroidal melanocytes (NCMs). BRCA1-deficient fibroblasts (Fibro-BKO) were exposed to the EVs and analyzed for their growth *in vitro* and their reprograming potential *in vivo* following inoculation into NOD-SCID mice. Mass spectrometry of proteins from UM-EVs and NCM-EVs was performed to determine a protein signature that could elucidate potential key players in UM progression. In-depth analyses showed the presence of exosomal markers, and proteins involved in cell-cell and focal adhesion, endocytosis, and PI3K-Akt signaling pathway. Notably, we observed high expression levels of HSP90, HSP70 and integrin V in UM-EVs. Our data bring new evidence on the involvement of UM-EVs in cancer progression and metastasis.

Keywords: Uveal melanoma; extracellular vesicles; liver metastasis; liquid biopsy; mass spectrometry

---

1. Introduction

Uveal Melanoma (UM) is the most common primary intraocular tumor in adults [1,2], and the second most common type of melanoma. It develops within the uveal tract of the eye, most frequently in the choroid [3,4]. Although there has been tremendous progress in understanding the genetic landscape [5–8], diagnosis [9–11], and treatment [12,13] of UM, the overall survival rate has not changed in the last three decades [14]. Its annual incidence is estimated at 3.75 and 5.2 cases per million individuals in Canada and the United States, respectively [15,16], while in Europe it varies according to latitude (2–8 cases per million) [17]. While the rate of UM occurrence is relatively low, approximately 50% of patients develop metastasis, primarily to the liver (90%) [18]. The 1-year survival rate of UM patients dramatically drops to 15% once it metastasizes [13,19] due to the absence of effective treatments and the high tumor burden at the time of detection [20]. While metastases are rarely detected at UM primary diagnosis, evidence has shown that circulating tumor cells can be found at diagnosis, suggesting that systemic involvement is an early phenomenon [21]. Moreover, the mechanisms underlying this process are not well understood. This implies that current clinical surveillance tools are not sensitive enough to detect premetastatic stages thereby underscoring the need for better and more sensitive biomarkers to

complement and validate existing clinical surveillance. Extracellular vesicles (EVs) have been shown to harbor selective biomarkers in various cancers and to provide valuable clinical information [22]. However, the role of EVs as biomarkers and mediators of metastasis has not been widely explored in UM.

EVs are nanoparticles emitted under physiological and pathological conditions such as cancer. They are highly heterogeneous based on their size, shape and subcellular origin [23]. Minimal information for the study of EVs have now been standardized [24]; these include and are not limited to the size, floating density, as well as the presence of classical markers such as tetraspanins, annexins, Alix, and heat shock proteins (HSPs) [25,26]. The underlying molecular mechanism involved in EV formation, delivery of cargo inside EVs and ultimately in their release is still not clear [26,27]. In contrast, their uptake by target cells has been shown to occur via numerous pathways (i.e., endocytosis, micropinocytosis, phagocytosis) [28,29]. EVs are loaded with RNA [30,31], DNA [27,32], lipid [33,34] and proteins [35,36], and play a vital role in intercellular communications [23,24,37,38]. Notably, cancer-derived EVs promote cell proliferation, migration, invasion, angiogenesis and metastases [39–41].

A growing body of evidence proposes that EV cargo could be used as circulating biomarkers in liquid biopsy-based platform, particularly in the context of cancer. miRNA profiling of UM-derived exosomes has been performed [42,43]. In addition, the proteome profile of UM secretome and that of UM-derived EVs have also been reported [22,44,45]. However, none has addressed protein differential expression between healthy- and UM-derived EVs.

We performed this study to investigate the effects of EVs derived from UM cell lines on the behaviour of target cells, and to compare the protein contents in EVs derived from UM cells and normal choroidal melanocytes (NCMs). We have previously demonstrated that blood-derived EVs from patients with ocular and cutaneous melanoma are uptaken by and reprogram single oncosuppressor-mutated (SOM) cells into malignant cells [46–48]. Here, we showed that as opposed to NCM-EVs, UM-EVs increased the proliferation of target SOM cells such as BRCA1-deficient fibroblasts (Fibro-BKO) and induced their malignant transformation. In addition, proteomic analyses showed that UM-derived EVs were enriched in proteins involved in cell-cell and focal adhesion, endocytosis, and metastatic niche organization. Altogether, these data shed light on the role of EVs in driving cancer progression, and their potential use in a liquid biopsy platform to monitor patients affected by UM.

2. Results

2.1. Primary NCMs Were Efficiently Cultured from Human Eyes

UM can arise de novo or from pre-existing benign nevi, stemming from malignant transformation of melanocytes of the uveal tract, mainly the choroid. As NCMs are not available commercially, and in order to perform comparative analyses of UM-EVs and to study their effects, we established primary NCM cultures as a control counterpart. NCM cultures were established from 3 donors as described under Material and Methods section (Figure S1 and Table S1). Geneticin was used to suppress growth of retinal pigmented epithelium (RPE) cells and fibroblasts, thus ensuring pure NCM cultures, as previously described [49]. The majority of NCM cells displayed a spindle morphology with brown pigmented cytoplasmic granules (Figures S1 and S2A). In addition, these cells stained positive for MART-1/Melan A, vimentin, S100 and HMB45, which is an indicator of melanogenesis [49] (Figures S2B,C). This suggests that our purification protocol yielded pure NCMs. Of note, EVs derived from donors 2G.PPccF1968Y and 2G.PPXG1981Y (NCM cells) were used for NanoSight, transmission electron microscopy (TEM), and Western blots. EVs derived from donors 2G.PPwC1963Y and 2G.PPXG1981Y (NCM cells) were used for mice experiments (Table S1B).

2.2. EVs Derived from UM Cells and NCMs are Efficiently Internalized by Target Cells

As our first goal was to determine the effects of EVs on target cells, we characterized the nature of these particles, and determined their behaviour when added to target cell cultures. EVs were isolated both from NCMs and from established UM cell cultures. Selected UM cell lines show typical UM-initiating mutations (characteristics shown in Table S1B) and we used MEL270 and OMM2.5, which are matched primary and metastatic, respectively, cell lines derived from the same UM patient. We confirmed the identity of the EVs both physically and phenotypically. As assessed by NanoSight for nanoparticle tracing analysis (NTA) and TEM, the isolated EVs were round-shaped vesicles with a mean diameter of 181 nm for UM-EVs (mean range 163 nm (MEL270) to 214 nm (MP46)), and 278 nm for EVs from NCMs (Figure 1A). As expected NCMs emitted a lower amount of EVs compared to the UM cell lines. (Figure 1B). In addition, by using TEM-based immunogold labeling and Western blot, we observed that these vesicles expressed

selective markers of exosomes (i.e., CD81, CD63, TSG101) (Figure 1C,D). Detailed analyses of NTA and TEM of EVs are shown in Figures S3A–J and S4A–J respectively.

In order to exert their effects, EVs must be internalized by target cells and deliver their cargo. To assess EV uptake by target cells, we tagged them with PKH67. To eliminate excess free PKH67 which may interfere with interpretation of EV uptake, labeled EV preparations were passed through an Optiprep density gradient (Figure S5A). NTA, immunogold TEM, and Western blot analyses revealed enrichment of PKH67-labeled EVs in fraction 3 that was devoid of free-floating dye (Figure S5B–E). Following incubation of purified PKH67-tagged EVs with Fibro-BKO and immortalized human hepatocytes (i.e., IHH; used herein because the liver is the primary site for UM metastasis[19,50]), we observed that treated cells efficiently internalized EVs (Figure 2A–D and 2F–I, respectively). In contrast, cells incubated with preparations from PKH67 samples without EVs did not show any green puncta signal in either Fibro-BKO (Figure 2E) or IHHs (Figure 2J). These data show that pure pools of EVs from UM cells are efficiently internalized by target cells.

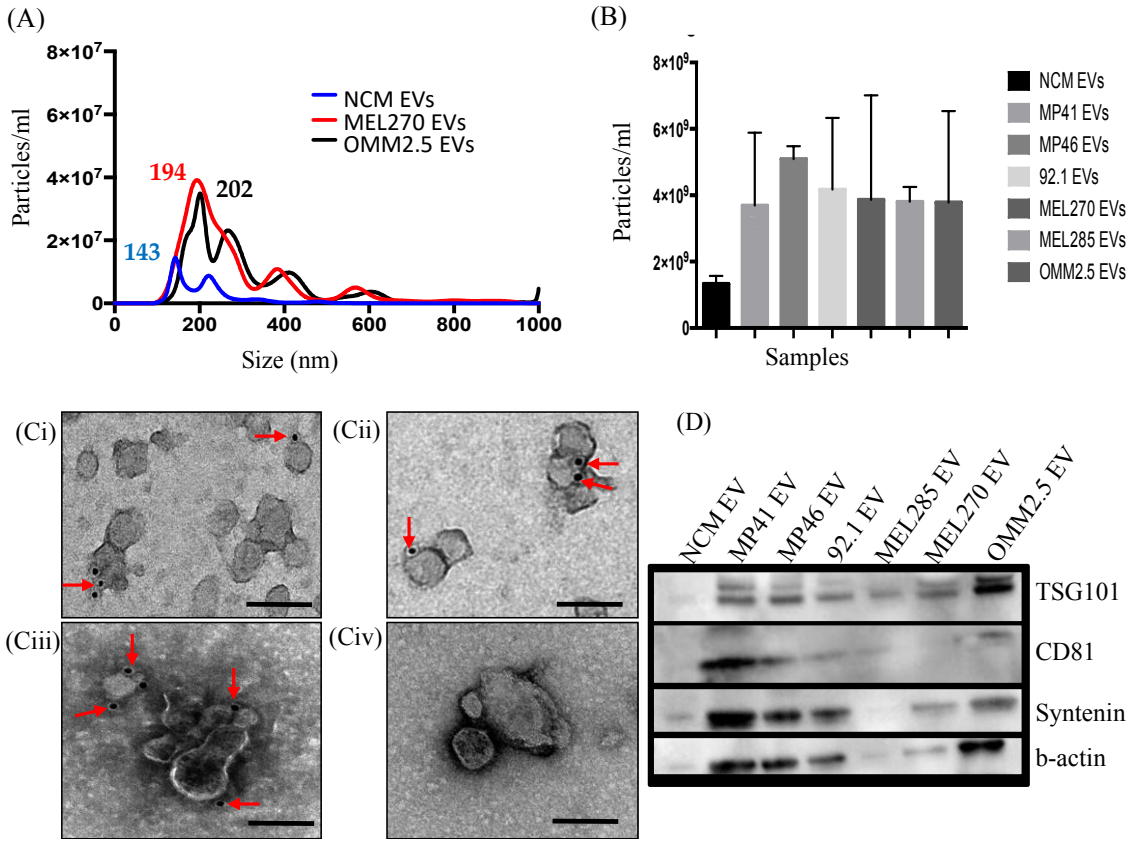

Figure 1. Characterization of extracellular vesicles (EVs) derived from normal choroidal melanocytes (NCMs) and Uveal Melanoma (UM) cells. (A and B) Nanoparticle tracing analysis NTA of EVs derived MEL270, metastatic UM cells (OMM2.5) and NCMs. (B) NTA data showing concentrations of EVs from different cell sources. Data are expressed as mean ± SD (n = 3). (C) Representative micrographs of immunoGold-TEM on MP46-EVs (Ci–Cii) 92.1-EVs (Ciii) and NCM-EVs (Civ) labelled with a cocktail of antibodies against CD81 (Ci), TSG101 (Cii) and CD63 (Ciii) (red arrows). Scale bars 200 nm. (D) Proteins isolated from EVs derived from different cell sources were analyzed by Western blot for the expression of specific exosome markers.

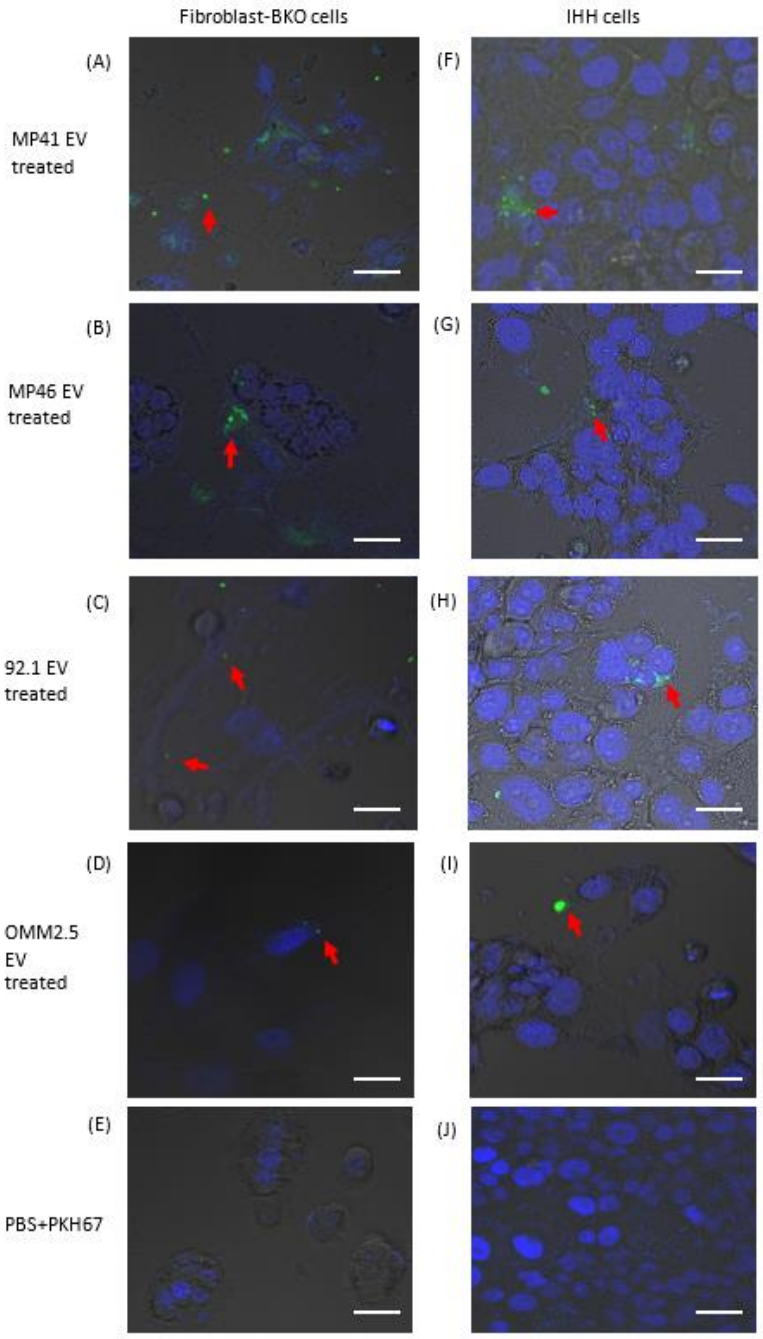

Figure 2. Isolated EVs were efficiently internalized by target cells. EVs from UM cells and NCMs were labeled with PKH67 dye and purified using Optiprep dentity gradient and ultracentrifugation. PKH67-labeled EVs were added to Fibro-BKO cells (A–D) and IHH (F–I). EV uptake (red arrows) was monitored under confocal microscopy 6 h later. (E,J) Cells were exposed to PKH67 solution processed as was the case for labeled EVs. Scale bars 20 μm.

2.3. Exposure to UM-EVs Increases the Proliferation, Migration and Invasion of Fibro-BKO Cells

EVs regulate different biological functions via the transfer of their cargo into target cells [46,47,51–54]. We have previously demonstrated that blood-derived EVs from patients with ocular and cutaneous melanoma are uptaken by and reprogram single oncosuppressor-mutated (SOM), such as Fibro-BKO cells into malignant cells [46–48]. We wanted to investigate the behavior of Fibro-BKO cells and analyze their growth potential when exposed to either culture medium without EVs (No-EVs), NCM-EVs or UM-EVs. Fibro-BKO cells were treated for 3 weeks, and their population doubling levels (i.e., PDL) were measured at successive cell passages. NCM-EVs did not affect the behavior of Fibro-BKO cells when compared to cells treated with EV-free culture medium (Figure 3A,B). When compared to Fibro-BKO cells exposed to NCM-EVs, cells treated with UM-EVs displayed increased proliferation as shown by the increase in cell PD, an effect that was significant at 3 weeks of exposure (1 PD increase with a range of 0.5 to 1.39) (Figure 3A,B). In parallel, we verified if exposure to cancer EVs altered cell viability *in vitro*. During the length of cell exposure (i.e., 3 weeks), we did not observe any effect of cancer cell-derived EVs on the percentage of viable cells (Figure S6).

Furthermore, we sought to investigate the effect of EVs on Fibro-BKO migration and invasion. EVs derived from NCM (2G.PPccF68Y) and UM cells (MEL270 and OMM2.5) were incubated with Fibro-BKO for 12 h and 24 h to analyze cell migration and invasion, respectively (Figure 3C–F). Fibro-BKO cells treated with UM-EVs exhibited higher migration and invasion compared to Fibro-BKO cells treated with NCM-EVs or only Phosphate Buffer Saline (PBS, vehicle). The migratory and invasion capacity of UM-EVs treated Fibro-BKO cells were approximately two times higher than those treated with NCM-EVs or PBS (Figure 3C–F). Moreover, Transwell invasion assay suggested that primary uveal melanoma derived EVs (MEL270) displayed enhanced invasion capability compared to metastatic uveal melanoma EVs (OMM2.5) (Figure 3E–F). Overall, these results indicate that UM-EVs enhance the proliferation, migration and invasion capabilities of Fibro-BKO cells compared to control groups (NCM-EVs or PBS).

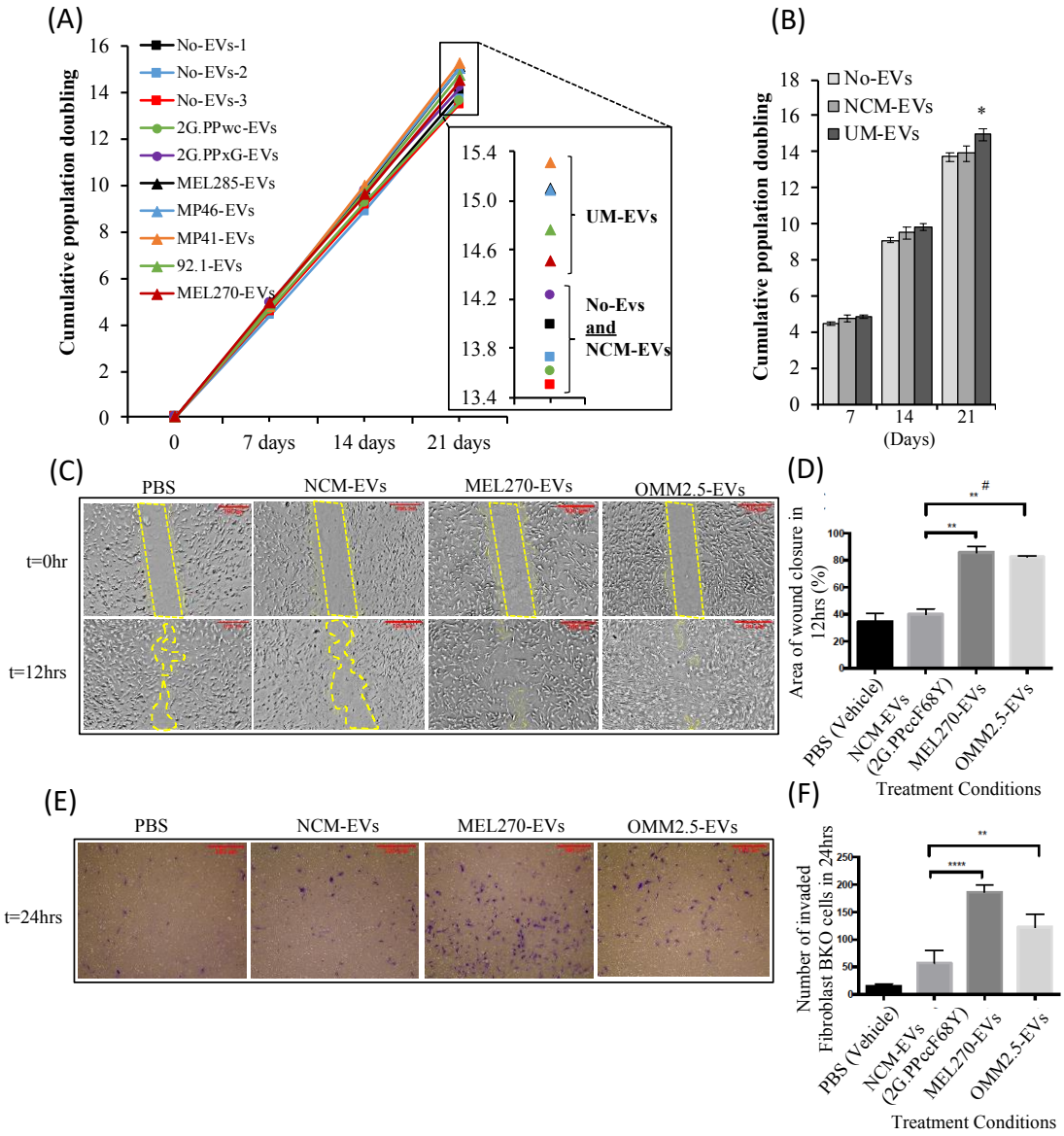

Figure 3. UM-EVs promote proliferation, migration and invasion of BRCA1-deficient fibroblast (Fibro-BKO) cells. (A–C) Fibro-BKO cells were cultured for 3 weeks in the presence of culture medium without EVs (No-EVs), NCM-EVs (from PPWc and PPxG eye donors) or UM-EVs. (A,B) Cells were analyzed for their growth potential by measuring population doubling capability at every passage. Data in inserts represent cumulative population doublings at the end of the treatment periods (A). Column graphs represent pooled data from three EV-free medium (No-EVs) samples, two NCM-EVs preparations and five UM-EVs preparations. Data are mean ± SD. p values < 0.05 (*) (B). (C–F) Fibro-BKO cells were cultured for 12 h (C,D; cell migration) or 24 h (E,F; cell

invasion) in the presence of culture medium without EVs (PBS), NCM-EVs or UM-EVs. Data are mean ± SD. (D) p value = 0.0086 (**), p value = 0.0051 (#). (F) p value = 0.0072 (**), p value < 0.0001 (****), MEL270 UM-EVs/OMM2.5 UM-EVs, p value = 0.0033 (**) (n = 3). Scale bar:100 μm, magnification 100×.

2.4. Fibro-BKO Cells Treated with UM-EVs Promote Tumor Growth *In Vivo*

Cancer EVs have been reported to regulate cancer invasion and metastasis [52,55–59]. Furthermore, we have previously shown that cancer EVs carrying mutated DNA and RNA induced malignant transformation of Fibro-BKO [60]. We analyzed the transforming abilities of UM-EVs on Fibro-BKO cells: at the end of a 3-week exposure to culture medium without EVs (No-EVs), NCM-EVs or UM-EVs, Fibro-BKO cells were inoculated subcutaneously into NOD/SCID mice. Mice injected with Fibro-BKO treated with EV-free culture medium or NCM-EVs did not develop any visible tumors at euthanasia (4 weeks following inoculation). In contrast, all mice injected with Fibro-BKO cells exposed to UM-EVs developed tumors with varying sizes (Figure 4A). Histopathological analyses of developing xenotransplants displayed features of adenocarcinomas (hematoxylin and eosin (H&E) staining) showing mitotic figures and high proliferation index (80–90% Ki67 positivity) (Figure 4B). Notably, we observed that UM-EVs-treated cells had completely changed their fate since developing tumors stained negative for vimentin, which is normally expressed on fibroblasts (Figure 4B). However, independent of UM-EVs used, we did not observe any positivity for MelanA, suggesting that fibroblast are refractory of phenotypic switch. Together, these data show that cancer UM-EVs significantly enhanced target Fibro-BKO cells proliferation, migration and invasion *in vitro* and induced their malignant transformation when injected into mice.

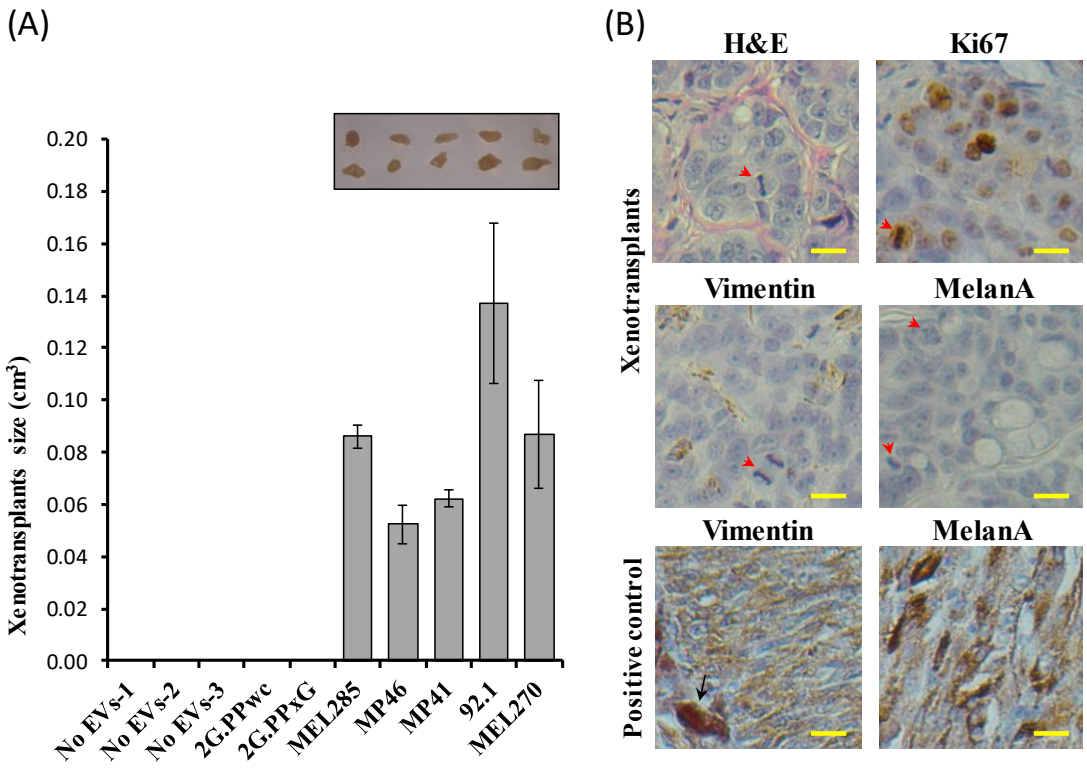

Figure 4. *In vivo* tumorigenicity assay of Fibro-BKO cells treated with UM-EVs (A)Exposed cells were injected subcutaneously into NOD/SCID mice that were monitored for 4 weeks for tumors growth. At euthanasia, developing tumors were excised and their sizes were measured. (B) Formalin-fixed paraffin-embedded tumors were processed for H&E staining, and immunolabeled with anti-Ki67, anti-Vimentin and anti-MelanA antibodies. Scale bar: 10 µm. Red arrowheads pointed to mitotic figures, and black arrow pointed to a melanophage. Positive controls are from choroidal melanoma specimens.

2.5. UM-EVs Carry Proteins Involved in Metastatic Niche Formation

To gain an in-depth understanding of EV protein cargo isolated from both UM cells and NCMs, we performed a whole proteome analysis by quantitative mass spectrometry (MS). We undertook these analyses to determine putative factors that might explain the effects we observed following treatments of target cells with EVs, in particular the factors that might underlie UM metastasis. Using a quantitative proteomic analysis, we identified 2154 proteins of which 1835 (85%) overlap with EV proteins previously reported in the Vesiclepedia database [61]. In addition,

we reported 319 novel proteins now added to the Vesiclepedia database (Figure 5A). Of the identified proteins, 33.06% (708 proteins) were shared between NCM-EVs and UM-EVs, whereas 66.93% (1433 proteins) were exclusive to UM-EVs and 1 protein was exclusive to NCM-EVs (Figure 5B). The shared proteins between the two datasets included typical EV protein signatures such as ESCRT components TSG101, CD81, CD63, CD9, and syntenin. Notably, each UM-EV set shared more proteins with other UM-EVs than with NCM-EVs. Comparing amongst cell lines, 60–80% of EV proteins from each UM cell line were found to overlap with every other UM cell line. In contrast, an average 33% of EV proteins from any UM cell line overlapped with NCM-EV proteins, which allows the conclusion that UM-EV cargo clustered differently from NCM-EV cargo (Figure 5C). In addition, tyrosinase related protein 1 (TYRP1; which is critical in the melanin biosynthesis pathway), melanotransferrin (MELTF) and melanocyte protein (PMEL) were present in almost all EV samples. Moreover, vimentin (VIM; an intermediate filament protein that is overexpressed in epithelial tumors such as UMs), melanoma-associated antigens D1 and D2 (MAGED1 and MAGED2) and melanoma antigen (MLANA) were present mainly in UM-EVs when compared with NCM-EVs. Altogether, these data indicate that the isolated EVs have a melanocytic origin.

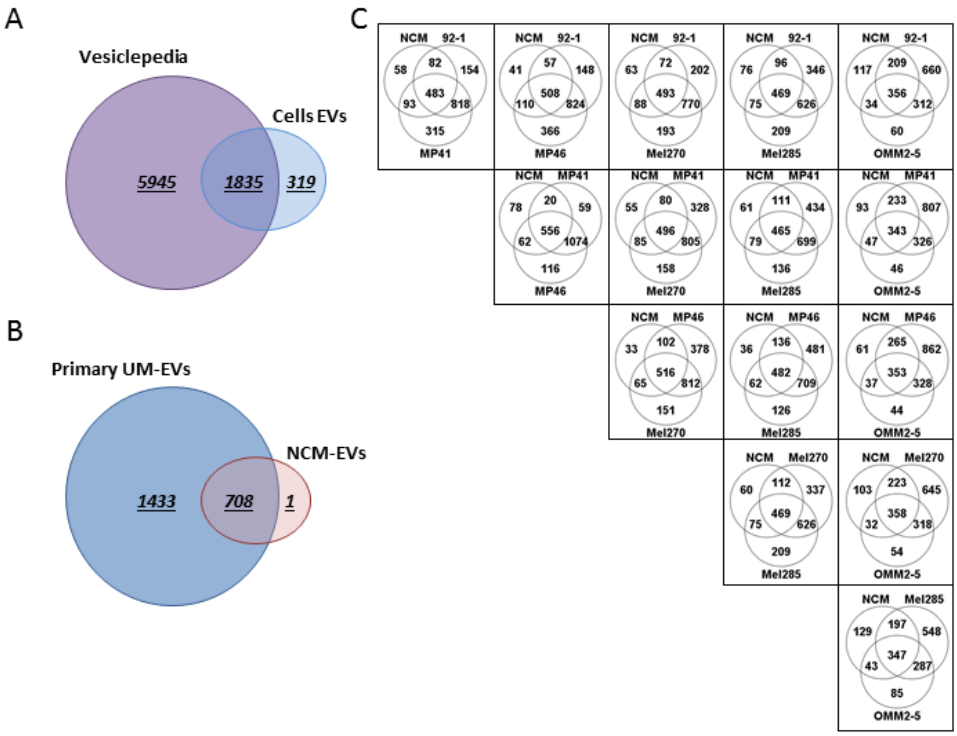

Figure 5. UM-EVs and NCM-EVs carried different sets of proteins. Venn diagram analyses. (A) The majority of proteins isolated from EVs derived from UM cells and NCMs were shared with data published in Vesiclepedia database. (B) NCM-EVs and primary UM-EVs shared 708 proteins, while 1 and 1433 proteins were exclusively present in NCM-EVs and primary UM-EVs, respectively. (C) Based on their protein cargo, primary UM-EVs clustered differently from NCM-EVs. A total of 20 to 265 proteins were exclusively shared between NCM-EVs and primary UM-EVs, while 287 to 1074 proteins were exclusively shared between EVs isolated from the different primary UM lines.

Extensive comparisons of EV cargo in primary UM cell lines and NCMs were conducted (Figure 6). In relation to NCM-EVs, we found that 232 proteins were upregulated and 76 proteins were downregulated in UM-EVs (Figure 6A,B). Of the upregulated proteins, 200 were exclusively present in UM-EVs (Table S2). To identify the physiological processes to which these EVs-derived proteins are implicated, we clustered the most differentially expressed proteins (i.e., 232 overexpressed and 76 down-expressed in UM-EVs) into gene ontology (GO) categories using the DAVID bioinformatics platform (Table S4). Characterization by biological process highlighted categories consistent with the known functions of EVs. Upregulated proteins primarily clustered in the categories of cell-cell adhesion, small GTPase mediated signal transduction, and movement of cell or subcellular component (Figure 7A). Various other categories were present with lower protein counts but similar significance values ($p < 0.05$). These included leukocyte transendothelial migration, signaling cascades (VEGFR, Wnt, MAPK), cell division and migration. In contrast, down-regulated proteins clustered mainly in homeostatic processes such as endocytosis, immune response, retina homeostasis and platelet degranulation (Figure 7A). Molecular functions clustering using Kyoto Encyclopedia of Genes and Genomes (KEGG) pathway analysis revealed that UM-EVs were enriched in proteins involved in cell motility and cellular transit (actin cytoskeleton), cellular uptake (endocytosis, phagocytosis), and cancer associated signaling pathways (PI3K-Akt, Ras, Rap1, cAMP, Ras) (Figure 7B), whereas proteins related to immune escape of cancer, such as those involved in complement and coagulation cascades, were downregulated (Figure 7B).

(A)

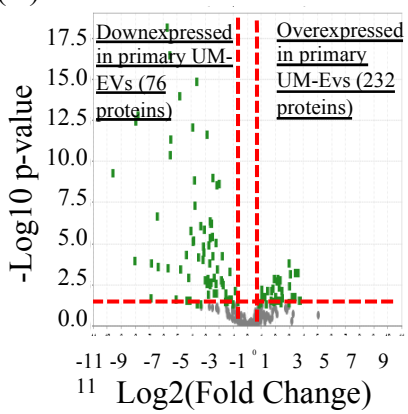
Downexpressed in primary UM-EVs (76 proteins)
Overexpressed in primary UM-Evs (232 proteins)
-Log10 p-value
17.5
15.0
12.5
10.0
7.5
5.0
2.5
0.0
-11 -9 -7 -5 -3 -1 0 1 3 5 7 9 11
Log2(Fold Change)

(B)

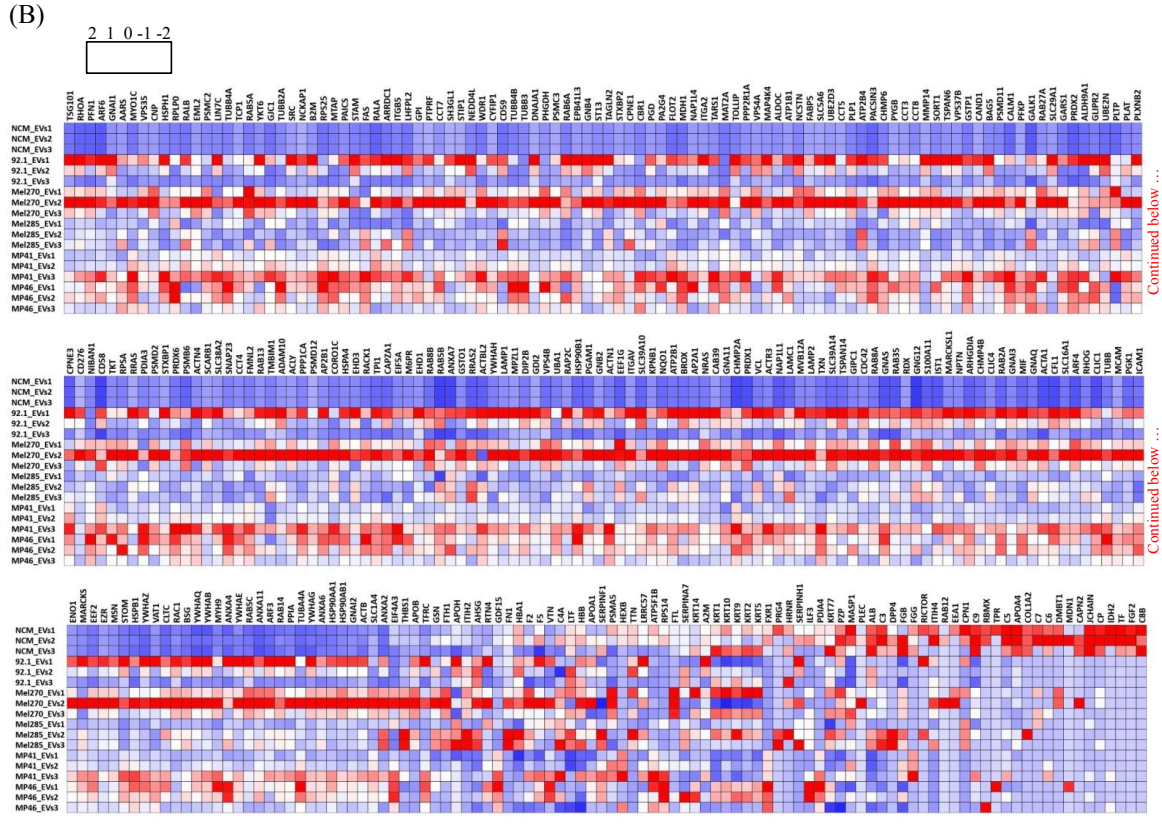
2 1 0 -1 -2
NCM_EVs1
NCM_EVs2
NCM_EVs3
92.1_EVs1
92.1_EVs2
92.1_EVs3
Mel270_EVs1
Mel270_EVs2
Mel270_EVs3
Mel285_EVs1
Mel285_EVs2
Mel285_EVs3
MP41_EVs1
MP41_EVs2
MP41_EVs3
MP46_EVs1
MP46_EVs2
MP46_EVs3
Continued below …
Continued below …

(C)

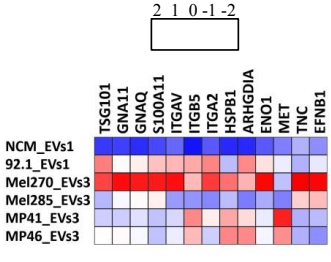
2 1 0 -1 -2
TSG101
GNA11
GNAQ
S100A11
ITGAV
ITGB5
ITGA2
HSPB1
ARHGDIA
ENO1
MET
TNC
EFNB1
NCM_EVs1
92.1_EVs1
Mel270_EVs3
Mel285_EVs3
MP41_EVs3
MP46_EVs3

(D)

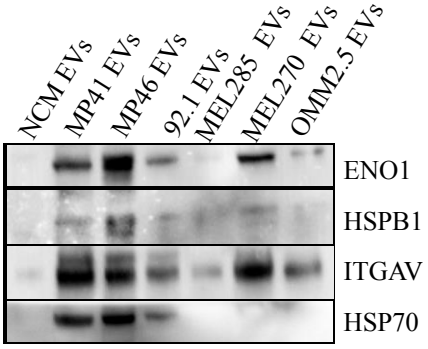
NCM EVs
MP41 EVs
MP46 EVs
92.1 EVs
MEL285 EVs
MEL270 EVs
OMM2.5 EVs
ENO1
HSPB1
ITGAV
HSP70

Figure 6. Primary UM-EVs are enriched in proteins involved in the regulation of tumor growth, homeostasis and metastasis organotropism. (A) Volcano plot representation of 308 proteins significantly and differentially expressed between primary UM-EVs and NCM-EVs. (B) Heatmap chart representing the 308 differentially expressed proteins. Note that primary UM-EV contents clustered differently from that of NCM-EVs. The full list of proteins is shown in Table S2. (C) Heatmap chart depicting the relative expression levels of proteins linked to tumorigenesis, cancer homeostasis, and metastasis organotropism. (D) Immunoblot validation of the relative expression levels of some proteins that emerged from MS data mining (see C). Note: HSP90 shown (Figure S7 (E)) was probed on a different membrane. In B,C, the key color represents Log(2) of protein quantitative ration where blue and red refer to downexpressed and overexpressed proteins in UM-EVs, respectively.

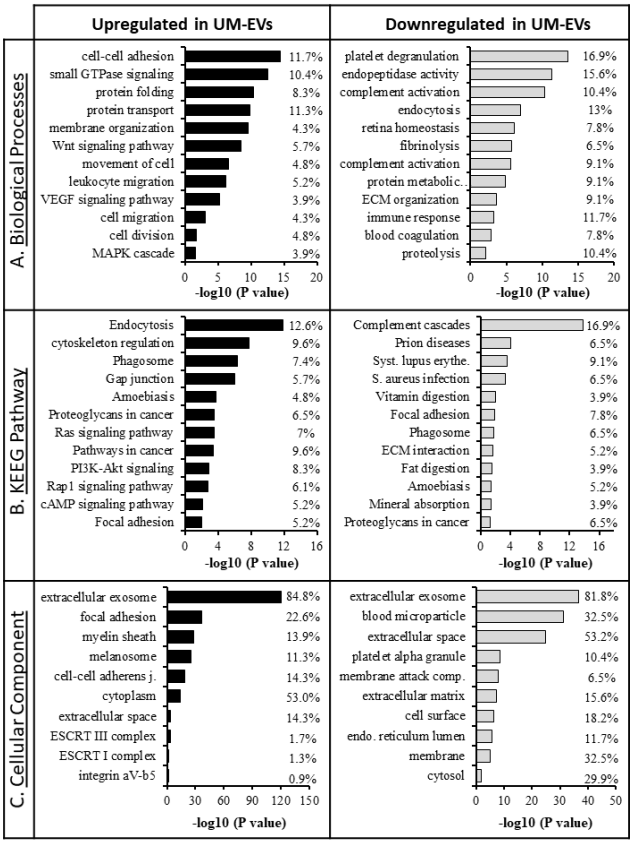

Figure 7. Gene ontology GO classification of proteomic data for differentially expressed proteins in primary UM-EVs and NCM-EVs. The most enriched categories in (A) biological process, (B) molecular function, and (C) cellular component. Left panel—UM-EVs, right panels—NCM-EVs.

Appropriately, when clustering the proteins based on cellular component, we found that the majority clustered into extracellular exosomes (i.e., EVs), for both upregulated and down-regulated groups (Figure 7C). There were certain cellular components exclusively present in the upregulated group, including ESCRT complexes I and III, and the integrin alpha v beta v (ITGαvβv) complex that were found to be significant ($p < 0.05$). UniProt tissue expression analysis [62] associated the UM-EVs proteins with Cajal-Retzius cells, B-cell lymphoma, brain, epithelium, liver and lung. In the down-regulated EV protein group, no proteins were found to be associated with the lungs and 35 proteins were clustered with the liver category, while the upregulated proteins had 58 total proteins in liver and 62 in lung categories.

We then mined our data by focusing on proteins that regulate tumor growth and those that modulate the metastatic niche environment (Figure 6C). The majority of upregulated proteins have been previously linked to tumorigenesis or cancer homeostasis, including signaling molecules (integrin αV, GNAQ, GNA11, the latter two being associated with UM tumorigenesis), molecular chaperon (HSPB1), and an ESCRT-I complex subunit (i.e., TSG101). Interestingly, integrin αV was associated with liver metastasis organotropism [56]. In addition, alpha-enolase (ENO1) was 11 times more expressed in UM-EVs than in NCM-EVs. This protein is a cancer cell surface biomarker found in EVs from melanoma and non-small cell lung carcinoma cells, and is expected to be used as a biomarker for many tumors [63,64]. Further, the chemoattractant S100A11 and ARHGDIA (RhoGDP) were upregulated in UM-EVs. Their expression is commonly increased in tumors and are often associated with tumor progression [65,66]. We validated the proteomic data by analyzing the expression of key proteins using immunoblotting (i.e., ENO1, HSPs, HSPB1 and integrin αV). Western blot analyses confirmed the pattern of protein expression as displayed in the heatmap chart from proteomic analyses (Figure 6D).

2.6. Metastatic UM-EVs Display Different Protein Expression Patterns Compared to Primary UM-EVs

To further analyze the differential protein cargo between primary and metastatic UM-EVs, we compared the expression of proteins in MEL270 primary UM cells and its metastatic derivative OMM2.5. Our analyses identified 1630 proteins of which 676 (42%) were shared, while 868 (53%) and 86 (5%) were exclusively expressed in MEL270 UM-EVs and OMM2.5 UM-EVs, respectively (Figure 8A). Notably, all primary UM-EVs shared more proteins with MEL270 UM-EVs (508 to 704 proteins) than with OMM2.5 UM-EVs (47 to 89 proteins), suggesting that primary UM-EV cargo clustered differently from metastatic UM-EV cargo (Figure 8B), and that these cargo regulated different cellular processes depending on donor UM cells (primary vs. metastatic).

When compared to OMM2.5-derived EVs, we found that 198 proteins were upregulated and 64 proteins were downregulated in MEL270-derived EVs (Figure 8C,D). Of the upregulated proteins, 116 were exclusively present in MEL270 UM-EVs (Table S3).

To determine the physiological processes associated with both primary and metastatic UM-EVs proteins, DAVID bioinformatics platform was utilized once more to functionally categorize proteins that demonstrated significant differential expression patterns between our primary UM cell line (MEL270) and the metastatic counterpart (OMM 2.5) (i.e., 198 overexpressed and 64 down-expressed in MEL270 UM-EVs secretions) (Table S5A,B). When referring to biological processes, the proteins upregulated in MEL270 UM-EVs clustered into leukocyte migration, small GTPase mediated signal transduction, integrin and tumor necrosis factor mediated signaling pathways, and MAPK cascade.

In contrast, the down-regulated proteins took part in platelet degranulation, extracellular matrix (ECM) organization and disassembly, ossification, and cell adhesion (Figure 9A). KEGG pathway analysis revealed upregulated proteins were mainly clustered into cellular uptake and processing (proteasome, endocytosis, phagocytosis), ECM-receptor interactions, and hematopoietic cell lineage, whereas downregulated proteins clustered mainly into ECM-receptor interaction, collagen and coagulation cascades, and immune responses. PI3K-Akt signaling and proteins commonly associated with small cell lung cancer were seen in both up and down-regulated protein groups (Figure 9B). Clustering proteins by cellular components found an enrichment for extracellular exosome associated proteins, consistent with previous data (Figure 9C).

When we mined the differentially expressed proteins by focusing solely on those involved in metastasis regulation (Figure 8E), we found that overexpressed proteins in MEL270 UM-EVs

belong to factors involved in metastasis organotropism (different classes of integrins, Coronin 1C and CD151), and mainly liver metastasis (i.e., ITGA5/B5) [56]. Other overexpressed proteins in MEL270 UM-EVs are involved in growth regulation (i.e., PCNA and CDK1) [67,68]. In contrast, we found that overexpressed proteins in OMM2.5 UM-EVs are those implicated in extracellular matrix (ECM) organization at metastatic niche sites. These include collagens, ECM1 and matrix metalloproteases (i.e., MMP2) [69–71]. These data suggest that while proteins carried in primary UM-derived EVs mainly helped in metastatic organotropism, those transported by metastatic counterparts were more involved in the maintenance of the metastatic niche.

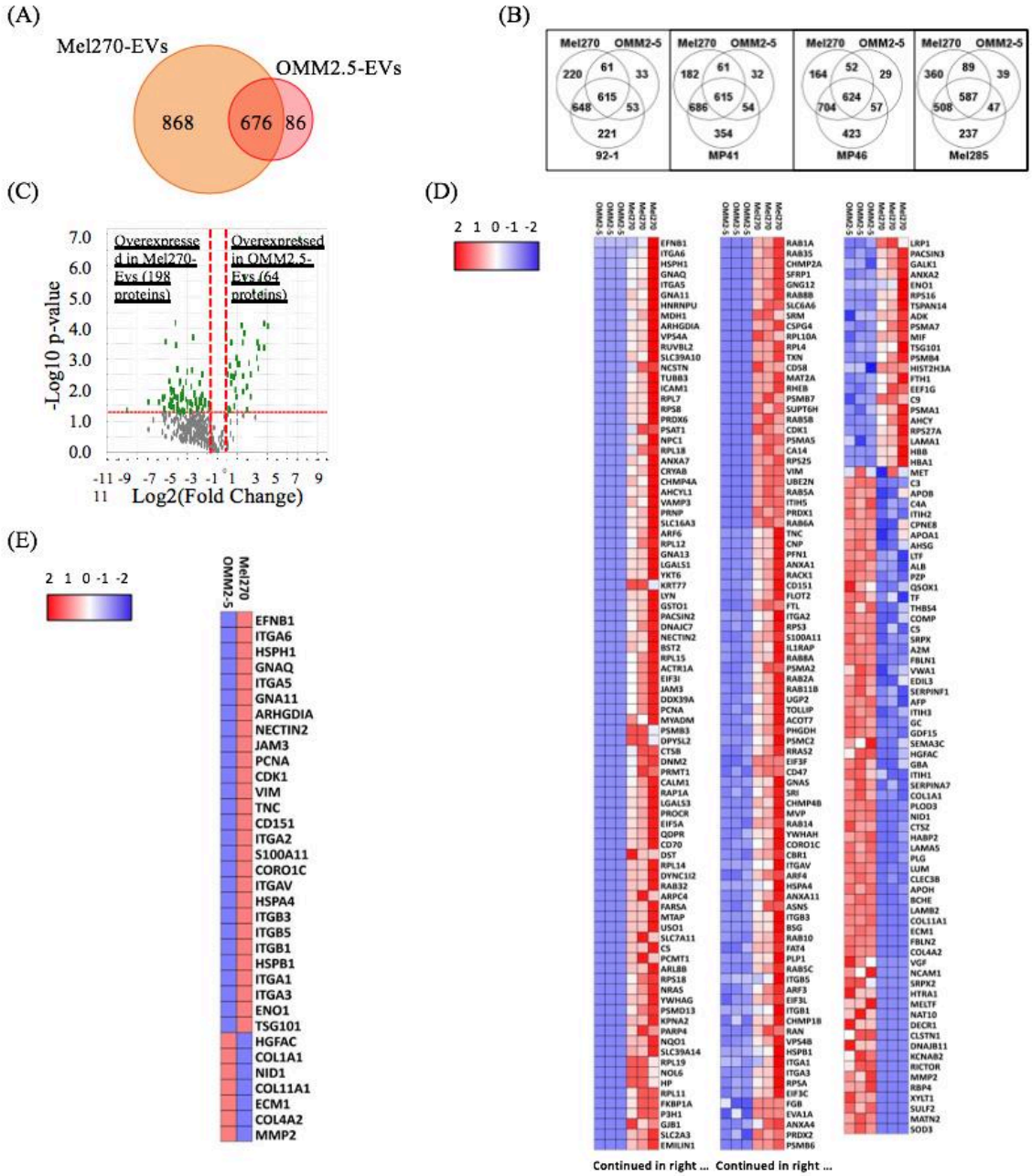

Figure 8. Primary UM-EV protein cargo clustered differently from that of metastatic UM-EVs. (A,B) Venn diagram analyses. Primary and metastatic UM-EVs shared 676 proteins, while 868 and 86 proteins were exclusively present in primary MEL270 UM-EVs and metastatic OMM2.5 UM-EVs, respectively (A). Based on their protein cargo, primary UM-EVs clustered differently from metastatic UM-EVs. 47 to 89 proteins were exclusively shared between primary UM-EVs and metastatic UM-EVs, while 508 to 704 proteins were exclusively shared between EVs isolated from the different primary UM lines (B). (C) Volcano plot representation of 262 proteins significantly and differentially expressed between primary and metastatic UM-EVs (MEL270 vs. OMM2.5). (D) Heatmap chart representing the 262 differentially expressed proteins. Note that primary MEL270 UM-EV contents clustered differently from that of metastatic OMM2.5 UM-EVs. The full list of proteins is shown in Table S3. (E) Heatmap chart depicting the relative expression levels of proteins linked to metastasis organotropism and metastasis regulation. In (D,E), the key color represents Log(2) of protein quantitative ration where blue and red refer to downexpressed and overexpressed proteins, respectively.

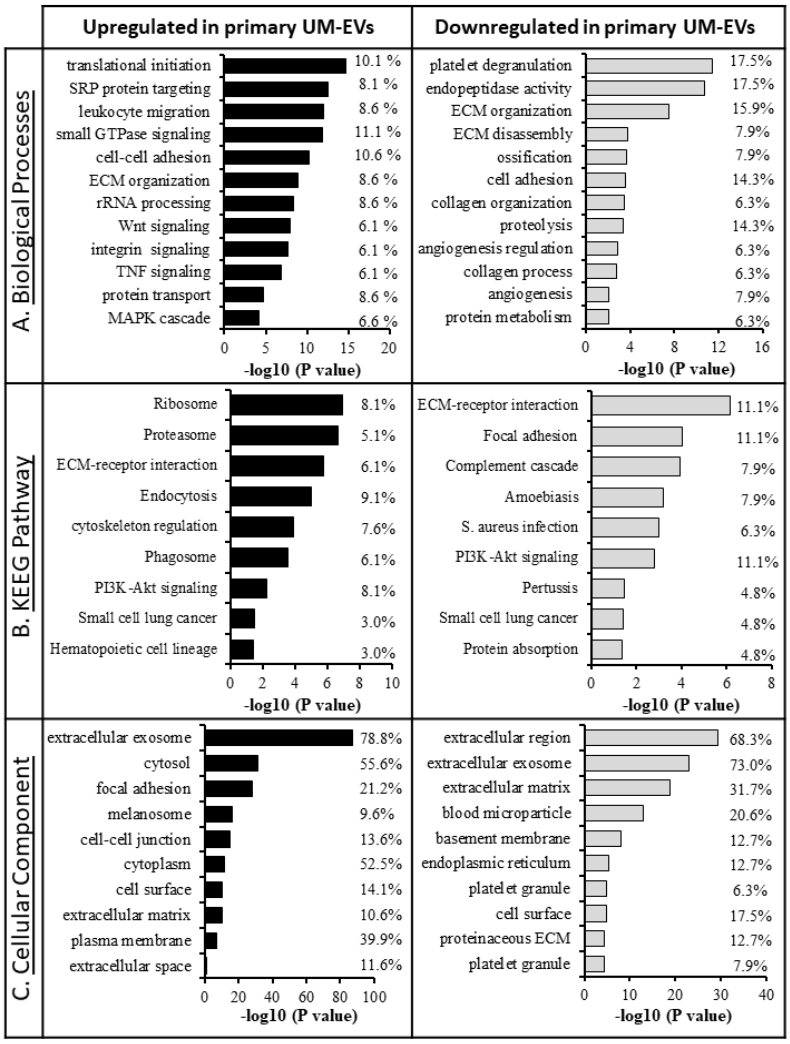

Figure 9. GO classification of proteomic data for differentially expressed proteins in primary MEL270 UM-EVs and metastatic OMM2.5 UM-EVs. The most enriched categories in (A) biological process, (B) molecular function, and (C) cellular component. Left panel—primary UM-EVs, right panels—metastatic UM-EVs.

3. Discussion

UM is the only malignancy in which diagnosis is made by clinical examination and generally without a biopsy. Unfortunately, the very limited number of metastatic UM cases that are deemed appropriate for surgical resection limits the possibility to obtain surgical samples that can be analyzed to understand the metastatic process. Given the high mortality rate, the asymptomatic nature and the lack of monitoring biomarkers, a liquid biopsy platform would be extremely

valuable in the diagnosis and treatment of UM. Attempts have been made to profile miRNA contents of UM-isolated exosomes [42,43], as well as the proteome from both UM secretome and UM-derived EVs [22,44,45]. However, research focusing on reliable and clinically valuable metastatic biomarkers in UM has remained limited, and an in-depth analysis of the protein composition of EV cargo in UM is virtually not available. Furthermore, studies addressing the differential expression pattern of EV cargo proteins between normal melanocytes and melanoma cells have been neither done nor published. It was already known that circulating EV levels increase with advancing stages of cancer, suggesting potential roles in cancer progression and invasion [72]. Furthermore, we previously reported that EVs from different malignancies carry oncogenic factors that trigger malignant transformation in target cells [60]. In the present study, we wanted to verify whether EVs isolated from UM cell lines would trigger malignant transformation of Fibro BKO. Moreover, we wanted to perform a label-free LC-MS/MS analyses on proteins isolated from EVs derived from both UM cells and NCMs to determine potential factors that may underlay the observed biological effects and to apply the findings as a base for a liquid biopsy platform.

Considering that UM arises from melanocytes of the uveal tract [13] and due to the lack of a commercial source of normal uveal melanocytes we established a control line for comparative analyses isolating NCMs from the choroid tissue of donor eyes. The identity of NCMs was confirmed at both structural (cell shape) and phenotypical levels using a set of specific markers [49,73].

In our experiments we demonstrated that not only were UM-EVs efficiently internalized by Fibro BKO cells, but we also confirmed that these cells undergo dramatic changes after exposure to EVs as shown by increased proliferation, migration, invasion and acquisition of malignant characteristics. Moreover, factors carried by EVs belong to different molecular categories (i.e., DNA, mRNA, miRNA, proteins) and their roles in cancer biology have been extensively highlighted [32,74–77]. Recently, we provided evidence that cancer EVs actively transfer mutated cancer genes to target cells as well as a bulk of coding and non-coding RNAs acting as modulators of essential cellular pathways that impact cancer growth and progression [60]. Herein, we decided to deepen these analyses by focusing on UM-EV protein cargo.

The proteomic analyses performed in this study confirmed the differential expression of several proteins involved in cancer cell growth, movement and adhesion, and metastatic niche

remodeling. Although relatively rare, UM is a deadly disease mainly as a result of the high risk of metastases occurring primarily in the liver [18,78]. Our analysis revealed several typical proteins implicated in the establishment of premetastatic niche that were differently expressed in the EVs from UM cells compared to those from NCMs. It has previously been reported that tumor-derived EVs expressing ITGαvβv are implicated in liver metastasis organotropism [56]. We observed high integrin αV protein levels in all UM-EVs analyzed when compared to NCM-EVs. Concurrently, DAVID bioinformatic analysis demonstrated that key proteins involved in the ITGαvβv complex were statistically significant in our dataset ($p < 0.05$). In relation to the integrins present in our UM-EV samples, there was upregulation of various signal transduction molecules such as S100A. It has been demonstrated that when integrins carried in cancer EVs were internalized by target cells, they activate SRC phosphorylation and pro-inflammatory S100 gene expression [56]. Further, EVs from melanoma were found to upregulate S100 proteins in recipient target organ cells resulting in vascular leakiness and promotion of metastasis [79]. Taken together, this suggests that UM-EVs promote a tumor induced inflammatory response and metastatic niche formation. Such data may provide insight into UM's remarkable tropism to the liver.

Additionally, the expression patterns of both HSP90 and ENO1 were found uniformly increased across all UM-EVs. HSP90 is a molecular chaperone reported to be of crucial importance in cancer cell growth and survival owing to its involvement in promoting the MAPK and P13K/AKT pathways [80,81]. In similar fashion, ENO1 is linked to the AKT signaling pathway, is involved in promoting gastric cancer cell proliferation and metastasis and serves as a potential biomarker for certain cancers [72,74]. The PI3K-AKT signaling pathway was also highlighted in our KEGG pathway analysis as our UM-EVs contain a number of proteins linked to this signaling cascade. Other proteins involved in the process of metastasis were also identified in a set of UM-EVs (i.e., hepatocyte growth factor receptor tyrosine kinase (MET, in MP41 UM-EVs and MP46 UM-EVs), tenascin C (TNC, in MEL270 UM-EVs and MEL285 UM-EVs), ephrin-B2 (EFNB2, in MEL285 UM-EVs)) [82–84]. However, their expression was not uniformly increased in EVs derived from all UM cells.

Notably, when we mined for proteins differentially expressed between primary and metastatic UM-EVs (MEL270 UM-EVs vs. OMM2.5 UM-EVs), we found that primary UM-derived EVs were enriched for proteins involved in the regulation of cell growth (i.e., PCNA and CDK1) [67,68] and in metastatic organotropism (i.e., integrins, Coronin 1C and CD151) [56,85,86].

Coronin 1C is highly expressed in invasive human cancers and correlates positively with increased metastatic risk [85]. CD151 is a tetraspanin associated with tumor metastasis, and is correlated with poor prognosis, decreased overall survival and increased recurrence [86]. Similarly, HSPB1 [87] was also increased in EVs derived from MEL270. HSPB1 has been reported to play an important role in UM micrometastasis [87] and acts as switch between tumor dormancy and tumor progression in breast cancer [88]. In contrast, proteins transported by metastatic UM-EVs are involved in the maintenance of the metastatic niche, mainly ECM modeling and organization (i.e., collagens, ECM1 and matrix metalloproteases (i.e., MMP2)) [70,71,89–91]. Previously, we reported that collagen IV-conveyed signals are essential cues for liver metastasis in several tumor types including UM and identified mediators of collagen IV signaling as potential therapeutic targets in the management of hepatic metastases [70]. In addition, ECM1 promotes migration and invasion by inducing EMT [89], and MMP-2 is recognized as a crucial contributor to liver metastasis [71]

Our proteomic analysis unravels other markers that could be valuable as diagnostic and prognostic tools (i.e., Nidogen1; NID1). NID1 is a basement membrane glycoprotein that is involved in ECM cellular interactions, cell migration and invasion, promotes melanoma metastasis, and is correlated with poor clinical outcomes. In our study, high levels of NID1 were found in EVs derived from OMM2.5 (metastatic) cells. Previously, NID1 has been proposed as a new biomarker for disease progression and therapeutic target in breast cancer and melanoma [92].

In this study, we used an *in vivo* model to test whether UM-EVs could promote tumorigenesis. As shown by our group previously, exposure of cancer patient-derived EVs to single-oncogene mutated cells (such as Fibro-BKO, HEK 293 and PTEN KO MCF) resulted in malignant transformation of the recipient cells and induction of tumors *in vivo*. Here we injected NOD-SCID mice with Fibro-BKO cells exposed to UM cell-derived EVs and found a similar effect: Fibro-BKO cells exposed to UM cell-derived EVs developed tumors *in vivo*, while those exposed to NCM-derived EVs did not. Our *in vivo* study provides evidence that EVs derived from UM cancer cells have the potential to promote tumorigenesis in primed cells.

The selective enrichment of metastatic factors and signaling pathway components in UM-derived EVs will contribute to our overall understanding of the regulatory networks involved in the establishment of the tumor microenvironment. This information will be helpful in elucidating the pathophysiological functions of tumor-derived EVs, and aid in the development of UM

diagnostics and therapeutics. In light of the data shown here, further studies to assess the downstream pathways that are altered in recipient cells are needed. Furthermore, understanding the role EVs play in mediating pro-tumor and in particular pro-metastasis processes in target organs, such as the liver are needed. Finally, validation of protein signatures, and potential biomarkers, are needed in EVs isolated from UM patient blood.

4. Material and Methods

4.1. Cell Culture Conditions

Human eyes (n = 3, Table S1) were obtained from Centre universitaire d'ophtalmologie (Centre Hospitalier Universitaire de Québec, Canada), following an informed consent from the donor's next of kin. Eyes were used in accordance to a protocol approved by the IRB of the Research Institute (RI) of the McGill University Health Centre (MUHC) (IRB #2019-5314).

NCM cultures were established from donor eyes [49,73]. In brief, the cornea, lens, vitreous humor and iris were removed. A total of four incisions were made toward the optic nerve to obtain a petal-like structure (Figure S1). The choroid was detached from the sclera, transferred into a solution of 0.02% EDTA at 37 °C for 30 min, and incubated in a mixture of collagenases IA and IV in trypsin (0.5 mg/mL each) (Sigma-Aldrich, St. Louis, MO, USA) to remove retinal pigment epithelium (RPE) cells. The choroid was then incubated in dispase II (Boehringer Ingelheim, Ingelheim am Rhein, Germany) and diluted in Melanocyte Growth Medium M2 medium (Promocell, Heidelberg, Germany) for 18 h at 37 °C. The reaction was stopped in Complete Protease Inhibitor Cocktail (Roche Diagnostics, Mannheim, Germany). Digested tissue was shaken to obtain single cell suspensions. Cells were passed through a 40 µm cell strainer, pelleted at 100 g for 5 min, resuspended in M2 medium, and cultured on FNC (0407, Athena, Baltimore, MD, USA) coated T25 tissue culture flasks. Culture medium was changed every three days. After reaching 80% confluency, cells were cryopreserved in liquid nitrogen using cryo-SFM (PromoCell, Heidelberg, Germany) for further usage. In the case of contamination with RPE cells or fibroblasts, culture medium was supplemented with 100 µg/mL geneticin (Sigma-Aldrich) for 7 days prior to subcultivation.

MP41, MP46 and 92.1 were purchased from ATCC (American Type Culture Collection). MEL270, MEL285 and OMM2.5 were kindly gifted by Dr. Vanessa Morales (University of

Tennessee), human BRCA1-deficient fibroblasts were from Dr. Goffredo Arena and Immortalized human hepatocytes were gifted by Dr. Peter Metrakos (McGill University).

UM cell lines (MP41, MP46, 92.1, MEL 270, MEL285 and OMM2.5) were maintained in Roswell Park Memorial Institute media (RPMI 1640) supplemented with 10% Fetus Bovine Serum, 0.1% 10U/mL penicillin and 10 μg/mL streptomycin, 4 mM L-glutamine and 10 μg/mL insulin, 1 mM NaPyruvate. All the media components were purchased from Corning. Human BRCA1-deficient fibroblasts (Fibro-BKO) [47] and immortalized human hepatocytes (IHH) were maintained in DMEM-F12 medium supplemented with 10% FBS, and penicillin-streptomycin antibiotics.

4.2. EV Isolation

UM cell lines were cultured in T75 flasks until they reached 80% confluency; then cell culture medium was replaced by medium supplemented with EV-depleted FBS. NCM cells were cultured in T25 flasks in M2 medium until they reached 80% confluency; then medium was changed with fresh M2 medium. Cells were allowed an additional 24 h incubation before conditioned media collection. Conditioned media from all cell cultures were subjected to a series of sequential differential centrifugation steps. The supernatants were centrifuged at 500 g for 10 min to remove contaminating cells, followed by centrifugation at 2000 g for 20 min to remove cell debris. Supernatants were passed through a 0.2 μm syringe filter (Corning), transferred to 26.3 mL polycarbonate tubes (# 355618; Beckman Coulter), and centrifuged at 16,500× g for 20 min at 4 °C to remove apoptotic bodies and cell debris. Supernatants were transferred to new 26.3 mL polycarbonate tubes and ultracentrifuged at 120,000× g (40,000 rpm) for 70 min at 4 °C using 70 Ti rotor in Optima XE ultracentrifuge machine (Beckman Coulter). The crude EVs pellets were washed with PBS at 120,000× g for 70 min at 4 °C, resuspended in 500 μL PBS, and stored in -80 °C until use.

For proteomic analyses of EVs, samples were purified using iodixanol (OptiPrep™ density gradient[93,94] (Sigma-Aldrich). Briefly, a density gradient was prepared by serial dilutions of iodixanol stock (60% w/v): (i) five volumes of 60% iodixanol were mixed with 1 volume of 0.25 M sucrose, 0.9 M NaCl and 120 mM HEPES solution (pH 7.4) to obtain 50% iodixanol, (ii) 2 volumes of 50% iodixanol were mixed with three volumes of 0.25 M sucrose, 150 mM NaCl and 20 mM HEPES (SNH) solution (pH 7.4) to obtain 20% iodixanol, and (iii) 1 volume of 50%

iodixanol was mixed with 9 volumes of SNH solution to prepare 5% iodixanol. EVs in 1.92 mL of HEPES-buffer were mixed with 2.88 mL of 50% iodixanol to obtain EVs-containing 30% iodixanol solution. The discontinuous iodixanol density gradient was prepared by carefully layering 2.5 mL of 5% iodixanol and 3 mL of 20% of iodixanol sequentially with the help of stainless steel 316 syringe needle (Sigma-Aldrich) in 13.26 mL Ultra-Clear tubes (Beckman Coulter). EVs in 30% iodixanol solution (4.8 mL) were carefully placed at the bottom of the tubes containing the iodixanol gradients using the syringe needle without disturbing the gradient. Tubes were spun at 38,000 rpm for 2 h using SW41 Ti swinging bucket rotor in LS8 ultracentrifuge at 4 °C. One millilitre fractions were collected (n = 10), diluted in PBS and centrifuged at 120,000× g for 70 min. The pellet of each fraction was resuspended in PBS and stored for EV characterization (i.e., NanoSight for nanoparticle tracing analysis (NTA) (Figure S8), Western blot (Figure S9) and transmission electron microscopy (TEM) (Figure S10)). In parallel, a control iodixanol density gradient was centrifuged with the sample. After centrifugation, 1 mL fractions were collected and 100 µL of each fraction was added to 96-well plates to read the absorbance at 340 nm to determine its density. Fraction 3 was enriched in EVs and was used for further analyses (Figure S5)

4.3. EV Characterization: TEM and Size Distribution Analyses

For TEM, EVs were processed in 0.1% sodium cacodylate washing buffer (250 mL EMS, 35× g sucrose, 250 mL water) and centrifuged at 120,000× g for 70 min. EV pellets were resuspended in 2.5% glutaraldehyde fixation solution (250 mL EMS, 50 mL 25% glutaraldehyde, 250 mL water). 10 µL of fixed EVs was put on TEM copper grids and left to settle for 20 min. Grids were washed with 0.02 M glycine for 10 min, and EVs were blocked in 2% bovine serum albumin/2% casein/0.5% ovalbumin solution. Primary antibodies (CD63, CD81, TSG101) were applied for overnight incubation at 4 °C in blocking buffer in 1:1 ratio. Grids were washed in Dulbecco's PBS (DPBS) and incubated with 20 nm gold anti-mouse (ab27242) and 10 nm gold anti-rabbit-conjugated secondary antibodies (ab272234) (1:20 ratio) at room temperature for 30 min. After washing with DPBS, EVs were stained with 4% uranyl acetate for 3 min and air-dried overnight. The grids are examined using FEI Tecnai^{TM} G2 Spirit BioTwin 120 kV Cryo-TEM. To quantitatively assess the size of the EVs, at least 100 vesicles were counted. In parallel, an aliquot of 5 µL of EVs sample was run on a Nanosight NS500 system (Nanosight Ltd., Amesbury, UK),

and the concentration and size distribution was analyzed using the NTA 1.3 software (Malvern Panalytical).

4.4. Cell Exposure to EVs

Fibro-BKO were used as target cells to analyze the biological effects of EVs isolated from NCMs and UM cell lines. When Fibro-BKO reached 30% confluence, they were treated with complete DMEM-F12 medium supplemented with 10^8 EVs/mL. At 80–90% cell confluency, cells were passaged 1 in 6 using 0.05% Trypsin-EDTA (Wisent). Cell count and viability was assessed using a hemocytometer and trypan blue exclusion staining.

4.5. Population Doubling Level (PDL) Calculation

Cells were considered at population doubling zero at the first time they were exposed to NCM-EVs or UM-EVs. At every passage, cell number was determined and population doubling was calculated using the following formula; PDL = log(Nh/Ni)/log2, where Nh is the number of cells harvested at the end of the incubation time and Ni is the number of cells inoculated at the beginning of the incubation time. Cumulative PDL was calculated by adding the previous calculated PDL.

4.6. EV Labeling and Cellular Uptake Assay

Isolated EVs were labeled with PKH67 green fluorescent probe according to the manufacturer's instructions (Sigma-Aldrich). Briefly, EVs were resuspended in Diluent C and mixed with equal volume of the stain solution (4 µL PKH 67 in 1 mL Diluent C) for 5 min. The reaction was stopped by adding 2 mL of 2% BSA. Control samples, consisting of EVs-free medium with Diluent C were run in parallel. All samples were passed through OptiPrep™ density gradient to purify EVs from unbound PKH67 dye. Fraction 3 (enriched in EVs, see previous sections) was collected from both control (PBS + PKH67 dye) and samples (EVs + PKH67 dye), and centrifuged at 120,000× g for 70 min at 4 °C. Pellets were resuspended in culture medium and added to Fibro-BKO and IHH cultures in four-well chamber slides (Ibidi, Gräfelfing, Germany) for 6 h. Stained cells were visualized using an LSM780 confocal microscope (Carl Zeiss, Oberkochen, Germany).

4.7. Immunofluorescence

Cells (20,000) were plated in four-well chamber slides for 24 h, fixed with 4% paraformaldehyde for 30 min, permeabilized with 0.1% Triton X for 15 min, and incubated in

blocking buffer (1% BSA in PBS) for 1 h. Primary antibodies against MLANA (MelanA) (TA801623), Vimentin (ab92547), HMB45 (sc-59305), S100 (ab4066), cytokeratin 18 (ab32118), cytokeratin 8 (ab59400) were added to cells at 1:1000 in blocking buffer and incubated overnight at 4°C. Slides were washed 5 times in PBS, and cells were counterstained for 1 h with fluorophore-conjugated secondary antibodies (1:1000 in blocking buffer). Cells were washed in PBS and the slides were mounted on coverslips with NucBlue (R37605; ThermoFisher, Waltham, MA, USA). Cells were visualized using an LSM780 confocal microscope.

4.8. Migration Assay

Cell migration was evaluated using wound-healing assay. Briefly, Fibroblast-BKO cells were seeded into 12 well plate at a density of 0.5×10^6 cells per well. After reaching confluence, the monolayers were scratched using 200 µL pipette tips and washed twice with PBS. Fresh complete media was added with EVs (NCM-EVs, MEL270 UM-EVs, OMM2.5 UM-EVs) or without EVs (PBS, vehicle) and photographed at 0 h and 12 h using inverted microscope at 100× magnification. The areas of wound closure were calculated using ImageJ software (ImageJ 1.53a, https://imagej.nih.gov/ij/). The wound-healing assay was carried out in triplicate (n = 3).

4.9. Transwell Invasion Assay

Invasion assay was conducted using the croning® BioCoatTM Matrigel® invasion chamber (354480) according to the manufacturer's protocols. Briefly, the inserts were rehydrated with DMEM medium for 2 h in the incubator. A total of 5×10^5 Fibroblast BKO cells pretreated with EVs derived from NCM (2G.PPccF68Y), MEL270 and OMM2.5 or control (without EVs treatments), were seeded onto the matrigel coated insert in 400 µL serum-free DMEM. Then, 750 µL of DMEM with 10% FBS was added into the lower well of the Transwell chamber. After 24hrs of incubation in the incubator (at 37 °C, 5% CO_2), the membrane of the insert was stained with a staining solution (Millipore Sigma, ECM508) for 20 min at room temperature. The inserts were washed twice with distilled water and the cells on the upper surface (non-invaded) of the insert were removed by scrubbing with cotton tipped swabs and washed away with distilled water. Finally, the invaded cells were counted under the inverted microscope at 100X magnification. At least five images were taken at random location per insert and transwell invasion assay was performed in triplicates (n = 3).

4.10. Protein Isolation from Cells and EVs

EVs and cells were lysed using RIPA buffer supplemented with Complete™ mini protease inhibitor (Sigma-Aldrich) at 4 °C for 30 min. Samples were pulse sonicated for 2 s (three times), and were spun at 13,000× g for 30 min at 4 °C. Supernatants were quantified using micro BCA and Pierce BCA (Fisher Scientific) for EVs and cells, respectively. Proteins samples were processed for Western blot and proteomic analyses by mass spectrometry.

4.11. Western Blot

25 µg of cell proteins and 10 µg of EVs proteins were separated using 12% precast polyacrylamide gel and transferred onto polyvinylidene fluoride (PVDF) membranes (BioRad, Hercules, CA, USA). Membranes were blocked for 1 h in 5% non-fat dry milk in Tris buffer saline with 0.05% Tween-20 (TBST). Membranes were probed with anti-TSG101 (1:1000) (ab125011), anti-CD63 (1:1000) (ab59479), anti-CD81 (1:1000) (ab109201) GM130 (ab59400) (all from abcam, Cambridge, United Kingdom), and β-actin (1:10000) (A2228-200 µL) (Sigma-Aldrich). Membranes were washed in TBST and were treated with corresponding horseradish peroxidase-conjugated secondary antibodies anti-rabbit hP (7074S) and anti-mouse hP (7076P2) (Cell Signalling Technology, Denver, MA, USA). Blots were developed using ECL prime Western blot detection (GE healthcare, Chicago, IL, USA) and visualized using the ChemiDoc™ XRS+ System (Biorad, Hercules, CA, USA).

4.12. Label-Free LC-MS/MS Proteomics Analysis of EVs and Database Search

LC-MS/MS proteomic analyses were done on EVs proteins (10 µg) as previously described [95]. Samples were run in triplicates. Raw data were converted into *.mgf (Mascot generic format) to use the Mascot2.6.2 search engine (Matrix Science, London, United Kingdom) to search against human protein sequences (Uniprot 2019). The database search results were loaded onto Scaffold Q + Scaffold_4.10.0 (Proteome Sciences, London, United Kingdom) for spectral counting, statistical treatment, data visualization and quantification. Additional filters were applied, such as protein identification which was considered if they had quantifiable protein area in 2 or more of the biological triplicates, protein threshold greater than 99.0%, and peptide threshold greater than 95.0%. Samples with low total protein counts and low spectrum counts were excluded from the analyses. The identified protein list in Scaffold were exported to Microsoft Excel and uploaded

into the DAVID Bioinformatics database (Database for Annotation, Visualization and Integrated Discovery version 6.8) [95,96] for the analysis of functional gene enrichment and annotation, and KEGG pathway. In addition, bioinformatic analysis and Vesiclepedia database search were performed using the FunRich software (Functional Enrichment Analysis Tool version 3.1.3) [97].

4.13. *In Vivo* Tumor Growth

The 5-week-old female NOD-SCID mice (Jackson Laboratory) were used with approval and in compliance with the MUHC Animal Compliance Office (Protocols 2012–7280). All animal protocols were carried out according to institutional guidelines. Cells growing in log phase were harvested by trypsinization and washed twice with HBSS. Mice (n = 2 per group) were injected subcutaneously in the flanks with 2 million cells in 200 µL HBSS/Matrigel mixture. Mice were followed for tumor growth, and sizes of the xenotransplants were determined at euthanasia.

4.14. Immunohistochemistry Labelling Procedure

Mice xenotransplants were collected, fixed in 10% buffered formalin, embedded in paraffin, and stained with H&E (hematoxylin and eosin) according to standard protocols or processed for immunohistochemistry. Briefly, 5 µm tissue sections were dewaxed in xylene and rehydrated with distilled water. After antigen unmasking and blocking of endogenous peroxidase (3% hydrogen peroxide), the slides were incubated with rabbit anti-Ki67 (abcam, ab15580), rabbit anti-MelanA (abcam, ab51061) or rabbit anti-Vimentin (abcam, ab92547) primary antibodies. Labeling was performed using EnVision+ System-HRP anti-rabbit (Dako, K4003) and the Liquid DAB+ Substrate Chromogen System (Dako, K3468). Sections were counterstained lightly with Hematoxylin before mounting.

4.15. Statistical Analysis

Data were analyzed using Student's t test for unpaired samples. The criterion for significance (p value <0.05) was set as mentioned in figures.

5. Conclusions

Metastasis is rarely found during diagnosis of primary UM and many patients already have organ specific micrometastases by the time the ocular tumor is detected [98]. Moreover, CTCs have been detected at primary UM diagnosis, preceding the clinical detection of metastasis [99].

There remains an urgent need for tools that will aid in the screening and monitoring of tumor burden. As the molecular contents of EVs reflect their cellular origin, EVs derived from cancer patient plasma can prove vital to the understanding of tumor progression, metastatic risk and allow real time evaluations of therapeutic outcome. This ability renders them prone to be used in liquid biopsy for detection of cancer biomarkers [100,101]. In the present study, we profiled the proteome of pure preparations of EVs in the context of UM and characterized their behaviour. The next step is to perform a comparative proteome profiling of EVs derived from both healthy individuals and from patients presenting with either uveal nevi or melanoma, with the ultimate goal of developing a non-invasive method to detect UM metastasis with high sensitivity and specificity.

Supplementary Materials: The following are available online at https://www.mdpi.com/2072-6694/12/10/2923/s1 Figure S1: Isolation and maintenance of normal choroidal melanocytes (NCM). Figure S2: Phenotypical characterization of cultured human NCM. Figure S3: Nanoparticle tracking analysis of EVs derived from UM and NMC cells. Figure S4: Transmission electron microscope images displayed represented data of EVs derived from UM and NCM cells. Figure S5: Purification of PKH67-labelled EVs. Figure S6: UM-EVs did not affect the viability of Fibro-BKO cells. Figure S7: Complete Western-blot PVDF membrane. Figure S8: Measuring size and concentration of EVs derived from NCM (blue), MEL270 UM-EVs (red) and OMM2.5 UM-EVs (black). Figure S9: Western blot analysis of common EV marker CD63 (A) and control beta actin (B). Figure S10: Immunoelectron microscopy images of EVs isolated from MP41 (A) and MEL270 (B) cell lines. Table S1: Cells used in this study. Table S2: Differentially Expressed Proteins between NCM-EVs and primary UM-EVs ($p < 0.05$). Table S3: Differentially Expressed Proteins between primary MEL270 UM-EVs and metastatic OMM2.5 UM-EVs ($p < 0.05$). Table S4A: DAVID analysis of upregulated proteins between NCM-EVs and primary UM-EVs. Table S4B: DAVID analysis of downregulated proteins between NCM-EVs and primary UM-EVs. Table S5A: DAVID analysis of upregulated proteins between primary MEL270 UM-EVs and metastatic OMM2.5 UM-EVs. Table S5B: DAVID analysis of downregulated proteins between primary MEL270 UM-EVs and metastatic OMM2.5 UM-EVs. Table S5C: DAVID analysis of upregulated proteins between primary MEL270 UM-EVs and metastatic OMM2.5 UM-EVs. Lists of proteins clustered into the DAVID subcategories referred to in Figure 8. Table S5D: DAVID analysis of downregulated proteins between primary MEL270 UM-EVs and metastatic OMM2.5 UM-EVs. Lists of proteins clustered into the DAVID subcategories referred to in Figure 8.

Author Contributions: conceptualization, J.B., G.A, M.A. and T.T.; methodology, J.B., M.A. and T.T.; validation, M.A., T.T., A.L.; formal analysis, M.A., T.T., A.L.; investigation, M.A., T.T., A.L.; resources, J.B.; writing—original draft preparation, J.B., M.A., T.T., A.L.; writing—review and editing, J.B., M.A., T.T., A.L., P.B., S.P., E.J., G.A. and T.F.; supervision, J.B.; funding acquisition, J.B. ; All authors have read and agreed to the published version of the manuscript.

Funding: This work was supported by the start up funding of Julia Burnier (Department of Oncology, McGill University).

Acknowledgments: We would like to acknowledge the technical expertise and scientific support of the Proteomics and Histopathology facility of the MUHC-RI, especially Lorne Taylor and Amy Wong. We would also like to acknowledge the Facility for Electron Microscopy Research of McGill University especially Jeannie Mui and Kelly Sears for help in microscope operation. We would like to thank Janusz Rak for his generosity in allowing us to utilize Nanosight. Thank you also to Dongsic Choi for his help in the proteomic analysis of EVs. Thank you to the group of Solange Landreville (Laval University) for the help with the primary choroidal melanocyte culture.

Conflicts of Interest: The authors declare no conflict of interest.

References

1. Jovanovic, P.; Mihajlovic, M.; Djordjevic-Jocic, J.; Vlajkovic, S.; Cekic, S.; Stefanovic, V. Ocular melanoma: An overview of the current status. Int. J. Clin. Exp. Pathol. 2013, 6, 1230–1244.
2. Jager, M.J.; Brouwer, N.J.; Esmaeli, B. The Cancer Genome Atlas Project: An Integrated Molecular View of Uveal Melanoma. Ophthalmology 2018, 125, 1139–1142, doi:10.1016/j.ophtha.2018.03.011.
3. Ragusa, M.; Barbagallo, C.; Statello, L.; Caltabiano, R.; Russo, A.; Puzzo, L.; Avitabile, T.; Longo, A.; Toro, M.D.; Barbagallo, D.; et al. miRNA profiling in vitreous humor, vitreal exosomes and serum from uveal melanoma patients: Pathological and diagnostic implications. Cancer Biol. Ther. 2015, 16, 1387–1396, doi:10.1080/15384047.2015.1046021.
4. Krantz, B.A.; Dave, N.; Komatsubara, K.M.; Marr, B.P.; Carvajal, R.D. Uveal melanoma: Epidemiology, etiology, and treatment of primary disease. Clin. Ophthalmol. 2017, 11, 279–289, doi:10.2147/OPTH.S89591.

5. Field, M.G.; Harbour, J.W. Recent developments in prognostic and predictive testing in uveal melanoma. Curr. Opin. Ophthalmol. 2014, 25, 234–239, doi:10.1097/ICU.0000000000000051.
6. Kivelä, T.; Kujala, E. Prognostication in eye cancer: The latest tumor, node, metastasis classification and beyond. Eye 2013, 27, 243–252, doi:10.1038/eye.2012.256.
7. Coupland, S.E.; Lake, S.L.; Zeschnigk, M.; Damato, B.E. Molecular pathology of uveal melanoma. Eye 2013, 27, 230–242, doi:10.1038/eye.2012.255.
8. Harbour, J.W.; Chao, D.L. A molecular revolution in uveal melanoma: Implications for patient care and targeted therapy. Ophthalmology 2014, 121, 1281–1288, doi:10.1016/j.ophtha.2013.12.014.
9. Tarlan, B.; Kıratlı, H. Uveal Melanoma: Current Trends in Diagnosis and Management. Turk. J. Ophthalmol. 2016, 46, 123–137, doi:10.4274/tjo.37431.
10. Shields, J.A.; McDonald, P.R. Improvements in the Diagnosis of Posterior Uveal Melanomas. JAMA Ophthalmol. 1974, 91, 259–264, doi:10.1001/archopht.1974.03900060269004.
11. Rennie, I.G. Things that go bump in the light. The differential diagnosis of posterior uveal melanomas. Eye 2002, 16, 325–346, doi:10.1038/sj.eye.6700117.
12. Yang, J.; Manson, D.K.; Marr, B.P.; Carvajal, R.D. Treatment of uveal melanoma: Where are we now? Ther. Adv. Med. Oncol. 2018, 10, 1758834018757175, doi:10.1177/1758834018757175.
13. Carvajal, R.D.; Schwartz, G.K.; Tezel, T.; Marr, B.; Francis, J.H.; Nathan, P.D. Metastatic disease from uveal melanoma: Treatment options and future prospects. Br. J. Ophthalmol. 2017, 101, 38–44, doi:10.1136/bjophthalmol-2016-309034.
14. Papastefanou, V.P.; Cohen, V.M.L. Uveal melanoma. J. Skin Cancer 2011, 2011, 573974, doi:10.1155/2011/573974.
15. Ghazawi, F.M.; Darwich, R.; Le, M.; Rahme, E.; Zubarev, A.; Moreau, L.; Burnier, J.V.; Sasseville, D.; Burnier, M.N.; Litvinov, I.V. Uveal melanoma incidence trends in Canada: A national comprehensive population-based study. Br. J. Ophthalmol. 2019, 103, 1872–1876, doi:10.1136/bjophthalmol-2018-312966.
16. Aronow, M.E.; Topham, A.K.; Singh, A.D. Uveal Melanoma: 5-Year Update on Incidence, Treatment, and Survival (SEER 1973-2013). Ocul. Oncol. Pathol. 2018, 4, 145–151, doi:10.1159/000480640.

17. Virgili, G.; Gatta, G.; Ciccolallo, L.; Capocaccia, R.; Biggeri, A.; Crocetti, E.; Lutz, J.-M.; Paci, E.; Group, =EUROCARE Working Incidence of uveal melanoma in Europe. Ophthalmology 2007, 114, 2309–2315, doi:10.1016/j.ophtha.2007.01.032.
18. Kaliki, S.; Shields, C.L.; Shields, J.A. Uveal melanoma: Estimating prognosis. Indian J. Ophthalmol. 2015, 63, 93–102, doi:10.4103/0301-4738.154367.
19. Postow, M.A.; Kuk, D.; Bogatch, K.; Carvajal, R.D. Assessment of overall survival from time of metastastasis in mucosal, uveal, and cutaneous melanoma. J. Clin. Oncol. 2014, 32, 9074, doi:10.1200/jco.2014.32.15_suppl.9074.
20. Song, J.; Merbs, S.L.; Sokoll, L.J.; Chan, D.W.; Zhang, Z. A multiplex immunoassay of serum biomarkers for the detection of uveal melanoma. Clin. Proteom. 2019, 16, 10, doi:10.1186/s12014-019-9230-8.
21. Callejo, S.A.; Antecka, E.; Blanco, P.L.; Edelstein, C.; Burnier, M.N. Identification of circulating malignant cells and its correlation with prognostic factors and treatment in uveal melanoma. A prospective longitudinal study. Eye 2007, 21, 752–759, doi:10.1038/sj.eye.6702322.
22. Surman, M.; Stępień, E.; Przybyło, M. Melanoma-Derived Extracellular Vesicles: Focus on Their Proteome. Proteomes 2019, 7, 21.
23. van Niel, G.; D'Angelo, G.; Raposo, G. Shedding light on the cell biology of extracellular vesicles. Nat. Rev. Mol. Cell Biol. 2018, 19, 213.
24. Théry, C.; Witwer, K.W.; Aikawa, E.; Alcaraz, M.J.; Anderson, J.D.; Andriantsitohaina, R.; Antoniou, A.; Arab, T.; Archer, F.; Atkin-Smith, G.K.; et al. Minimal information for studies of extracellular vesicles 2018 (MISEV2018): A position statement of the International Society for Extracellular Vesicles and update of the MISEV2014 guidelines. J. Extracell. Vesicles 2018, 7, 1535750, doi:10.1080/20013078.2018.1535750.
25. Simpson, R.J.; Jensen, S.S.; Lim, J.W.E. Proteomic profiling of exosomes: Current perspectives. Proteomics 2008, 8, 4083–4099, doi:10.1002/pmic.200800109.
26. Jeppesen, D.K.; Fenix, A.M.; Franklin, J.L.; Higginbotham, J.N.; Zhang, Q.; Zimmerman, L.J.; Liebler, D.C.; Ping, J.; Liu, Q.; Evans, R.; et al. Reassessment of Exosome Composition. Cell 2019, 177, 428–445.e18, doi:10.1016/j.cell.2019.02.029.
27. Lee, T.H.; Chennakrishnaiah, S.; Meehan, B.; Montermini, L.; Garnier, D.; D'Asti, E.; Hou, W.; Magnus, N.; Gayden, T.; Jabado, N.; et al. Barriers to horizontal cell transformation by

extracellular vesicles containing oncogenic H-ras. Oncotarget 2016, 7, 51991–52002, doi:10.18632/oncotarget.10627.

28. Horibe, S.; Tanahashi, T.; Kawauchi, S.; Murakami, Y.; Rikitake, Y. Mechanism of recipient cell-dependent differences in exosome uptake. BMC Cancer 2018, 18, 47, doi:10.1186/s12885-017-3958-1.
29. Feng, D.; Zhao, W.-L.; Ye, Y.-Y.; Bai, X.-C.; Liu, R.-Q.; Chang, L.-F.; Zhou, Q.; Sui, S.-F. Cellular Internalization of Exosomes Occurs Through Phagocytosis. Traffic 2010, 11, 675–687, doi:10.1111/j.1600-0854.2010.01041.x.
30. Bellingham, S.A.; Coleman, B.M.; Hill, A.F. Small RNA deep sequencing reveals a distinct miRNA signature released in exosomes from prion-infected neuronal cells. Nucleic Acids Res. 2012, 40, 10937–10949, doi:10.1093/nar/gks832.
31. Di Vizio, D.; Morello, M.; Dudley, A.C.; Schow, P.W.; Adam, R.M.; Morley, S.; Mulholland, D.; Rotinen, M.; Hager, M.H.; Insabato, L.; et al. Large oncosomes in human prostate cancer tissues and in the circulation of mice with metastatic disease. Am. J. Pathol. 2012, 181, 1573–1584, doi:10.1016/j.ajpath.2012.07.030.
32. Kahlert, C.; Melo, S.A.; Protopopov, A.; Tang, J.; Seth, S.; Koch, O.; Zhang, J.; Weitz, J.; Chin, L.; Futreal, A.; et al. Identification of doublestranded genomic dna spanning all chromosomes with mutated KRAS and P53 DNA in the serum exosomes of patients with pancreatic cancer. J. Biol. Chem. 2014, 289, 3869–3875, doi:10.1074/jbc.C113.532267.
33. Brzozowski, J.S.; Jankowski, H.; Bond, D.R.; McCague, S.B.; Munro, B.R.; Predebon, M.J.; Scarlett, C.J.; Skelding, K.A.; Weidenhofer, J. Lipidomic profiling of extracellular vesicles derived from prostate and prostate cancer cell lines. Lipids Health Dis. 2018, 17, 211, doi:10.1186/s12944-018-0854-x.
34. Skotland, T.; Sandvig, K.; Llorente, A. Lipids in exosomes: Current knowledge and the way forward. Prog. Lipid Res. 2017, 66, 30–41, doi:10.1016/j.plipres.2017.03.001.
35. Théry, C.; Boussac, M.; Véron, P.; Ricciardi-Castagnoli, P.; Raposo, G.; Garin, J.; Amigorena, S. Proteomic Analysis of Dendritic Cell-Derived Exosomes: A Secreted Subcellular Compartment Distinct from Apoptotic Vesicles. J. Immunol. 2001, 166, 7309–7318, doi:10.4049/jimmunol.166.12.7309.

36. Liang, B.; Peng, P.; Chen, S.; Li, L.; Zhang, M.; Cao, D.; Yang, J.; Li, H.; Gui, T.; Li, X.; et al. Characterization and proteomic analysis of ovarian cancer-derived exosomes. J. Proteom. 2013, 80, 171–182, doi:10.1016/j.jprot.2012.12.029.
37. Zaborowski, M.P.; Balaj, L.; Breakefield, X.O.; Lai, C.P. Extracellular Vesicles: Composition, Biological Relevance, and Methods of Study. Bioscience 2015, 65, 783–797, doi:10.1093/biosci/biv084.
38. Inamdar, S.; Nitiyanandan, R.; Rege, K. Emerging applications of exosomes in cancer therapeutics and diagnostics. Bioeng. Transl. Med. 2017, 2, 70–80, doi:10.1002/btm2.10059.
39. Al-Nedawi, K.; Meehan, B.; Micallef, J.; Lhotak, V.; May, L.; Guha, A.; Rak, J. Intercellular transfer of the oncogenic receptor EGFRvIII by microvesicles derived from tumour cells. Nat. Cell Biol. 2008, 10, 619–624, doi:10.1038/ncb1725.
40. Aga, M.; Bentz, G.L.; Raffa, S.; Torrisi, M.R.; Kondo, S.; Wakisaka, N.; Yoshizaki, T.; Pagano, J.S.; Shackelford, J. Exosomal HIF1α supports invasive potential of nasopharyngeal carcinoma-associated LMP1-positive exosomes. Oncogene 2014, 33, 4613–4622, doi:10.1038/onc.2014.66.
41. Xu, J.; Liao, K.; Zhou, W. Exosomes Regulate the Transformation of Cancer Cells in Cancer Stem Cell Homeostasis. Stem Cells Int. 2018, 2018, 4837370, doi:10.1155/2018/4837370.
42. Kilic, E.; Smit, K.; van Poppelen, N.; Lunavat, T.; Derks, K.; Vaarwater, J.; Verdijk, R.; Mensink, H.; Lötvall, J.; de Klein, A. miRNA profiling of uveal melanoma exosomes as a metastatic risk biomarker. Acta Ophthalmol. 2017, 95, doi:10.1111/j.1755-3768.2017.03642.
43. Eldh, M.; Olofsson Bagge, R.; Lässer, C.; Svanvik, J.; Sjöstrand, M.; Mattsson, J.; Lindnér, P.; Choi, D.-S.; Gho, Y.S.; Lötvall, J. MicroRNA in exosomes isolated directly from the liver circulation in patients with metastatic uveal melanoma. BMC Cancer 2014, 14, 962, doi:10.1186/1471-2407-14-962.
44. Pardo, M.; García, Á.; Antrobus, R.; Blanco, M.J.; Dwek, R.A.; Zitzmann, N. Biomarker Discovery from Uveal Melanoma Secretomes: Identification of gp100 and Cathepsin D in Patient Serum. J. Proteome Res. 2007, 6, 2802–2811, doi:10.1021/pr070021t.
45. Angi, M.; Kalirai, H.; Prendergast, S.; Simpson, D.; Hammond, D.E.; Madigan, M.C.; Beynon, R.J.; Coupland, S.E. In-depth proteomic profiling of the uveal melanoma secretome. Oncotarget 2016, 7, 49623–49635, doi:10.18632/oncotarget.10418.

46. Abdouh, M.; Hamam, D.; Gao, Z.-H.; Arena, V.; Arena, M.; Arena, G.O. Exosomes isolated from cancer patients' sera transfer malignant traits and confer the same phenotype of primary tumors to oncosuppressor-mutated cells. J. Exp. Clin. Cancer Res. 2017, 36, 113, doi:10.1186/s13046-017-0587-0.
47. Hamam, D.; Abdouh, M.; Gao, Z.-H.; Arena, V.; Arena, M.; Arena, G.O. Transfer of malignant trait to BRCA1 deficient human fibroblasts following exposure to serum of cancer patients. J. Exp. Clin. Cancer Res. 2016, 35, 80, doi:10.1186/s13046-016-0360-9.
48. Abdouh, M.; Gao, Z.H.; Arena, V.; Arena, M.; Burnier, M.N.; Arena, G.O. Oncosuppressor-Mutated Cells as a Liquid Biopsy Test for Cancer-Screening. Sci. Rep. 2019, 9, 2384, doi:10.1038/s41598-019-38736-y.
49. Valtink, M.; Engelmann, K. Serum-free cultivation of adult normal human choroidal melanocytes. Clin. Exp. Ophthalmol. 2007, 245, 1487–1494, doi:10.1007/s00417-007-0588-3.
50. Collaborative Ocular Melanoma Study Group.The COMS Randomized Trial of Iodine 125 Brachytherapy for Choroidal Melanoma: V. Twelve-Year Mortality Rates and Prognostic Factors: COMS Report No. 28; JAMA Ophthalmology,Chicago, IL, USA. 2006; Volume 124.
51. Abdouh, M.; Zhou, S.; Arena, V.; Arena, M.; Lazaris, A.; Onerheim, R.; Metrakos, P.; Arena, G.O. Transfer of malignant trait to immortalized human cells following exposure to human cancer serum. J. Exp. Clin. Cancer Res. 2014, 33, 86, doi:10.1186/s13046-014-0086-5.
52. Van Niel, G.; Raposo, G.; Candalh, C.; Boussac, M.; Hershberg, R.; Cerf–Bensussan, N.; Heyman, M. Intestinal epithelial cells secrete exosome–like vesicles. Gastroenterology 2001, 121, 337–349, doi:10.1053/gast.2001.26263.
53. Logozzi, M.; De Milito, A.; Lugini, L.; Borghi, M.; Calabrò, L.; Spada, M.; Perdicchio, M.; Marino, M.L.; Federici, C.; Iessi, E.; et al. High levels of exosomes expressing CD63 and caveolin-1 in plasma of melanoma patients. PLoS ONE 2009, 4, e5219, doi:10.1371/journal.pone.0005219.
54. Lee, T.H.; D'Asti, E.; Magnus, N.; Al-Nedawi, K.; Meehan, B.; Rak, J. Microvesicles as mediators of intercellular communication in cancer--the emerging science of cellular "debris". Semin. Immunopathol. 2011, 33, 455–467.
55. Yuana, Y.; Sturk, A.; Nieuwland, R. Extracellular vesicles in physiological and pathological conditions. Blood Rev. 2013, 27, 31–39, doi:10.1016/j.blre.2012.12.002.

56. Hoshino, A.; Costa-Silva, B.; Shen, T.L.; Rodrigues, G.; Hashimoto, A.; Tesic Mark, M.; Molina, H.; Kohsaka, S.; Di Giannatale, A.; Ceder, S.; et al. Tumour exosome integrins determine organotropic metastasis. Nature 2015, 527, 329–335, doi:10.1038/nature15756.
57. Lindoso, R.S.; Collino, F.; Camussi, G. Extracellular vesicles derived from renal cancer stem cells induce a pro-tumorigenic phenotype in mesenchymal stromal cells. Oncotarget 2015, 6, 7959–7969, doi:10.18632/oncotarget.3503.
58. Oikkonen, L.; Lise, S. Making the most of RNA-seq: Pre-processing sequencing data with Opossum for reliable SNP variant detection. Wellcome open Res. 2017, 2, 6, doi:10.12688/wellcomeopenres.10501.2.
59. Rimmer, A.; Phan, H.; Mathieson, I.; Iqbal, Z.; Twigg, S.R.F.; Consortium, W.; Wilkie, A.O.M.; McVean, G.; Lunter, G. Integrating mapping-, assembly- and haplotype-based approaches for calling variants in clinical sequencing applications. Nat. Genet. 2014, 46, 912–918, doi:10.1038/ng.3036.
60. Abdouh, M.; Floris, M.; Gao, Z.-H.; Arena, V.; Arena, M.; Arena, G.O. Colorectal cancer-derived extracellular vesicles induce transformation of fibroblasts into colon carcinoma cells. J. Exp. Clin. Cancer Res. 2019, 38, 257, doi:10.1186/s13046-019-1248-2.
61. Pathan, M.; Fonseka, P.; Chitti, S. V.; Kang, T.; Sanwlani, R.; Van Deun, J.; Hendrix, A.; Mathivanan, S. Vesiclepedia 2019: A compendium of RNA, proteins, lipids and metabolites in extracellular vesicles. Nucleic Acids Res. 2018, 47, D516–D519, doi:10.1093/nar/gky1029.
62. Consortium, U. UniProt: A worldwide hub of protein knowledge. Nucleic Acids Res. 2019, 47, D506–D515, doi:10.1093/nar/gky1049.
63. Pan, D.; Chen, J.; Feng, C.; Wu, W.; Wang, Y.; Tong, J.; Zhou, D. Preferential Localization of MUC1 Glycoprotein in Exosomes Secreted by Non-Small Cell Lung Carcinoma Cells. Int. J. Mol. Sci. 2019, 20, 323.
64. Sun, L.; Guo, C.; Cao, J.; Burnett, J.; Yang, Z.; Ran, Y.; Sun, D. Over-expression of alpha-enolase as a prognostic biomarker in patients with pancreatic cancer. Int. J. Med. Sci. 2017, 14, 655–661, doi:10.7150/ijms.18736.
65. Cho, H.J.; Hwang, Y.S.; Yoon, J.; Lee, M.; Lee, H.G.; Daar, I.O. EphrinB1 promotes cancer cell migration and invasion through the interaction with RhoGDI1. Oncogene 2018, 37, 861–872, doi:10.1038/onc.2017.386.

66. Keijser, S.; Missotten, G.S.; Bonfrer, J.M.; De Wolff-Rouendaal, D.; Jager, M.J.; De Keizer, R.J.W. Immunophenotypic markers to differentiate between benign and malignant melanocytic lesions. Br. J. Ophthalmol. 2006, 90, 213–217, doi:10.1136/bjo.2005.080390.
67. Kelman, Z. PCNA: Structure, functions and interactions. Oncogene 1997, 14, 629–640.
68. Diril, M.K.; Ratnacaram, C.K.; Padmakumar, V.C.; Du, T.; Wasser, M.; Coppola, V.; Tessarollo, L.; Kaldis, P. Cyclin-dependent kinase 1 (Cdk1) is essential for cell division and suppression of DNA re-replication but not for liver regeneration. Proc. Natl. Acad. Sci. USA 2012, 109, 3826–3831, doi:10.1073/pnas.1115201109.
69. Wu, Q.; Chen, D.; Luo, Q.; Yang, Q.; Zhao, C.; Zhang, D.; Zeng, Y.; Huang, L.; Zhang, Z.; Qi, Z. Extracellular matrix protein 1 recruits moesin to facilitate invadopodia formation and breast cancer metastasis. Cancer Lett. 2018, 437, 44–55, doi:10.1016/j.canlet.2018.08.022.
70. Burnier, J.V.; Wang, N.; Michel, R.P.; Hassanain, M.; Li, S.; Lu, Y.; Metrakos, P.; Antecka, E.; Burnier, M.N.; Ponton, A.; et al. Type IV collagen-initiated signals provide survival and growth cues required for liver metastasis. Oncogene 2011, 30, 3766–3783, doi:10.1038/onc.2011.89.
71. Mook, O.R.F.; Frederiks, W.M.; Van Noorden, C.J.F. The role of gelatinases in colorectal cancer progression and metastasis. Biochim. Biophys. Acta-Rev. Cancer 2004, 1705, 69–89, doi:10.1016/j.bbcan.2004.09.006.
72. Zhang, X.; Yuan, X.; Shi, H.; Wu, L.; Qian, H.; Xu, W. Exosomes in cancer: Small particle, big player. J. Hematol. Oncol. 2015, 8, 83, doi:10.1186/s13045-015-0181-x.
73. Weidmann, C.; Pomerleau, J.; Trudel-vandal, L.; Landreville, S. Differential responses of choroidal melanocytes and uveal melanoma cells to low oxygen conditions. Mol. Vis. 2017, 23, 103–115.
74. Skog, J.; Würdinger, T.; van Rijn, S.; Meijer, D.H.; Gainche, L.; Sena-Esteves, M.; Curry, W.T., Jr.; Carter, B.S.; Krichevsky, A.M.; Breakefield, X.O. Glioblastoma microvesicles transport RNA and proteins that promote tumour growth and provide diagnostic biomarkers. Nat. Cell Biol. 2008, 10, 1470–1476, doi:10.1038/ncb1800.
75. Hood, J.L.; San Roman, S.; Wickline, S.A. Exosomes released by melanoma cells prepare sentinel lymph nodes for tumor metastasis. Cancer Res. 2011, 71, 3792–3801, doi:10.1158/0008-5472.CAN-10-4455.

76. Fujita, Y.; Yoshioka, Y.; Ochiya, T. Extracellular vesicle transfer of cancer pathogenic components. Cancer Sci. 2016, 107, 385–390, doi:10.1111/cas.12896.
77. Valadi, H.; Ekström, K.; Bossios, A.; Sjöstrand, M.; Lee, J.J.; Lötvall, J.O. Exosome-mediated transfer of mRNAs and microRNAs is a novel mechanism of genetic exchange between cells. Nat. Cell Biol. 2007, 9, 654–659, doi:10.1038/ncb1596.
78. Group Collaborative Ocular Melanoma Study Development of Metastatic Disease After Enrollment in the COMS Trials for Treatment of Choroidal Melanoma: Collaborative Ocular Melanoma Study Group Report No. 26. JAMA Ophthalmol. 2005, 123, 1639–1643, doi:10.1001/archopht.123.12.1639.
79. Peinado, H. Melanoma exosomes educate bone marrow progenitor cells. Nat. Med. 2013, 18, 883–891, doi:10.1038/nm.2753.Melanoma.
80. Rong, B.; Yang, S. Molecular mechanism and targeted therapy of Hsp90 involved in lung cancer: New discoveries and developments (Review). Int. J. Oncol. 2018, 52, 321–336, doi:10.3892/ijo.2017.4214.
81. Mielczarek-Lewandowska, A.; Hartman, M.L.; Czyz, M. Inhibitors of HSP90 in melanoma. Apoptosis 2019, 25, 12–28, doi:10.1007/s10495-019-01577-1.
82. Surriga, O.; Rajasekhar, V.K.; Ambrosini, G.; Dogan, Y.; Huang, R.; Schwartz, G.K. Crizotinib, a c-Met Inhibitor, Prevents Metastasis in a Metastatic Uveal Melanoma Model. Mol. Cancer Ther. 2013, 12, 2817–2826, doi:10.1158/1535-7163.MCT-13-0499.
83. Cheng, H.; Chua, V.; Liao, C.; Purwin, T.J.; Terai, M.; Kageyama, K.; Davies, M.A.; Sato, T.; Aplin, A.E. Co-targeting HGF/cMET Signaling with MEK Inhibitors in Metastatic Uveal Melanoma. Mol. Cancer Ther. 2017, 16, 516–528, doi:10.1158/1535-7163.MCT-16-0552.
84. Kääriäinen, E.; Nummela, P.; Soikkeli, J.; Yin, M.; Lukk, M.; Jahkola, T.; Virolainen, S.; Ora, A.; Ukkonen, E.; Saksela, O.; et al. Switch to an invasive growth phase in melanoma is associated with tenascin-C, fibronectin, and procollagen-I forming specific channel structures for invasion. J. Pathol. 2006, 210, 181–191, doi:10.1002/path.2045.
85. Castagnino, A.; Castro-Castro, A.; Irondelle, M.; Guichard, A.; Lodillinsky, C.; Fuhrmann, L.; Vacher, S.; Agüera-González, S.; Zagryazhskaya-Masson, A.; Romao, M.; et al. Coronin 1C promotes triple-negative breast cancer invasiveness through regulation of MT1-MMP traffic and invadopodia function. Oncogene 2018, 37, 6425–6441, doi:10.1038/s41388-018-0422-x.

86. Ke, A.W.; Shi, G.M.; Zhou, J.; Wu, F.Z.; Ding, Z. Bin; Hu, M.Y.; Xu, Y.; Song, Z.J.; Wang, Z.J.; Wu, J.C.; et al. Role of overexpression of CD151 and/or c-Met in predicting prognosis of hepatocellular carcinoma. Hepatology 2009, 49, 491–503, doi:10.1002/hep.22639.
87. Crabb, J.W.; Hu, B.; Crabb, J.S.; Triozzi, P.; Sauntharajah, Y.; Tubbs, R.; Singh, A.D. iTRAQ quantitative proteomic comparison of metastatic and non-metastatic uveal melanoma tumors. PLoS ONE 2015, 10, e0135543, doi:10.1371/journal.pone.0135543.
88. Lee, Y.-J.; Lee, H.-J.; Choi, S.; Jin, Y.B.; An, H.J.; Kang, J.-H.; Yoon, S.S.; Lee, Y.-S. Soluble HSPB1 regulates VEGF-mediated angiogenesis through their direct interaction. Angiogenesis 2012, 15, 229–242, doi:10.1007/s10456-012-9255-3.
89. Chen, H.; Jia, W.; Li, J. ECM1 promotes migration and invasion of hepatocellular carcinoma by inducing epithelial-mesenchymal transition. World J. Surg. Oncol. 2016, 14, 195, doi:10.1186/s12957-016-0952-z.
90. Liu, Y.; Zhang, J.; Chen, Y.; Sohel, H.; Ke, X.; Chen, J.; Li, Y.X. The correlation and role analysis of COL4A1 and COL4A2 in hepatocarcinogenesis. Aging (Albany NY) 2020, 12, 204–223, doi:10.18632/aging.1026102610.
91. Wu, Y.H.; Chang, T.H.; Huang, Y.F.; Huang, H.D.; Chou, C.Y. COL11A1 promotes tumor progression and predicts poor clinical outcome in ovarian cancer. Br. Dent. J. 2014, 217, 3432–3440, doi:10.1038/onc.2013.307.
92. Alečković, M.; Wei, Y.; LeRoy, G.; Sidoli, S.; Liu, D.D.; Garcia, B.A.; Kang, Y. Identification of Nidogen 1 as a lung metastasis protein through secretome analysis. Genes Dev. 2017, 31, 1439–1455, doi:10.1101/gad.301937.117.
93. Choi, D.-S.; Gho, Y.S. Isolation of Extracellular Vesicles for Proteomic Profiling BT—Proteomic Profiling: Methods and Protocols. In Methods in Molecular Biology; Posch, A., Ed.; Springer: New York, NY, USA, 2015; pp. 167–177, ISBN 978-1-4939-2550-6.
94. Choi, D.; Montermini, L.; Kim, D.; Meehan, B.; Roth, F.P. The impact of oncogenic EGFRvIII on the proteome of extracellular vesicles released from glioblastoma cells. Mol. Cell. Proteom. 2018, 17, 1948–1964.
95. Huang, D.W.; Sherman, B.T.; Lempicki, R.A. Bioinformatics enrichment tools: Paths toward the comprehensive functional analysis of large gene lists. Nucleic Acids Res. 2009, 37, 1–13, doi:10.1093/nar/gkn923.

96. Huang, D.W.; Sherman, B.T.; Lempicki, R.A. Systematic and integrative analysis of large gene lists using DAVID bioinformatics resources. Nat. Protoc. 2008, 4, 44.
97. Kalra, H.; Simpson, R.J.; Ji, H.; Aikawa, E.; Altevogt, P.; Askenase, P.; Bond, V.C.; Borràs, F.E.; Breakefield, X.; Budnik, V.; et al. Vesiclepedia: A Compendium for Extracellular Vesicles with Continuous Community Annotation. PLoS Biol. 2012, 10, e1001450.
98. Damato, B. Does ocular treatment of uveal melanoma influence survival? Br. J. Cancer 2010, 103, 285–290, doi:10.1038/sj.bjc.6605765.
99. Anand, K.; Roszik, J.; Gombos, D.; Upshaw, J.; Sarli, V.; Meas, S.; Lucci, A.; Hall, C.; Patel, S. Pilot Study of Circulating Tumor Cells in Early-Stage and Metastatic Uveal Melanoma. Cancers 2019, 11, 856, doi:10.3390/cancers11060856.
100. Eguchi, A.; Kostallari, E.; Feldstein, A.E.; Shah, V.H. Extracellular vesicles, the liquid biopsy of the future. J. Hepatol. 2019, 70, 1292–1294, doi:10.1016/j.jhep.2019.01.030.
101. Zhao, Z.; Fan, J.; Hsu, Y.-M.S.; Lyon, C.J.; Ning, B.; Hu, T.Y. Extracellular vesicles as cancer liquid biopsies: From discovery, validation, to clinical application. Lab Chip 2019, 19, 1114–1140, doi:10.1039/C8LC01123K.

Chapter 4 (General Discussion)

An obstacle to improving treatment of UM is the rarity of UM as a disease and in turn the sheer lack of understanding surrounding metastatic spread. Systemic therapies which attempt to control metastases are often suboptimal in UM and targeted options are under development [17, 82, 83]. Selumetinib an inhibitor of MEK1 and MEK2, and other similar drugs, are therapies which target the overactivation of the Gα11/q pathway. While promising in UM, there have yet to be major improvements to survival and in the case of selumetinib, many adverse effects of the treatment were reported [41, 46, 216]. It is suggested that therapies targeting one arm of the Gα11/q pathway are insufficient and multiple effector pathways can rescue the blocked route resulting in reduced efficacy of certain targeted options [41].

Inconsistencies in the efficacy of cancer treatment is an unfortunate consequence of tumor and cellular heterogenicity. To compound, the propensity of lesions to metastasize accentuates the gaps in knowledge. The seed to soil theory originally formed in 1889 [217], has since undergone extensive developments demarking a sequential series of genetic and epigenetic events associated with metastasis. Malignant cells acquire an enhanced motility, reduced dependence on cell to cell adhesion, invasive capabilities, and improved survival, promoting colonization to distant tissues [85, 86]. This process is associated with epithelial-mesenchymal transition (EMT), where cells lose adhesive attachments, release matrix metalloproteinases (MMPs) and become aggressively invasive [218, 219]. Partial EMT in which cells maintain variable degrees of both epithelial and mesenchymal phenotypes is often observed in cancer [218]. These transient and reversible phenotypes are correlated with increased malignancy and may confer resistance to anti-cancer therapies [218-221]. However, EMT is not a requirement for metastasis and the extent of EMT is often not universal for all caners [222, 223]. In breast and pancreatic cancer, metastasis may not be dependent on EMT, however may confer a certain amount of chemoresistance [224, 225].

Therapies to combat cancer have been developed to target different aspects of the above framework, either encompassing a broader range of cancer phenotypes or focusing in on precise genetic aberrations, protein and nucleic acid targets. Broadening the scope of current therapies in UM would bring us ever closer to effective options. In Chapter 2, we present the first study investigating the use of MF, an abortifacient, as a potential anti-cancer therapy in UM. MF has been shown to target EMT associated phenotypes (adhesion, migration, and invasion) *in vitro* and

in vivo [108-110, 120, 226]. To date, the application of MF in the context of UM had never been investigated and therefore we sought to determine if MF could influence UM growth *in vitro*.

The potency of MF as a cancer inhibiting drug was tested on a panel of human UM cell lines. At lower concentrations (5-20μM) MF affects the growth of UM cells in a dose dependent manner leading to a an eventual cytostatic state. While at higher doses (30-40μM), MF is cytotoxic to UM cells *in vitro*, significantly reducing cellular viability and resulting in an increase in hypodiploid cells, caspase 3 and 7 activity, DNA fragmentation, and release of cfDNA all associated with an apoptotic cell death mechanism. Our findings confirm MF has the ability to disrupt the growth of UM cells and become cytotoxic.

These results are consistent with previous reports of the ability of MF to inhibit cellular proliferation in a dose-dependent fashion and result in cell cycle arrest. MF is known to target cancer hallmarks: specifically, the accelerated proliferation, migratory and invasive capability of cancer cells [109, 110, 227-229]. Further, our preliminary results have shown that MF is potent enough to disturb the migratory and invasive capability of UM cells *in vitro*. In accordance with previous research in other cancer types [109, 126], a trend is seen in which MF causes marked decreases in the migratory and invasiveness of UM cells at cytostatic doses. Investigations to confirm the influence of MF on UM cellular motility would be required, including fluorescent labelling of fibrillar actin to observe effects on cytoskeleton.

MF has been demonstrated to function through the classical PR pathway, inhibiting transcription of downstream products. Another mechanism by which MF may act is through inhibition of progesterone induced blocking factor (PIBF). PIBF is found upregulated in cancer and allows T cells to deactivate natural killer cells in the tumor microenvironment. This process of immune evasion can be potentiated with progesterone or inhibited through MF [230-232].

However, MF can function in absence of the PR receptor [110]. Here, our results were the first to characterize the mRNA expression of various PR receptors in UM. We demonstrated a clear lack of classical PR mRNA expression, reporting in place non-classical PR and glucocorticoid receptor mRNA expression in UM. PAQR8, PGRMC1, and PGRMC2, expressed in UM cells, have all been associated with cancer signaling pathways including anti-apoptotic signaling, cholesterol metabolism, cell cycle regulation and chemoresistance [233-237]. Upon MF treatment, receptor mRNA expression levels were significantly reduced suggesting a possible adaptive mechanism adopted by UM cells in order to avoid the cytotoxic effects of MF. However,

further studies are of necessity to investigate how MF may be impacting receptor protein expression and signaling.

Of novelty, quantification of cfDNA release was employed as a means to monitor MF treatment response in UM cells. Our group had recently optimized and implemented a method to monitor circulating tumor DNA (ctDNA) in relation to treatment response in UM using digital droplet PCR to quantify four UM driver mutations (*GNAQ, GNA11, PLCβ4* and *CYSTLR2*). ctDNA levels in plasma and aqueous humor correlated with tumor growth in a rabbit model of UM and was detachable prior to tumor discovery. These same methods were translated to a patient cohort, proving ctDNA was not only detectable in UM patient blood but correlated with malignancy [69]. Here, we found an increase in cfDNA for all UM cell lines in a dose dependent manner following MF treatment consistent with massive cellular death. These data suggest a potential application of ctDNA and liquid biopsy techniques to monitor MF treatment response in an *in vivo* model of UM.

In vitro investigations of MF have translated to *in vivo* models of ovarian and lung cancer with promising initial results to reduce tumor growth [108, 111]. In patient cohorts similar conclusions lead to a reduction in growth and improvement in perceived quality of life for patients with end stage metastatic disease [112]. The application of MF in the setting of cancer is promising, and repurposing MF as a safe adjuvant therapy could become a possibility. However, it remains clear that our current knowledge on the mechanisms of action of MF are lacking and therefore further *in vitro* and *in vivo* investigations are necessary to determine the value of such treatment in clinic. To date, our manuscript is an encouraging beginning, expanding the current body of knowledge on prospective therapies in UM with the goal to ameliorate gaps in treatment for metastatic UM patients.

Individual cellular adaptations such as EMT, are not the only mechanisms defining metastatic spread [224, 225]. While aggressively malignant individual cells can incite metastases, widespread intercellular communication with the microenvironment and host is an imperative aspect of dissemination. Termed the pro-metastatic secretome, tumors release an abundance of cytokines, chemokines, angiogenic factors, various nucleic acids, proteins and EVs to shape the local and distant microenvironments [95, 238]. These messengers then function as immunomodulators, remodel the extracellular matrix, and recruit cancer associated effector cells to promote metastatic spread [95, 149, 207].

Though protein aggregates and nucleic acids are released straight into the extracellular space by tumors, EVs provide a secure means of transferring malignant signals through harsh conditions and farther distances. Ranging from 50-1000nm in diameter, EVs are cancer messengers encasing selectively loaded proteins and nucleic acid cargo in a lipid bilayer with specific surface patterns to target and interact with appropriate recipient cells [149]. These messengers have become the next frontier in cancer research and biomarker discovery. Expanding the liquid biopsy scene, EVs have an increased abundance in the blood of cancer patients, and harbour a signature proteome, transcriptome and genome which parallels their cell of origin [95, 146, 149, 179, 207]. The formation of a pre-metastatic niche suggests EVs secreted from the primary tumor transport tumorigenic cargo with oncogenic potential and transform recipient cells in a distant tissue [95, 98, 99, 169, 207]. In ovarian and pancreatic cancers, EVs have been shown to function through immunomodulation, angiogenesis, and direct cellular reprogramming to aid in the formation of these pre-metastatic niches [99].

The current reservoir of knowledge in UM concerning EVs and their functional intentions as potential mediators of metastasis is scarce [239, 240]. To summarize, miRNA profiles of EVs derived from metastatic UM patient liver perfusate and patient serum have been investigated [212, 213]. Limited insight into the proteomic profile of UM-derived EVs is available. Surman *et al.* reported on the protein content and glycosylation pattern of UM cell line (Mel 202)-derived EVs, finding associations with cancer-signaling molecules [214].

Therefore, in Chapter 3 we sought to contribute to the limited information surrounding UM EVs as a means to gain insight into the metastatic potential of UM. This was the first study to focus on the EV proteomic profile of a large panel of primary and metastatic human UM cell lines and to explore the oncogenic potential of these EVs *in vivo*. Taking into account the entire EV proteome provided a thorough picture and highlighted key metastatic players we might not have explored on our own. As an example, our results demonstrated a heightened expression of integrin αV protein levels in all UM-EVs in comparison to NCM-EVs. Presence of ITGαvβv in cancer derived EVs has previously been associated with liver organotropism [241]. While other tumor-associated proteins were found upregulated in UM EVs compared to control. Included are HSP90 and ENO1 both with links to the MAPK and P13K/AKT pathways, promotion of cellular survival, metastasis and have biomarker potential in certain cancers [242-244]. Overall, UM cell line EVs expressed higher levels of proteins associated with various cancer signaling cascades, including

cellular growth, adhesion, motility, and proteins associated with pre-metastatic niches. An in-depth discussion on UM-EV protein content in relation to metastasis can be found in Chapter 3.

An *in vivo* mouse model was used to further determine the functional capabilities of UM derived EVs. Treatment of fibro-BKO cells with UM-EVs and subsequent injection into NOD-SCID mice resulted in tumor formation *in vivo*. In contrast, cells treated with NCM-EVs were not able to produce tumors. This matches previous research demonstrating the oncogenic potential of EVs derived from cancer patient sera [169]. Further our results confirmed UM-EVs were efficiently internalized by recipient cells and enhanced proliferation, migration and invasion of the cells in question. Recipient cells (onco-suppressor mutated fibroblasts and immortalized human hepatocytes) were selected to represent cells of the potential premetastatic niche in UM metastasis. A more specific explanation which informed our decision to use BRCA1 knockout fibroblasts can be found in a previous study by Abdouh M. *et al.* [169]. Following the results of our study, it would be pertinent to assess the interactions between recipient cells and UM-EVs to determine the signaling cascades and biological alterations that may be occurring in recipient cells upon exposure.

Selective EV cargo from various cancer types have been characterized and oncogenic drivers or potential biomarkers identified. Further tracking of EVs in *in vivo* models allows researchers to determine their route of dissemination and the locations in which they may be preferentially acting to create a microenvironment for eventual tumor cell colonization. These advances help us gain a broader understanding of metastasis as a systemic event. The population of EVs secreted from any given cell or tumor is extremely heterogenous; therefore, selectively isolating a given subclass denies a thorough exploration of the cargo and functional intentions of the entire EV population. Here we provided this broader account in UM and these advances hope to enhance our current knowledge on metastatic progression.

Chapter 5 (Future Directions)

UM has a higher incidence than any other ocular cancer and metastasis rates that extend to 50% of the patient cohort with 2-year survival below 10% [3, 4, 6, 10, 67, 245]. This thesis included valuable insights into the treatment and propagation of UM, building a foundation to further the UM community and eventually improve patient outcome. The two studies focused on aspects of the UM research field which had yet to be investigated, namely a possible new adjuvant

therapy and investigations into UM-EVs. Both sets of data also demonstrate the role of liquid biopsy in monitoring treatment response and as a source of potential biomarkers. This is especially important in UM, where intraocular biopsies and resections are not commonly performed for diagnosis.

In Chapter 2, MF demonstrated potent cytotoxicity on our panel of human UM cell lines. To expand these findings, there should be an assessment of MF's influence on the cytoskeleton, migratory and invasive properties of UM. It would then prove beneficial to determine the mechanism of action of MF in UM. We provided evidence that UM cells expressed non-classical PR mRNA in place of classical PR. Therefore, it should be determined whether MF does indeed interact with one of these non-classical PRs or another receptor to exert the observed inhibitory effects. Subsequent downstream pathway analysis would provide a thorough picture of the mechanisms by which this drug may be acting. Finally, an *in vivo* model would further confirm whether MF may be relevant in the treatment of UM and metastatic progression. With the detection of heightened levels of cfDNA release following MF treatment, it would prove interesting to use liquid biopsies to monitor tumor response to MF in an *in vivo* model.

Chapter 3 shifted focus to EVs as possible mediators of metastatic disease in UM. We are the first to elucidate the EV proteomic profile of six UM cell lines with comparison to normal choroidal melanocytes and demonstrate the oncogenic potential of UM-EVs *in vivo*. We identified differential expression of potential biomarkers implicated in tumorigenesis and metastatic niche formation. To progress these results, it would prove pertinent to investigate the interactions of UM-EVs with recipient cells and determine if organotrophic mechanisms are indeed involved. Further understanding the surface composition of EVs, their cargo delivery and downstream signaling in targeted cells would lead way for possible therapeutic targets.

Bibliography:

1. Lin, J.Y. and D.E. Fisher, Melanocyte biology and skin pigmentation. Nature, 2007. 445(7130): p. 843-50.
2. Amaro, A., et al., The biology of uveal melanoma. Cancer Metastasis Rev, 2017. 36(1): p. 109-140.
3. Chang AE, K.L., Menck HR., The National Cancer Data Base report on cutaneous and noncutaneous melanoma: a summary of 84,836 cases from the past decade. The American College of Surgeons Commission on Cancer and the American Cancer Society. Cancer, 1998. 83(8): p. 1664–1678.
4. McLaughlin, C.C., et al., Incidence of noncutaneous melanomas in the U.S. Cancer, 2005. 103(5): p. 1000-7.
5. Wick, M.R., Cutaneous melanoma: A current overview. Semin Diagn Pathol, 2016. 33(4): p. 225-41.
6. Krantz, B.A., et al., Uveal melanoma: epidemiology, etiology, and treatment of primary disease. Clin Ophthalmol, 2017. 11: p. 279-289.
7. Singh, A.D., M.E. Turell, and A.K. Topham, Uveal melanoma: trends in incidence, treatment, and survival. Ophthalmology, 2011. 118(9): p. 1881-5.
8. Virgili, G., Gatta, G., Ciccolallo, L., Capocaccia, R., Biggeri, A., Crocetti, E., et al., Survival in patients with uveal melano- ma in Europe. Archives of Ophthalmology, 2008. 126(10): p. 1413–1418.
9. Aronow, M.E., A.K. Topham, and A.D. Singh, Uveal Melanoma: 5-Year Update on Incidence, Treatment, and Survival (SEER 1973-2013). Ocul Oncol Pathol, 2018. 4(3): p. 145-151.
10. Kaliki, S. and C.L. Shields, Uveal melanoma: relatively rare but deadly cancer. Eye (Lond), 2017. 31(2): p. 241-257.
11. Damato EM, D.B., Detection and time to treatment of uveal melanoma in the United Kingdom: an evaluation of 2,384 patients. Ophthalmology, 2012. 119(8): p. 1582–1589.
12. Andreoli MT, M.W., Leiderman YI., Epidemiological trends in uveal melanoma. Br J Ophthalmol., 2015. 99(11): p. 1550–1553.
13. Ghazawi, F.M., et al., Uveal melanoma incidence trends in Canada: a national comprehensive population-based study. Br J Ophthalmol, 2019. 103(12): p. 1872-1876.

14. Nathan, P., Cohen, V., Coupland, S., Curtis, K., Damato, B., Evans, J., et al. , Uveal melanoma UK national guidelines. European Journal of Cancer, 2015. 51(16): p. 2404–2412.
15. Kujala, E., T. Makitie, and T. Kivela, Very long-term prognosis of patients with malignant uveal melanoma. Invest Ophthalmol Vis Sci, 2003. 44(11): p. 4651-9.
16. F.P. Xu, L.T.T., A.A. Singh, A.D, Uveal melanoma: metastases, in: S. A. Damato B (Ed.), Clinical Ophthalmic Oncology. Springer, 2019.
17. Bustamante, P., et al., Uveal melanoma pathobiology: Metastasis to the liver. Semin Cancer Biol, 2020.
18. CollaborativeOcularMelanomaStudyGroup, Assessmentofmetastaticdisease status at death in 435 patients with large choroidal melanoma in the Collabora- tive Ocular Melanoma Study (COMS). COMS Report No. 15. . Arch Ophthalmol., 2001. 119: p. 670-676.
19. Diener-West, M.R., S.M.; Agugliaro, D.J.; Caldwell, R.; Cumming, K.; Earle, J.D.; Hawkins, B.S.; Hayman, J.A.; Jaiyesimi, I.; Jampol, L.M.; et al., Development of metastatic disease after enrollment in the COMS trials for treatment of choroidal melanoma: Collaborative ocular melanoma study group report No. 26. Arch. Ophthalmol., 2005. 123: p. 1639–1643.
20. Rietschel P, P.K., Hanlon C, Patel A, Abramson DH, Chapman PB., Variates of survival in metastatic uveal melanoma. J Clin Oncol., 2005. 23(31): p. 8076–8080.
21. Kuk D, S.A., Barker CA, et al., Prognosis of mucosal, uveal, acral, nonacral cutaneous, and unknown primary melanoma from the time of first metastasis. Oncologist., 2016. 21(7): p. 848–854.
22. Mafee, M.F., et al., Anatomy and pathology of the eye: role of MR imaging and CT. Neuroimaging Clin N Am, 2005. 15(1): p. 23-47.
23. Kels, B.D., A. Grzybowski, and J.M. Grant-Kels, Human ocular anatomy. Clin Dermatol, 2015. 33(2): p. 140-6.
24. Griewank, K.G., et al., Conjunctival melanomas harbor BRAF and NRAS mutations and copy number changes similar to cutaneous and mucosal melanomas. Clin Cancer Res, 2013. 19(12): p. 3143-52.

25. Kusters-Vandevelde, H.V., et al., Primary melanocytic tumors of the central nervous system: a review with focus on molecular aspects. Brain Pathol, 2015. 25(2): p. 209-26.
26. Shields CL, F.M., Thangappan A, Nagori S, Mashayekhi A, Lally DR et al., Metastasis of uveal melanoma millimeter-by-millimeter in 8033 consecutive eyes. Arch Ophthalmol, 2009. 127(8): p. 989–998.
27. Weis E, S.C., Lajous M, Shields JA, Shields CL., The Association Between Host Susceptibility Factors and Uveal Melanoma: a meta-analysis. Arch Ophthalmol 2006. 124(1): p. 54–60.
28. Hu, D.N., et al., Population-based incidence of uveal melanoma in various races and ethnic groups. Am J Ophthalmol, 2005. 140(4): p. 612-7.
29. Shah, C.P., et al., Intermittent and chronic ultraviolet light exposure and uveal melanoma: a meta-analysis. Ophthalmology, 2005. 112(9): p. 1599-607.
30. Horn, S., Figl, A., Rachakonda, P. S., Fischer, C., Sucker, A., Gast, A., et al., TERT promoter mutations in familial and spo- radic melanoma. [Research support, non-U.S. Gov't]. Science, 2013. 339(6122): p. 959–961.
31. Huang, F.W., Hodis, E., Xu, M. J., Kryukov, G. V., Chin, L., & Garraway, L. A., Highly recurrent TERT promoter muta- tions in human melanoma. [Research support, N.I.H., extramural research support, non-U.S. Gov't]. Science, 2013. 339(6122): p. 957–959.
32. Robertson, A.G., Shih, J., Yau, C., Gibb, E.A., Oba, J., Mungall, K.L., Hess, J.M., and V. Uzunangelov, Walter, V., Danilova, L., Lichtenberg, T.M., Kucherlapati, M., Kimes, P.K., Tang, M., Penson, A., Babur, O., Akbani, R., Bristow, C.A., Hoadley, K.A., Iype, L., Chang, M.T., Network, T.R., Cherniack, A.D., Benz, C., Mills, G.B., Verhaak, R.G.W., Griewank, K.G., Felau, I., Zenklusen, J.C., Gershenwald, J.E., Schoenfield, L., Lazar, A.J., Abdel-Rahman, M.H., Roman-Roman, S., Stern, M.H., Cebulla, C.M., Williams, M.D., Jager, M.J., Coupland, S.E., Esmaeli, B., Kandoth, C., Woodman, S.E., I, Integrative analysis identifies four molecular and clinical subsets in uveal melanoma. Cancer Cell, 2017. 32: p. 204–220 e215.
33. Dono, M., et al., Mutation frequencies of GNAQ, GNA11, BAP1, SF3B1, EIF1AX and TERT in uveal melanoma: detection of an activating mutation in the TERT gene promoter in a single case of uveal melanoma. Br J Cancer, 2014. 110(4): p. 1058-65.

34. Koopmans, A.E., et al., Prevalence and implications of TERT promoter mutation in uveal and conjunctival melanoma and in benign and premalignant conjunctival melanocytic lesions. Invest Ophthalmol Vis Sci, 2014. 55(9): p. 6024-30.
35. Bastian, B.C., The molecular pathology of melanoma: an integrated taxonomy of melanocytic neoplasia. Annu Rev Pathol, 2014. 9: p. 239-71.
36. Chien, J.L., et al., Choroidal nevus: a review of prevalence, features, genetics, risks, and outcomes. Curr Opin Ophthalmol, 2017. 28(3): p. 228-237.
37. Shields CL, F.M., Mashayekhi A, et al. , Clinical spectrum of choroidal nevi based on age at presentation in 3422 consecutive eyes. Ophthalmology, 2008. 115: p. 546 – 552.
38. C.L. Shields, L.A.D., M.D. Yu, D. Ancona-Lezama, M. Di Nicola, B.SEPK. Williams, J.A. Lucio-Alvarez, S.M. Ang, S.M. Maloney, R.J. Welch, J.A. Shields, Choroidal nevus transformation into melanoma per millimeter increment in thickness using multimodal imaging in 2355 cases: the 2019 Wendell L. Hughes lecture. Retina, 2019. 39(10): p. 1852–1860.
39. Singh AD, K.P., Topham A., Estimating the risk of malig- nant transformation of a choroidal nevus. Ophthalmology, 2005. 112: p. 1784–1789.
40. ShieldsCL, D., Ancona-LezamaD,etal., Choroidalnevus transformation into melanoma using multimodal imaging in 3806 cases. The 2020 Taylor R. Smith and Victor T. Curtin Lecture. Retina 2018.
41. Smit, K.N., et al., Uveal melanoma: Towards a molecular understanding. Prog Retin Eye Res, 2020. 75: p. 100800.
42. Yavuzyigitoglu, S., et al., Correlation of Gene Mutation Status with Copy Number Profile in Uveal Melanoma. Ophthalmology, 2017. 124(4): p. 573-575.
43. Van Raamsdonk, C.D., et al., Mutations in GNA11 in uveal melanoma. N Engl J Med, 2010. 363(23): p. 2191-9.
44. Yavuzyigitoglu, S., et al., Uveal Melanomas with SF3B1 Mutations: A Distinct Subclass Associated with Late-Onset Metastases. Ophthalmology, 2016b. 123(5): p. 1118-28.
45. Vader, M.J.C., Madigan, M.C., Versluis, M., Suleiman, H.M., Gezgin, G., Gruis, N.A., Out- Luiting, J.J., Bergman, W., Verdijk, R.M., Jager, M.J., van der Velden, P.A., GNAQ and GNA11 mutations and downstream YAP activation in choroidal nevi. . Br. J. Cancer, 2017. 117: p. 884–887.

46. Moore, A.R., et al., Recurrent activating mutations of G-protein-coupled receptor CYSLTR2 in uveal melanoma. Nat Genet, 2016. 48(6): p. 675-80.
47. Moore, A.R., et al., GNA11 Q209L Mouse Model Reveals RasGRP3 as an Essential Signaling Node in Uveal Melanoma. Cell Rep, 2018. 22(9): p. 2455-2468.
48. O'Hayre, M., Vazquez-Prado, J., Kufareva, I., Stawiski, E.W., Handel, T.M., Seshagiri, S., Gutkind, J.S., The emerging mutational landscape of G proteins and G-protein-coupled receptors in cancer. Nat. Rev. Cancer, 2013. 13: p. 412–424.
49. Yoo, J.H., Shi, D.S., Grossmann, A.H., Sorensen, L.K., Tong, Z., Mleynek, T.M., Rogers, A., Zhu, W., Richards, J.R., Winter, J.M., Zhu, J., Dunn, C., Bajji, A., Shenderovich, M., Mueller, A.L., Woodman, S.E., Harbour, J.W., Thomas, K.R., Odelberg, S.J., Ostanin, K., Li, D.Y., ARF6 is an actionable node that orchestrates oncogenic GNAQ signaling in uveal melanoma. . Cancer Cell 2016. 29: p. 889–904.
50. Chen, X., et al., RasGRP3 Mediates MAPK Pathway Activation in GNAQ Mutant Uveal Melanoma. Cancer Cell, 2017. 31(5): p. 685-696 e6.
51. Feng, X., et al., Hippo-independent activation of YAP by the GNAQ uveal melanoma oncogene through a trio-regulated rho GTPase signaling circuitry. Cancer Cell, 2014. 25(6): p. 831-45.
52. Feng, X., Degese, M.S., Iglesias-Bartolome, R., Vaque, J.P., Molinolo, A.A., Rodrigues, M., Zaidi, M.R., Ksander, B.R., Merlino, G., Sodhi, A., Chen, Q., Gutkind, J.S., Hippo-independent activation of YAP by the GNAQ uveal melanoma oncogene
through a trio-regulated rho GTPase signaling circuitry. . Cancer Cell, 2014. 25: p. 831–845.
53. Ramos, A., and Camargo, F.D., The Hippo signaling pathway and stem cell biology. Trends Cell Biol., 2012. 22: p. 339–346.
54. Zhao, B., Li, L., Lei, Q., and Guan, K.L., The Hippo-YAP pathway in organ size control and tumorigenesis: an updated version. Genes Dev., 2010. 24: p. 862–874.
55. Harbour, J.W., Onken, M.D., Roberson, E.D., Duan, S., Cao, L., Worley, L.A., Council, M.L., Matatall, K.A., Helms, C., Bowcock, A.M., Frequent mutation of BAP1 in metastasizing uveal melanomas. . Science, 2010. 330: p. 1410–1413.
56. Koopmans, A.E., et al., Clinical significance of immunohistochemistry for detection of BAP1 mutations in uveal melanoma. Mod Pathol, 2014. 27(10): p. 1321-30.

57. al., H.N.e., BRCA1-associated protein 1 interferes with BRCA1/BARD1 RING heterodimer activity. Cancer Res., 2009. 69: p. 111.
58. Yu, H., Pak, H., Hammond-Martel, I., Ghram, M., Rodrigue, A., Daou, S., Barbour, H., Corbeil, L., Hebert, J., Drobetsky, E., Masson, J.Y., Di Noia, J.M., Affar el, B., Tumor suppressor and deubiquitinase BAP1 promotes DNA double-strand break repair. . Proc. Natl. Acad. Sci. U. S. A. , 2014. 111: p. 285–290.
59. Wessely, A., et al., The Role of Immune Checkpoint Blockade in Uveal Melanoma. Int J Mol Sci, 2020. 21(3).
60. Harbour, J.W., et al., Frequent mutation of BAP1 in metastasizing uveal melanomas. Science, 2010. 330(6009): p. 1410-3.
61. Yang, J., et al., Treatment of uveal melanoma: where are we now? Ther Adv Med Oncol, 2018. 10: p. 1758834018757175.
62. Bailey, P., Chang, D.K., Nones, K., Johns, A.L., Patch, A.M., Gingras, M.C., Miller, D.K., Christ, A.N., Bruxner, T.J., Quinn, M.C., Nourse, C., Murtaugh, L.C., Harliwong, I., Idrisoglu, S., Manning, S., Nourbakhsh, E., Wani, S., Fink, L., Holmes, O., Chin, V., Anderson, M.J., Kazakoff, S., Leonard, C., Newell, F., Waddell, N., Wood, S., Xu, Q., Wilson, P.J., Cloonan, N., Kassahn, K.S., Taylor, D., Quek, K., Robertson, A., Pantano, L., Mincarelli, L., Sanchez, L.N., Evers, L., Wu, J., Pinese, M., Cowley, M.J., Jones, M.D., Colvin, E.K., Nagrial, A.M., Humphrey, E.S., Chantrill, L.A., Mawson, A., Humphris, J., Chou, A., Pajic, M., Scarlett, C.J., Pinho, A.V., Giry-Laterriere, M., Rooman, I., Samra, J.S., Kench, J.G., Lovell, J.A., Merrett, N.D., Toon, C.W., Epari, K., Nguyen, N.Q., Barbour, A., Zeps, N., Moran-Jones, K., Jamieson, N.B., Graham, J.S., Duthie, F., Oien, K., Hair, J., Grutzmann, R., Maitra, A., Iacobuzio-Donahue, C.A., Wolfgang, C.L., Morgan, R.A., Lawlor, R.T., Corbo, V., Bassi, C., Rusev, B., Capelli, P., Salvia, R., Tortora, G., Mukhopadhyay, D., Petersen, G.M., Australian Pancreatic Cancer Genome, I., Munzy, D.M., Fisher, W.E., Karim, S.A., Eshleman, J.R., Hruban, R.H., Pilarsky, C., Morton, J.P., Sansom, O.J., Scarpa, A., Musgrove, E.A., Bailey, U.M., Hofmann, O., Sutherland, R.L., Wheeler, D.A., Gill, A.J., Gibbs, R.A., Pearson, J.V., Waddell, N., Biankin, A.V., Grimmond, S.M. , Genomic analyses identify molecular subtypes of pancreatic cancer. Nature, 2016. 531: p. 47–52.

63. Ciriello, G., Gatza, M.L., Beck, A.H., Wilkerson, M.D., Rhie, S.K., Pastore, A., Zhang, H., McLellan, M., Yau, C., Kandoth, C., Bowlby, R., Shen, H., Hayat, S., Fieldhouse, R., Lester, S.C., Tse, G.M., Factor, R.E., Collins, L.C., Allison, K.H., Chen, Y.Y., Jensen, K., Johnson, N.B., Oesterreich, S., Mills, G.B., Cherniack, A.D., Robertson, G., Benz, C., Sander, C., Laird, P.W., Hoadley, K.A., King, T.A., Network, T.R., Perou, C.M., Comprehensive molecular portraits of invasive lobular breast cancer. Cell, 2015. 163: p. 506–519.
64. Martin, M., Masshofer, L., Temming, P., Rahmann, S., Metz, C., Bornfeld, N., van de Nes, J., Klein-Hitpass, L., Hinnebusch, A.G., Horsthemke, B., Lohmann, D.R., Zeschnigk, M., Exome sequencing identifies recurrent somatic mutations in EIF1AX and SF3B1 in uveal melanoma with disomy 3. . Nat. Genet, 2013. 45: p. 933–936.
65. Harbour JW, C.R., The DecisionDx-UM Gene Expression Profile Test Provides Risk Stratification and Individualized Patient Care in Uveal Melanoma. PLoS Curr., 2013. 5.
66. Onken, M.D., et al., Gene expression profiling in uveal melanoma reveals two molecular classes and predicts metastatic death. Cancer Res, 2004. 64(20): p. 7205-9.
67. Damato, E.M. and B.E. Damato, Detection and time to treatment of uveal melanoma in the United Kingdom: an evaluation of 2,384 patients. Ophthalmology, 2012. 119(8): p. 1582-9.
68. Manford, M., Simple visual hallucinations and epilepsy. Pract Neurol, 2020. 20(5): p. 345-346.
69. Bustamante, P., et al., Circulating tumor DNA tracking through driver mutations as a liquid biopsy-based biomarker for uveal melanoma. Journal of Experimental & Clinical Cancer Research, 2021. 40(1).
70. Frizziero, L., et al., Uveal Melanoma Biopsy: A Review. Cancers (Basel), 2019. 11(8).
71. Bedi, D.G., et al., Sonography of the eye. AJR Am J Roentgenol, 2006. 187(4): p. 1061-72.
72. MM., B., Intraocular biopsy of uveal melanoma Risk assessment and identification of genetic prognostic markers. Acta Ophthalmol., 2018. 96: p. 1-28.
73. TA., M., Fine-needle aspiration biopsy in the management of choroidal melanoma. Curr Opin Ophthalmol., 2013. 24(3): p. 262-266.

74. Onken, M.D.W., L.A.; Char, D.H.; Augsburger, J.J.; Correa, Z.M.; Nudleman, E.; Aaberg, T.M., Jr.; Altaweel, M.M.; Bardenstein, D.S.; Finger, P.T.; et al., Collaborative Ocular Oncology Group report number 1: Prospective validation of a multi-gene prognostic assay in uveal melanoma. Ophthalmology 2012. 119: p. 1596–1603.
75. Jovanovic, P., et al., Ocular melanoma: an overview of the current status. International journal of clinical and experimental pathology, 2013. 6(7): p. 1230- 1244.
76. Damato, B., Ocular treatment of choroidal melanoma in relation to the prevention of metastatic death - A personal view. Prog Retin Eye Res, 2018. 66: p. 187-199.
77. BE., D., Local resection of uveal melanoma. Dev Ophthalmol., 2012. 49: p. 66–80.
78. Group, C.O.M.S., The COMS random- ized trial of iodine 125 brachytherapy for choroidal melanoma: V. Twelve-year mortality rates and prognostic factors: COMS report no. 28. Arch Ophthalmol, 2006. 124(12): p. 1684–1693.
79. Eskelin, S., Pyrhonen, S., Summanen, P., Hahka-Kemppinen, M., Kivela, T., Tumor doubling times in metastatic malignant melanoma of the uvea: tumor progression before and after treatment. . Ophthalmology, 2000. 107: p. 1443–1449.
80. Lane, A.M., I.K. Kim, and E.S. Gragoudas, Survival Rates in Patients After Treatment for Metastasis From Uveal Melanoma. JAMA Ophthalmol, 2018. 136(9): p. 981-986.
81. Khoja, L., et al., Meta-analysis in metastatic uveal melanoma to determine progression free and overall survival benchmarks: an international rare cancers initiative (IRCI) ocular melanoma study. Ann Oncol, 2019. 30(8): p. 1370-1380.
82. Rowcroft A, L.B., Thomson BNJ, Banting S, Knowles B. , Systematic review of liver directed therapy for uveal melanoma hepatic metastases, HPB Oxford, 2019. 22(4): p. 497-505.
83. Servois, V., et al., Iterative treatment with surgery and radiofrequency ablation of uveal melanoma liver metastasis: Retrospective analysis of a series of very long-term survivors. Eur J Surg Oncol, 2019. 45(9): p. 1717-1722.
84. Bergers, G. and S.M. Fendt, The metabolism of cancer cells during metastasis. Nat Rev Cancer, 2021. 21(3): p. 162-180.
85. IJ., F., The pathogenesis of cancer metastasis: the ‘seed and soil’ hypothesis revisited. Nature reviews Cancer, 2003. 3: p. 453–458.

86. Lambert, A.W., D.R. Pattabiraman, and R.A. Weinberg, Emerging Biological Principles of Metastasis. Cell, 2017. 168(4): p. 670-691.
87. Moreno-Bueno, G., et al., The morphological and molecular features of the epithelial-to-mesenchymal transition. Nat Protoc, 2009. 4(11): p. 1591-613.
88. Scheel, C. and R.A. Weinberg, Cancer stem cells and epithelial-mesenchymal transition: concepts and molecular links. Semin Cancer Biol, 2012. 22(5-6): p. 396-403.
89. Thiery, J.P., Epithelial–mesenchymal transitions in tumour progression. Nat. Rev. Cancer, 2002. 2: p. 442–454.
90. Peinado, H., Olmeda, D. & Cano, A., Snail, Zeb and bHLH factors in tumour progression: an alliance against the epithelial phenotype? Nat. Rev. Cancer, 2007. 7: p. 415–428.
91. Moreno-Bueno, G.e.a., Genetic profiling of epithelial cells expressing E-cadherin repressors reveals a distinct role for Snail, Slug, and E47 factors in epithelial–mesenchymal transition. Cancer Res., 2006. 66: p. 9543–9556.
92. De Craene, B.e.a., The transcription factor snail induces tumor cell invasion through modulation of the epithelial cell differentiation program. Cancer Res, 2005. 65: p. 6237–6244.
93. Steeg, P.S., Targeting metastasis. Nat Rev Cancer, 2016. 16(4): p. 201-18.
94. S., P., The distribution of secondary growths in cancer of the breast. Lancet 1889. 1: p. 99–101.
95. Peinado, H., et al., Pre-metastatic niches: organ-specific homes for metastases. Nat Rev Cancer, 2017. 17(5): p. 302-317.
96. Kaplan, R.N.e.a., VEGFR1-positive haematopoietic bone marrow progenitors initiate the pre-metastatic
niche. Nature, 2005. 438: p. 820–827.
97. Hiratsuka, S.e.a., The S100A8-serum amyloid A3– TLR4 paracrine cascade establishes a pre-metastatic phase. . Nat. Cell Biol., 2008. 10: p. 1349–1355.
98. Costa-Silva, B., et al., Pancreatic cancer exosomes initiate pre-metastatic niche formation in the liver. Nat Cell Biol, 2015. 17(6): p. 816-26.
99. Feng, W., et al., Exosomes promote pre-metastatic niche formation in ovarian cancer. Mol Cancer, 2019. 18(1): p. 124.

100. Baulieu, E.-E., “Contragestion and other clinical applications of RU 486, an antiprogesterone at the receptor”. Science, 1989. 245: p. 1351–1357.
101. Cossu, G., et al., The Role of Mifepristone in Meningiomas Management: A Systematic Review of the Literature. Biomed Res Int, 2015. 2015: p. 267831.
102. Goldstone, P., C. Walker, and K. Hawtin, Efficacy and safety of mifepristone-buccal misoprostol for early medical abortion in an Australian clinical setting. Aust N Z J Obstet Gynaecol, 2017. 57(3): p. 366-371.
103. Schaff, E.A., Mifepristone: ten years later. Contraception, 2010. 81(1): p. 1-7.
104. Ho PC, Y.N.E., Tang OS. , Mifepristone: contraceptive and non-contraceptive uses. Curr Opin Obstet Gynecol, 2002. 14: p. 325–30.
105. Nieman, L.K., Recent Updates on the Diagnosis and Management of Cushing's Syndrome. Endocrinol Metab (Seoul), 2018. 33(2): p. 139-146.
106. Block, T., et al., Mifepristone Plasma Level and Glucocorticoid Receptor Antagonism Associated With Response in Patients With Psychotic Depression. J Clin Psychopharmacol, 2017. 37(5): p. 505-511.
107. Benagiano, G., C. Bastianelli, and M. Farris, Selective progesterone receptor modulators 3: use in oncology, endocrinology and psychiatry. Expert Opin Pharmacother, 2008. 9(14): p. 2487-96.
108. Goyeneche, A.A., Carón, R.W., Telleria, C.M., Mifepristone Inhibits Ovarian Cancer Cancer Cell Growth In Vitro and In Vivo. Clin Cancer Res., 2007. 13(11): p. 3370-3379.
109. Ritch, S.J., et al., Advanced assessment of migration and invasion of cancer cells in response to mifepristone therapy using double fluorescence cytochemical labeling. BMC Cancer, 2019. 19(1): p. 376.
110. Tieszen, C.R., et al., Antiprogestin mifepristone inhibits the growth of cancer cells of reproductive and non-reproductive origin regardless of progesterone receptor expression. BMC Cancer, 2011. 11: p. 207.
111. Check JH, S.L., Chern J and Dix E, Mifepristone Treatment Improves Length and Quality of Survival of Mice with Spontaneous Lung Cancer. Anticancer Res, 2010. 30: p. 119-122.

112. J.H. Check, E.D., R. Cohen, D. Check, C. Wilson, Efficacy of the progesterone receptor antagonist mifepristone for palliative therapy of patients with a variety of advanced cancer types. Anticancer Res., 2010. 30(2): p. 623–628.
113. Sitruk-Ware, R. and I.M. Spitz, Pharmacological properties of mifepristone: toxicology and safety in animal and human studies. Contraception, 2003. 68(6): p. 409-420.
114. Baulieu, E.E., Segal,S.J., The antiprogestin steroid RU 486 and human fertility control. New York: Plenum Press, 1985.
115. Deraedt R, V.B., Fournex R., Toxicological study on RU 486. In: Baulieu EE, Segal SJ, editors. The antiprogestin steroid RU 486 and human fertility control. New York: Plenum Press, 1985: p. 123–126.
116. Gaillard RC, H.W., Utilisation clinique du RU 486: contrôle du cycle menstruel et effet sur l'axe hypophyso-surrénalien [Clinical use of RU 486: control of the menstrual cycle and effect on the hypophyseal-adrenal axis]. . Ann Endocrinol (Paris), 1983. 44(5): p. 345-6.
117. Garfield RE, B.E., The antiprogesterone steroid RU 486: a short pharmacological and clinical review, with emphasis on the interruption of pregnancy. Baillieres Clin Endocrinol Metab., 1987. 1(1): p. 207-221.
118. Philibert D, M.M., Mary I, et al., Pharmacological profile of RU 486 in animals. In: Baulieu EE, Segal SJ, editors. The anti- progestin steroid RU 486 and human fertility control. New York: Plenum Press, 1985: p. 49–68.
119. Organization., W.H., Clinical Practice Handbook for Safe Abortion. Geneva, Switzerland: WHO, 2014.
120. Chen, W., et al., Pharmacokinetic differences of mifepristone between sexes in animals. J Pharm Biomed Anal, 2018. 154: p. 108-115.
121. R. Peyron, E.A., V. Targosz, L. Silvestre, M. Renault, F. Elkik, P. Leclerc, A. Ulmann, E.E. Baulieu, Early termination of pregnancy with mifepristone (RU 486) and the orally active prostaglandin misoprostol. N. Engl. J. Med., 1993. 328(21): p. 1509-1513.
122. Song, L.P., et al., Early medical abortion with self-administered low-dose mifepristone in combination with misoprostol. J Obstet Gynaecol Res, 2018. 44(9): p. 1705-1711.
123. Administration, U.S.F.a.D. Postmarket Drug Safety Information for Patients and Providers : Questions and Answers on Mifeprex. 2019; Available from:

https://www.fda.gov/drugs/postmarket-drug-safety-information-patients-and-providers/questions-and-answers-mifeprex.

124. Chen, J., et al., The unique pharmacological characteristics of mifepristone (RU486): from terminating pregnancy to preventing cancer metastasis. Med Res Rev, 2014. 34(5): p. 979-1000.

125. Islam, M.S., et al., Selective Progesterone Receptor Modulators-Mechanisms and Therapeutic Utility. Endocr Rev, 2020. 41(5).

126. Li DQ, W.Z., Bai J, Zhao J, Wang Y, Hu K, Du YH., Effects of mifepristone on invasive and metastatic potential of human gastric adenocarcinoma cell line MKN-45 in vitro and in vivo. World J Gastroenterol., 2004. 10(12): p. 1726-1729.

127. Murray MJ, L.B., Embryo implantation and tumor metastasis: common pathways of invasion and angiogenesis. Semin Reprod Endocrinol 1999. 17: p. 275-290.

128. Udayashankar, R., et al., Characterization of invasive trophoblasts generated from human embryonic stem cells. Hum Reprod, 2011. 26(2): p. 398-406.

129. Bardon S, V.F., Chalbos D, Rochefort H., RU486, a progestin and glucocorticoid antagonist, inhibits

the growth of breast cancer cells via the progesterone receptor. J Clin Endocrinol Metab, 1985. 60: p. 692-697.

130. Benad, P., et al., The anti-progestin RU-486 inhibits viability of MCF-7 breast cancer cells by suppressing WNT1. Cancer Lett, 2011. 312(1): p. 101-8.

131. Gaddy VT, B.J., Delk JN, Kallab AM, Porter AG, Schoenlein PV., Mifepristone induces growth arrest, caspase activation, and apoptosis of estrogen receptor-expressing, antiestrogen-resistant breast cancer cells. Clin Cancer Res., 2004. 10(15): p. 5215-25.

132. Musgrove EA, L.C., Cornish AL, Swarbrick A, Sutherland RL., Antiprogestin inhibition of cell cycle progression in T-47D breast cancer cells is accompanied by induction of the cyclin-dependent kinase inhibitor p21. Mol Endocrinol., 1997. 1: p. 54-66.

133. Li, A., et al., Effect of mifepristone on proliferation and apoptosis of Ishikawa endometrial adenocarcinoma cells. Fertil Steril, 2005. 84(1): p. 202-11.

134. Navo, M.A., et al., In vitro evaluation of the growth inhibition and apoptosis effect of mifepristone (RU486) in human Ishikawa and HEC1A endometrial cancer cell lines. Cancer Chemother Pharmacol, 2008. 62(3): p. 483-9.

135. Jiang J, W.R., Wang ZH, Sun HC, Xu Z, Xiu HM., Effect of mifepristone on estrogen and progesterone receptors in human endometrial and endometriotic cells in vitro. . Fertil Steril., 2002. 77(5): p. 995-1000.
136. Jovanovic-Pole A, L.Y., Kim Y, et al., Prevention of Brca1-mediated mammary tumorigenesis in mice by a progesterone antagonist. Science, 2006. 1467: p. 314.
137. G.H. Bakker, B.S.-H., M.S. Henkelmann, et al., Comparison of the actions of the antiprogestin mifepristone (RU486), the progestin megestrol acetate, the LHRH-analog buserelin, and ovariectomy in treatment of rat mammary tumors. Cancer Treat Rep, 1987. 71: p. 1021-1027.
138. Klijn JGM, S.-H.B., Foekens JA, progesterone antagonists and progesterone receptor modulators in the treatment of breast cancer. Steroids 2000. 65: p. 825-830.
139. Perrault D, E.E., Pritchard KI, et al. , Phase II study of the progesterone antagonist mifepristone in patients with untreated metastatic breast carcinoma: a National Cancer Institute of Canada Clinical Trials Group Study. J Clin Oncol, 1996. 14: p. 2709-2712.
140. Romieux G, M.T., Ulmann A, and e. al., The antiprogestin RU486 in advanced breast cancer: preliminary clinical trial. Bull Cancer 1987. 74: p. 455-559.
141. J.G.M. Klijn, F.H.D.J., G.H. Bakker, S.W.J. Lamberts, C.J. Rodenburg, J. Alexieva-Figusch, Antiprogestins: a new form of endocrine therapy for breast cancer. Cancer Res,, 1989. 49: p. 2851-2856.
142. Ramondetta LM, J.A., Sun CC, et al., Phase 2 trial of mifepristone (RU-486) in advanced or recurrent endometrioid adenocarcinoma or low-grade endometrial stromal sarcoma. Cancer, 2009. 115(9): p. 1867–1874.
143. Grunberg, S.M., Weiss, M. H., Spitz, I. M., Ahmadi, J., Sadun, A., Russell, C. A., Lucci, L., & Stevenson, L. L., Treatment of unresectable meningiomas with the antiprogesterone agent mifepristone. Journal of Neurosurgery, 1991. 74(6): p. 861-866.
144. S. M. Grunberg, C.R., J. Townsend, J. Ahmadi, L. Feun, and R. Fredericks, Eds., Phase III Double-Blind Randomized Placebo-Controlled Study on Mifepristone (RU) for the Treatment of Unresectable Meningioma. American Society of Clinical Oncology, Alexandria, Va, USA, 2001.

145. Check JH, C.D., Poretta T., Mifepristone Extends Both Length and Quality of Life in a Patient With Advanced Non-small Cell Lung Cancer that Has Progressed Despite Chemotherapy and a Check-point Inhibitor. . Anticancer Res, 2019. 39(4): p. 1923-1926.
146. Thery, C., et al., Minimal information for studies of extracellular vesicles 2018 (MISEV2018): a position statement of the International Society for Extracellular Vesicles and update of the MISEV2014 guidelines. J Extracell Vesicles, 2018. 7(1): p. 1535750.
147. Bu, H., et al., Exosomes: Isolation, Analysis, and Applications in Cancer Detection and Therapy. Chembiochem, 2019. 20(4): p. 451-461.
148. Lane, R., et al., Cell-derived extracellular vesicles can be used as a biomarker reservoir for glioblastoma tumor subtyping. Commun Biol, 2019. 2: p. 315.
149. van Niel, G., G. D'Angelo, and G. Raposo, Shedding light on the cell biology of extracellular vesicles. Nat Rev Mol Cell Biol, 2018. 19(4): p. 213-228.
150. Xu, R., et al., Extracellular vesicle isolation and characterization: toward clinical application. J Clin Invest, 2016. 126(4): p. 1152-62.
151. Zaborowski, M.P., et al., Extracellular Vesicles: Composition, Biological Relevance, and Methods of Study. Bioscience, 2015. 65(8): p. 783-797.
152. Zhao, H., et al., Tumor microenvironment derived exosomes pleiotropically modulate cancer cell metabolism. Elife, 2016. 5: p. e10250.
153. Thery, C., M. Ostrowski, and E. Segura, Membrane vesicles as conveyors of immune responses. Nat Rev Immunol, 2009. 9(8): p. 581-93.
154. Blanchard, N., et al., TCR activation of human T cells induces the production of exosomes bearing the TCR/CD3/zeta complex. J Immunol, 2002. 168(7): p. 3235-41.
155. Cocucci, E., Meldolesi, J., Ectosomes and exosomes: shed- ding the confusion between extracellular vesicles. Trends Cell Biol., 2015. 25(6): p. 364–372.
156. Cocucci, E. and J. Meldolesi, Ectosomes. Curr Biol, 2011. 21(23): p. R940-1.
157. Kowal J, A.G., Colombo M, Jouve M, Morath JP, Primdal-Bengtson B, Dingli F, Loew D, Tkach M, Théry C, Proteomic comparison defines novel markers to characterize heterogeneous populations of extracellular vesicle subtypes. Proc Natl Acad Sci USA, 2016. 113: p. E968 – E977.
158. Mathieu, M., et al., Specificities of secretion and uptake of exosomes and other extracellular vesicles for cell-to-cell communication. Nat Cell Biol, 2019. 21(1): p. 9-17.

159. Tkach, M., et al., Qualitative differences in T-cell activation by dendritic cell-derived extracellular vesicle subtypes. EMBO J, 2017. 36(20): p. 3012-3028.
160. Kamerkar, S., et al., Exosomes facilitate therapeutic targeting of oncogenic KRAS in pancreatic cancer. Nature, 2017. 546(7659): p. 498-503.
161. Valadi, H.e.a., Exosome-mediated transfer of mRNAs and microRNAs is a novel mechanism of genetic exchange between cells. Nat. Cell Biol., 2007. 9: p. 654–659.
162. Wu, J., et al., The malignant role of exosomes in the communication among colorectal cancer cell, macrophage and microbiome. Carcinogenesis, 2019. 40(5): p. 601-610.
163. Lee, C.H., et al., Discovery of a diagnostic biomarker for colon cancer through proteomic profiling of small extracellular vesicles. BMC Cancer, 2018. 18(1): p. 1058.
164. Rontogianni, S., et al., Proteomic profiling of extracellular vesicles allows for human breast cancer subtyping. Commun Biol, 2019. 2: p. 325.
165. Eldh M, O.B.R., Lässer C, Svanvik J, Sjöstrand M, Mattsson J, Lindnér P, Choi DS, Gho YS, Lötvall J., MicroRNA in exosomes isolated directly from the liver circulation in patients with metastatic uveal melanoma. . BMC Cancer, 2014. 14: p. 962.
166. Diamond, J.M., et al., Exosomes Shuttle TREX1-Sensitive IFN-Stimulatory dsDNA from Irradiated Cancer Cells to DCs. Cancer Immunol Res, 2018. 6(8): p. 910-920.
167. Kahlert, C., et al., Identification of double-stranded genomic DNA spanning all chromosomes with mutated KRAS and p53 DNA in the serum exosomes of patients with pancreatic cancer. J Biol Chem, 2014. 289(7): p. 3869-75.
168. Balaj, L.e.a., Tumour microvesicles contain retrotransposon elements and amplified oncogene sequences. Nat. Commun., 2011. 2: p. 180.
169. Abdouh, M., et al., Exosomes isolated from cancer patients' sera transfer malignant traits and confer the same phenotype of primary tumors to oncosuppressor-mutated cells. J Exp Clin Cancer Res, 2017. 36(1): p. 113.
170. Antonyak, M.A.e.a., Cancer cell-derived microvesicles induce transformation by transferring tissue transglutaminase and fibronectin to recipient cells. Proc. Natl Acad. Sci. USA, 2011. 108: p. 4852–4857.
171. Saenz-Cuesta, M., et al., Methods for extracellular vesicles isolation in a hospital setting. Front Immunol, 2015. 6: p. 50.

172. Davis, J.Q., et al., Selective externalization of an ATP-binding protein structurally related to the clathrin-uncoating ATPase/heat shock protein in vesicles containing terminal transferrin receptors during reticulocyte maturation. Journal of Biological Chemistry, 1986. 261(33): p. 15368-15371.
173. Harding, C., Heuser, J., Stahl, P., Receptor-mediated Endocytosis of Transferrin and Recycling of the Transferrin Receptor in Rat Reticulocytes. Cell Biol., 1983. 97: p. 329-339.
174. Johnstone, R.M., et al., Vesicle formation during reticulocyte maturation. Association of plasma membrane activities with released vesicles (exosomes). Journal of Biological Chemistry, 1987. 262(19): p. 9412-9420.
175. Todorova D, S.S., Lacroix R, Sabatier F, Dignat-George F. , Extracellular Vesicles in Angiogenesis. Circ Res., 2017. 120(10): p. 1658-1673.
176. Marar C, S.B., Wirtz D., Extracellular vesicles in immunomodulation and tumor progression. Nat Immunol, 2021. 22(5): p. 560-570.
177. Saint-Pol, J., et al., Targeting and Crossing the Blood-Brain Barrier with Extracellular Vesicles. Cells, 2020. 9(4).
178. Terlecki-Zaniewicz L, P.V., Bobbili MR, Lämmermann I, Perrotta I, Grillenberger T, Schwestka J, Weiß K, Pum D, Arcalis E, Schwingenschuh S, Birngruber T, Brandstetter M, Heuser T, Schosserer M, Morizot F, Mildner M, Stöger E, Tschachler E, Weinmüllner R, Gruber F, Grillari J. , Extracellular Vesicles in Human Skin: Cross-Talk from Senescent Fibroblasts to Keratinocytes by miRNAs. J Invest Dermatol. , 2019. 139(12): p. 2425-2436.
179. Consortium, E.-T., et al., EV-TRACK: transparent reporting and centralizing knowledge in extracellular vesicle research. Nat Methods, 2017. 14(3): p. 228-232.
180. Cvjetkovic, A., J. Lotvall, and C. Lasser, The influence of rotor type and centrifugation time on the yield and purity of extracellular vesicles. J Extracell Vesicles, 2014. 3.
181. Skotland, T., et al., An emerging focus on lipids in extracellular vesicles. Adv Drug Deliv Rev, 2020. 159: p. 308-321.
182. Stein, J.M., Luzio, J.P., Ectocytosis caused by sublytic autologous complement attack on human neutrophils. The sorting of endogenous plasma-membrane proteins and lipids into shed vesicles. Biochem J., 1991. 274 (Pt 2): p. 381–386.

183. Jeppesen, D.K., et al., Reassessment of Exosome Composition. Cell, 2019. 177(2): p. 428-445 e18.
184. Sodar, B.W., et al., Low-density lipoprotein mimics blood plasma-derived exosomes and microvesicles during isolation and detection. Sci Rep, 2016. 6: p. 24316.
185. Hurley, J.H., et al., Membrane budding. Cell, 2010. 143(6): p. 875-87.
186. Morelli, A.E.e.a., Endocytosis, intracellular sorting and processing of exosomes by dendritic cells. Blood, 2004. 104: p. 3257–3266.
187. Barres, C.e.a., Galectin-5 is bound onto the surface
of rat reticulocyte exosomes and modulates vesicle uptake by macrophages. Blood, 2010. 115: p. 696–705.
188. Frey, B.G., U. S., The immune functions of phosphatidylserine in membranes of dying cells and microvesicles. Semin. Immunopathol., 2011. 33: p. 497–516.
189. Fitzner, D., et al., Selective transfer of exosomes from oligodendrocytes to microglia by macropinocytosis. J Cell Sci, 2011. 124(Pt 3): p. 447-58.
190. Durcin, M., et al., Characterisation of adipocyte-derived extracellular vesicle subtypes identifies distinct protein and lipid signatures for large and small extracellular vesicles. J Extracell Vesicles, 2017. 6(1): p. 1305677.
191. Colombo, M., G. Raposo, and C. Thery, Biogenesis, secretion, and intercellular interactions of exosomes and other extracellular vesicles. Annu Rev Cell Dev Biol, 2014. 30: p. 255-89.
192. Purushothaman, A.e.a., Fibronectin on the surface of myeloma cell-derived exosomes mediates exosome-cell interactions. J. Biol. Chem., 2016. 291: p. 1652–1663.
193. Melo, S.A.e.a., Glypican-1 identifies cancer exosomes and detects early pancreatic cancer. Nature, 2015. 523: p. 177–182.
194. Laulagnier, K., et al., Amyloid precursor protein products concentrate in a subset of exosomes specifically endocytosed by neurons. Cell Mol Life Sci, 2018. 75(4): p. 757-773.
195. Laulagnier K., e.a., Mast cell– and dendritic cell–derived exosomes display a specific lipid composition and an unusual membrane organization. Biochemical Journal, 2004. 380: p. 161–171.

196. Muralidharan-Chari, V.e.a., ARF6-regulated shedding of tumor cell-derived plasma membrane microvesicles. Curr. Biol., 2009. 19: p. 1875–1885.
197. Doyle, L.M. and M.Z. Wang, Overview of Extracellular Vesicles, Their Origin, Composition, Purpose, and Methods for Exosome Isolation and Analysis. Cells, 2019. 8(7).
198. Zhang, H., et al., Identification of distinct nanoparticles and subsets of extracellular vesicles by asymmetric flow field-flow fractionation. Nat Cell Biol, 2018. 20(3): p. 332-343.
199. Caradec, J., et al., Reproducibility and efficiency of serum-derived exosome extraction methods. Clin Biochem, 2014. 47(13-14): p. 1286-92.
200. Linares, R., et al., High-speed centrifugation induces aggregation of extracellular vesicles. J Extracell Vesicles, 2015. 4: p. 29509.
201. Patel, G.K., et al., Comparative analysis of exosome isolation methods using culture supernatant for optimum yield, purity and downstream applications. Sci Rep, 2019. 9(1): p. 5335.
202. Tauro, B.J., et al., Comparison of ultracentrifugation, density gradient separation, and immunoaffinity capture methods for isolating human colon cancer cell line LIM1863-derived exosomes. Methods, 2012. 56(2): p. 293-304.
203. Gamez-Valero, A., et al., Size-Exclusion Chromatography-based isolation minimally alters Extracellular Vesicles' characteristics compared to precipitating agents. Sci Rep, 2016. 6: p. 33641.
204. Shu, S., et al., Purity and yield of melanoma exosomes are dependent on isolation method. J Extracell Vesicles, 2020. 9(1): p. 1692401.
205. Hamam, D., et al., Transfer of malignant trait to BRCA1 deficient human fibroblasts following exposure to serum of cancer patients. J Exp Clin Cancer Res, 2016. 35: p. 80.
206. Ruiz-Lopez, L., et al., The role of exosomes on colorectal cancer: A review. J Gastroenterol Hepatol, 2018. 33(4): p. 792-799.
207. Guo, Y., et al., Effects of exosomes on pre-metastatic niche formation in tumors. Mol Cancer, 2019. 18(1): p. 39.
208. Hood, J.L., R.S. San, and S.A. Wickline, Exosomes released by melanoma cells prepare sentinel lymph nodes for tumor metastasis. Cancer Res, 2011. 71(11): p. 3792-801.

209. Skog, J., et al., Glioblastoma microvesicles transport RNA and proteins that promote tumour growth and provide diagnostic biomarkers. Nat Cell Biol, 2008. 10(12): p. 1470-6.
210. San Lucas, F.A., et al., Minimally invasive genomic and transcriptomic profiling of visceral cancers by next-generation sequencing of circulating exosomes. Ann Oncol, 2016. 27(4): p. 635-41.
211. Qu, X., et al., Double-Stranded DNA in Exosomes of Malignant Pleural Effusions as a Novel DNA Source for EGFR Mutation Detection in Lung Adenocarcinoma. Front Oncol, 2019. 9: p. 931.
212. Eldh M, O.B.R., Lässer C, et al., MicroRNA in exosomes isolated directly from the liver circulation in patients with metastatic uveal melanoma. BMC Cancer, 2014. 14: p. 962.
213. Ragusa, M., et al., miRNA profiling in vitreous humor, vitreal exosomes and serum from uveal melanoma patients: Pathological and diagnostic implications. Cancer Biol Ther, 2015. 16(9): p. 1387-96.
214. Surman, M., et al., An Insight into the Proteome of Uveal Melanoma-Derived Ectosomes Reveals the Presence of Potentially Useful Biomarkers. Int J Mol Sci, 2019. 20(15).
215. Muller, L., et al., Isolation of biologically-active exosomes from human plasma. J Immunol Methods, 2014. 411: p. 55-65.
216. Carvajal, R.D., et al., Effect of selumetinib vs chemotherapy on progression-free survival in uveal melanoma: a randomized clinical trial. JAMA, 2014. 311(23): p. 2397-405.
217. S., P., The distribution of secondary growths in cancer of the breast. Lancet, 1889. 1: p. 571–573.
218. Saitoh, M., Involvement of partial EMT in cancer progression. J Biochem, 2018. 164(4): p. 257-264.
219. Geiger, T.R. and D.S. Peeper, Metastasis mechanisms. Biochim Biophys Acta, 2009. 1796(2): p. 293-308.
220. Friedl, P. and K. Wolf, Tumour-cell invasion and migration: diversity and escape mechanisms. Nat Rev Cancer, 2003. 3(5): p. 362-74.
221. Yu, M., et al., Circulating breast tumor cells exhibit dynamic changes in epithelial and mesenchymal composition. Science, 2013. 339(6119): p. 580-4.

222. De Craene, B. and G. Berx, Regulatory networks defining EMT during cancer initiation and progression. Nat Rev Cancer, 2013. 13(2): p. 97-110.
223. Li, W. and Y. Kang, Probing the Fifty Shades of EMT in Metastasis. Trends Cancer, 2016. 2(2): p. 65-67.
224. Fischer, K.R., et al., Epithelial-to-mesenchymal transition is not required for lung metastasis but contributes to chemoresistance. Nature, 2015. 527(7579): p. 472-6.
225. Zheng, X., et al., Epithelial-to-mesenchymal transition is dispensable for metastasis but induces chemoresistance in pancreatic cancer. Nature, 2015. 527(7579): p. 525-530.
226. Brandhagen, B.N., et al., Cytostasis and morphological changes induced by mifepristone in human metastatic cancer cells involve cytoskeletal filamentous actin reorganization and impairment of cell adhesion dynamics. BMC Cancer, 2013. 13: p. 35.
227. Goyeneche, A.A., R.W. Caron, and C.M. Telleria, Mifepristone inhibits ovarian cancer cell growth in vitro and in vivo. Clin Cancer Res, 2007. 13(11): p. 3370-9.
228. Goyeneche, A.A., E.E. Seidel, and C.M. Telleria, Growth inhibition induced by antiprogestins RU-38486, ORG-31710, and CDB-2914 in ovarian cancer cells involves inhibition of cyclin dependent kinase 2. Invest New Drugs, 2012. 30(3): p. 967-80.
229. Goyeneche, A.A. and C.M. Telleria, Antiprogestins in gynecological diseases. Reproduction, 2015. 149(1): p. R15-33.
230. Check JH, C.D., Therapy Aimed to Suppress the Production of the Immunosuppressive Protein Progesterone Induced Blocking Factor (PIBF) May Provide Palliation and/or Increased Longevity for Patients With a Variety of Different Advanced Cancers. Anticancer Res, 2019. 39(7): p. 3365-3372.
231. Check JH, N.P., Goldberg J, Yuen W and Angotti D., A model for potential tumor immunotherapy based on knowledge of immune mechanisms responsible for spontaneous abortion. Med Hypoth, 2001. 57: p. 337-343.
232. Srivastava, M.D., et al., Expression and modulation of progesterone induced blocking factor (PIBF) and innate immune factors in human leukemia cell lines by progesterone and mifepristone. Leuk Lymphoma, 2007. 48(8): p. 1610-7.
233. Cahill, M.A., et al., The emerging role of progesterone receptor membrane component 1 (PGRMC1) in cancer biology. Biochim Biophys Acta, 2016. 1866(2): p. 339-349.

234. Cahill, M.A. and H. Neubauer, PGRMC Proteins Are Coming of Age: A Special Issue on the Role of PGRMC1 and PGRMC2 in Metabolism and Cancer Biology. Cancers (Basel), 2021. 13(3).
235. Dressing GE, A.R., Pang Y, Thomas P. , Membrane progesterone receptors (mPRs) mediate progestin induced antimorbidity in breast cancer cells and are expressed in human breast tumors. . Horm Cancer., 2012. 3(3): p. 101-12.
236. Garg D, N.S., Baig KM, Driggers P, Segars J. , Progesterone-mediated non-classical signaling. Trends Endocrinol Metab., 2017. 28(9): p. 656–668.
237. S.T. Lin, E.W.M., J.F. Chang, R.Y. Hu, L.H. Wang, H.L. Chan, PGRMC1 contributes to doxorubicin-induced chemoresistance in MES-SA uterine sarcoma. Cell. Mol. Life Sci., 2015. 72: p. 2395–2409.
238. Hanahan, D. and R.A. Weinberg, Hallmarks of cancer: the next generation. Cell, 2011. 144(5): p. 646-74.
239. Lande, K., et al., Exosomes: Insights from Retinoblastoma and Other Eye Cancers. Int J Mol Sci, 2020. 21(19).
240. Liu, J., et al., Roles of Exosomes in Ocular Diseases. Int J Nanomedicine, 2020. 15: p. 10519-10538.
241. Hoshino, A., et al., Tumour exosome integrins determine organotropic metastasis. Nature, 2015. 527(7578): p. 329-35.
242. Mielczarek-Lewandowska, A., M.L. Hartman, and M. Czyz, Inhibitors of HSP90 in melanoma. Apoptosis, 2020. 25(1-2): p. 12-28.
243. Fu Q-F, L.Y., Fan Y, Hua S-N, Qu H-Y, Dong S-W, et al., Alpha-enolase promotes cell glycolysis, growth, migration, and invasion in non-small cell lung cancer through FAK-mediated PI3K/AKT pathway. Journal of Hematology & Oncology, 2015. 8: p. 22.
244. Principe M, C.P., Shih NY, Chattaragada MS, Rolla S, Conti L, et al., Targeting of surface alpha-enolase inhibits the invasiveness of pancreatic cancer cells. Oncotarget, 2015. 6: p. 11098-113.
245. Diener-West, M., et al., Development of metastatic disease after enrollment in the COMS trials for treatment of choroidal melanoma: Collaborative Ocular Melanoma Study Group Report No. 26. Arch Ophthalmol, 2005. 123(12): p. 1639-43.